Towards Improved EEG Interpretation in a Sensorimotor BCI for the Control of a Prosthetic or Orthotic Hand

Abdul-Khaaliq Mohamed

June 2011

A dissertation submitted to the Faculty of Engineering and the Built Environment, University of Witwatersrand, for the degree of Master of Science in Engineering.

Declaration

I declare that this dissertation is my own, unaided work, unless otherwise acknowledged. It is being submitted for the degree of Master of Science of Engineering at the University of Witwatersrand, Johannesburg. It has not been submitted before for any degree or examination at any other university.

Signed on: ____ day of _____ 20___

_____

Abstract

A brain computer interface (BCI), which reroutes neural signals from the brain to actuators in a prosthetic or orthotic hand, promises to aid those who suffer from hand motor impairments, such as amputees and victims of strokes and spinal cord injuries. Such individuals can greatly benefit from the return of some of the essential functionality of the hand through the renewed performance of the basic hand movements involved in daily activities. These hand movements include wrist extension, wrist flexion, finger extension, finger flexion and the tripod pinch. The core of this sensorimotor BCI solution lies in the interpretation of the neural information for the five essential hand movements extracted from EEG (electroencephalogram). It is necessary to improve on the interpretation of these EEG signals; hence this research explores the possibility of single-trial EEG discrimination for the five essential hand movements in an offline, synchronous manner.

The EEG was recorded from five healthy test subjects as they performed the actual and imagined movements for both hands. The research is then divided into three investigations which respectively attempt to differentiate the EEG for: 1) right and left combinations of the different hand movements, 2) wrist and finger movements on the same hand and 3) the individual five movements on the same hand. A general method is applied to all three investigations. It utilizes independent component analysis (ICA) and time-frequency techniques to extract features based on event-related (de)synchronisation (ERD/ERS) and movement-related cortical potentials (MRCP). The Bhattacharyya distance is used for feature reduction and Mahalanobis distance clustering and artificial neural networks are used as classifiers.

The best average accuracies of 89 %, 71 % and 57 % for the three respective investigations are obtained using ANNs and features related to ERD/ERS. Along with accuracies around 70 % for a few subjects in the five-movement differentiation investigation, these results indicated the possibility of offline, synchronous differentiation of single-trial EEG for the five essential hand movements. These hand movements can be used in part or in combination as imagined and performed motor tasks for BCIs aimed at controlling prosthetic or orthotic hands.

Acknowledgments

There are several people and institutions that have helped me through the process of this research and are hereby acknowledged. Firstly I would like to thank my wife, my parents and the rest of my family for their encouragement, patience and support. I would also like to thank my two supervisors i.e. Prof. Tshilidzi Marwala (University of Johannesburg) and Dr. Lester John (University of Cape Town) for all their help, guidance and support. Many thanks go to the University of Johannesburg and the University of Witwatersrand for their financial assistance. The assistance from the Univeristy of Cape Town in terms of expertise and the use of the necessary equipment is greatly appreciated. I would like to thank Prof. Ian. Jandrell along with my supervisors for allowing the co-operation of the three universities involved in this research.

Contents

List of Figures

List of Tables

Glossary of Terms and Abbreviations

Index Term	Description
AAR	Automatic artifact removal
ACA	Average of class accuracy, measuring the average of the percentage of correctly identified feature vectors for all classes
Accuracy of classification (AOC)	The percentage of correctly identified feature vectors (trials) in relation to the total number of feature vectors or trials.
Alpha	The frequency band of brain waves occurring between 8 and 12 Hz
ALS	Amyotrophic lateral sclerosis
ANN	Artificial neural network
Asynchronous BCI	A BCI associated with the self-paced movements of the user
BCI	Brain Computer Interface
BD	Bhattacharyya distance
Beta	The frequency band of brain waves occurring between 13 and 31 Hz
Bilateral	Occurring on, affecting, or acting in conjunction with parts on both sides of the body
Blind source separation	The separation of source signals from a set of mixed signals without information about the mixing process or the source signals.
BMPI	Beta movement performance/imagination
BP	Bereitschaftspotential
BPM	Beta pre-movement
CAR	Common average reference
COMB	Refers to the combination of TFSE and TFSM features
Contralateral	Occurring on, affecting, or acting in conjunction with a part on the opposite side of the body
CSP	Common spatial patterns
DC	Direct Current (refers to voltage that has an oscillating frequency

	close to or equal to zero)
Delta	The frequency band of brain waves occurring between 0 and 4 Hz
Dependent BCI	A BCI where the generation of brain activity is dependent on the body's natural output pathways
Discrete wavelet transform	This is a time frequency signal analysis technique using sampled wavelets
Dynamic movement	Related to the force, speed or energy of motion
ECoG	Electro-corticography (measured from the exposed surface of the cerebral cortex of the brain and not from the scalp as in the case EEG)
EEG	Electroencephalogram/ Electroencephalography/ Electroencephalographic
EMG	Electromyogram/ Electromyography/ Electromyographic
EOG	Electro-oculogram
ERD	Event-related desynchronisation
ERP	Event-related potential
ERS	Event-related synchronisation
FE	Finger extension
FF	Finger flexion
FMDI	Five movement differentiation investigation
FN	False negative
FP	False positive
Gabor transformation	A time frequency signal analysis technique that makes use of the Gaussian function and the Fourier transform
Gamma	The frequency band of brain waves occurring above 31 Hz
ICA	Independent Component Analysis
ICs	Independent Components
Imag	Imaginary
Imagined movement	Where a user/subject imagines themselves performing a movement but does not perform it physically
Independent BCI	A BCI where the generation of brain activity is not dependent on the body's natural output pathways, but rather on the user's intent
Ipsilateral	Occurring on, affecting, or acting in conjunction with a part on the same side of the body
Isometric plantarflexion	A movement of the foot which attempts to increase the angle between the front part of the foot and the shin (similar to depressing an automobile pedal), but without any movement due to an immovable resistance against the sole of the foot.
ITV	Inter-trial variance method of calculating non-phase locked ERD/ERS
Kinematic movement	Related to the type of physiological movement
LH	Left hand
M1	Primary motor cortex

MD	Mahalanobis distance
MLP	Multilayer perceptron
MMPI	Mu movement performance/imagination
MPM	Mu pre-movement
MRCP	Movement-related cortical potential
Mu	The frequency band of sensorimotor waves occurring between 8 and 12 Hz
Offline	Refers to methods where brain activity is recorded and analysis is done on the recordings
Online	Refers to analysis that is done as brain activity is recorded i.e. in real-time
Orthosis	An orthopaedic device that supports or corrects the function of a limb or the torso.
PCA	Principle Component Analysis
PMA	Pre-motor cortex/area
Pronation	Rotation of the forearm and thus the hand towards the centre of the body (pronation of the hand)
Prosthesis	An artificial device or extension that replaces a missing body part.
Real movement	Where a movement is executed or performed physically
Rebound rate	The rate at which the MRCP rebounds from its negative level (BP) after movement or imagination onset.
Reinnervation	The operation of grafting a viable nerve to restore the nerve supply of an organ or paralyzed muscle.
RH	Right hand
RLI	Right vs. Left investigation
Self-paced	Voluntary control by the user of the timing of actions
Single-trial	A singular occurrence of an event, such movement imagination of a limb, which is contained within one trial. Single-trial analysis involves examining neural patterns in each trial individually.
SL	Surface Laplacian
SMA	Supplementary motor cortex/area
SNR	Signal-to-noise ratio
Somatotopy	The correspondence of receptors in regions or parts of the body via respective nerve fibres to specific organised, functional areas of the cerebral cortex
Supination	Rotation of the forearm and thus the hand away from the centre of the body (supination of the hand)
Synchronous BCI	A BCI associated with movements which are initiated by external cues and not according to the voluntary intention of the user
Targeted muscle reinnervation	A method where the original nerves of the chest muscle or upper arm are cut or deactivated. The chest muscle or upper arm muscle, which is inactive due to the lost of the arm, is reinnervated with residual nerves of the amputated arm. The chest then provides an amplified source of motor commands from the arm nerves in the form of EMG, which can be used to control a

	motorised prosthetic arm.
TF	Time-frequency
TFSE	Used to refer to the time-frequency spectral features based on mu and beta ERD/ERS
TSFM	Used to refer to the time-frequency spectral features based on delta MRCP
Theta	The frequency band of brain waves occurring between 4 and 7 Hz
TN	True negative
TP	True positive
TR	Tripod pinch
Unilateral	Occurring on, affecting, or acting in conjunction with parts on one side of the body
WE	Wrist extension
WF	Wrist flexion
WFMI	Wrist vs. Finger movement investigation

Chapter 1

Introduction

1.1 Introduction

Consider the lifestyles of people who have lost an arm or hand in an accident or through an amputation or who have lost the control of their hand through a stroke or a spinal cord injury. Now consider the difficulties that such people must endure on a daily basis: they can no longer perform hand gestures, grasp and release a glass of water or write with a pen. Such individuals can greatly benefit from technology that can return some of the essential functionality of the hand by allowing the performance of the basic hand movements involved in the daily activities mentioned above (Section 1.2 elaborates upon these basic hand movements). A neurally controlled prosthetic hand is a possible solution for an amputee, whereby neural commands are rerouted from the brain to actuators in the prosthetic hand [1]. Similarly, an orthotic hand can be used to return basic hand movements to those who have suffered from spinal cord injuries or strokes and consequently lost the use of their arms.

This chapter provides basic background on different solutions for the neural control of prosthetic/orthotic hands and highlights some of their key challenges. The use of a brain-computer interface (BCI) based on electroencephalogram (EEG) is a safe and cheap solution that can address some of these challenges and can be applied to

amputees and victims of strokes and spinal cord injuries. This solution presents the problem of efficient, reliable EEG interpretation that will allow the control of a multi-functional prosthetic/orthotic hand capable of performing essential hand movements. This research aims to address this problem in part by investigating the possibility of EEG interpretation for five essential hand movements in a controlled laboratory experiment.

1.2 Hand Movement Selection

Five essential hand movements are chosen to allow people who have motor impairments of the hand to perform simple daily tasks. Considering the movements that patients learn during motor rehabilitation [2][3], five hand movements providing essential functionality are considered i.e. wrist extension, (WE), wrist flexion (WF), mass finger extension (FE), mass finger flexion (FF) and the tripod pinch (TR). These are shown in Figure 1.1 and occupational therapists consider these to be the most essential hand movements [2][3][4].

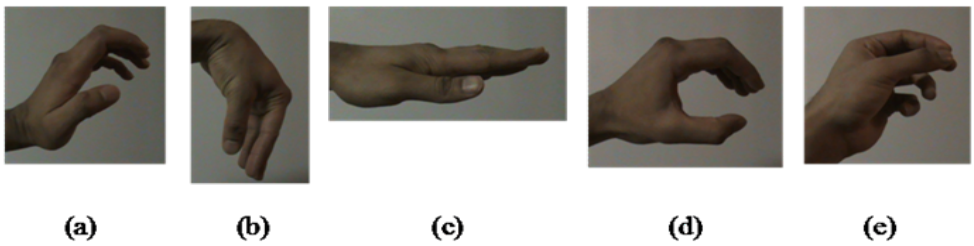

Figure 1.1: Most essential hand movements from a rehabilitation perspective: (a) wrist extension (WE), (b) wrist flexion (WF), (c) mass finger extension (FE), (d) mass finger flexion (FF) and (e) tripod grasp/pinch (TR). The tripod grasp is finer and more complex than the other movements

WE and WF provide a person with basic overall movement of the entire hand and in turn enable the performance of hand gestures such as waving. WF and WE facilitate the stability, positioning and load control of the hand, which in turn are essential for grasping strength and finer finger movement control [2][5]. FF and FE respectively allow the basic grasping and voluntary release of objects (such as a drinking glass) [3]. Training patients during rehabilitation to perform pinches such as the tripod pinch

stimulate finer hand motor skills and allow them to perform activities such as buttoning or writing with a pen [5].

1.3 Current Prosthetic or Orthotic Solutions

In order to allow the execution of the five essential hand movements the prosthetic or orthotic solution requires: 1) a physically suitable, mechatronic artificial device capable of sufficient degrees of freedom to perform the five different movements and 2) an efficient control system that can interpret the user's intention to perform one of the five movements and consequently execute the artificial device accordingly [6]. This is a challenging task since the human hand is an adaptable and complex system with a large number of degrees of freedom, sensors, actuators and tendons and a complex control system [6]. Despite these complexities, however, minimal effort is required by a person to use it for daily activities [6].

In contrast, current prosthetic and orthotic hand solutions are far from providing the capabilities of the human hand [6][7]. Commercially available prosthetic hands, such as the Otto Bock SensorHand [8], do not provide efficient grasping functionality [6][9]. Current prosthetics solutions also require a large amount of training, adjusting and concentration during use to enable a few degrees of freedom [6][9][7]. Other robotic and anthropomorphic hands can provide more degrees of freedom, but are heavy and bulky and are hence not suitable as a prosthetic [9]. The use of microactuators for example, in a complete redesign of the prosthetic hand could provide a lighter artificial device with more degrees of freedom and efficient grasping functionality [6].

However, with more degrees of freedom and improved functionality, efficient neural control still remains a limiting factor [6]. The processing of neural signals required for prosthetic/orthoctic hand control is challenging (as explained in Section 2.3) [1][9][10]. Hence, complex computational techniques and algorithms are required to detect, extract and translate relevant movement-related information from the neural signals [10][11][12] (see Chapter 5 and Section 2.4 for examples of such techniques). These methods are computationally expensive making real-time control more challenging [12]. Furthermore, the controller's accuracy decreases when the number

of movements to be identified increases [11]. Due to these challenges, most studies to date, which are related to neural prosthetics/orthotics, have focused the detection of simple hand movements [6][12]. However, some studies have attempted to allow more extensive control of more degrees of freedom [6][9][7] and this research contributes toward that effort.

1.4 Controlling of a Prosthetic or Orthotic Hand

A prosthetic/orthotic hand may be controlled mechanically by using a shoulder harness or by the movement of the elbow in the case of the WILMER elbow [13][14]. However these solutions are limited in functionality and provide unnatural control [15]. By connecting the prosthetic/orthotic hand more directly to the nervous system, it can be controlled in a manner similar to how a human hand is controlled [15]. In particular electromyography (EMG), electro-corticography (ECoG), and electroencephalography (EEG) can be use to infer control of a prosthetic/orthotic hand [13], provided that the relevant information can be extracted and translated [11][16].

Research efforts into EMG-based control of a prosthetic hand [6] have demonstrated the possibility of reliable, multifunctional control in real-time [7]. WE, WF, FE, FF and the TR are included in some EMG-based prosthetic hand studies [7][9] (the results of this study are shown in Section 7.5.1). Surface EMG does not require surgery and is an easily obtainable information source [6]. Although it requires external power, unlike mechanical harnesses, it does not hinder movement as some of them do [6]. Prosthetic control using this method, however, requires muscle control in the upper body, such as the upper arm or, in the case of targeted muscle reinnervation, the chest [6][15][17]. Hence this method cannot be applied in the case of complete paralysis, which may result from strokes or spinal cord injuries [13]. Another disadvantage of EMG-controlled prosthetic solutions is that adaptation to different levels of amputation is needed [15]. The use of ECoG or EEG as a source of control information could overcome these problems. Since ECoG and EEG deal with the brain directly, which produces all the control information for hand movement, it is hypothesized that they possess more control information than EMG. This may allow

the control of more advanced hand movements as neural understanding and interpretation improves.

Compared to EEG, ECoG (like other invasive techniques) has been shown to provide a better signal-to-noise ratio (SNR), overall better results and superiority in hand movement classification problems [10][18] to the point where individual finger movements can be discriminated [19][20]. Studies using the Braingate neural interface, which uses ECoG, have shown that tetraplegic patients can operate simple computer software without training [21]. However, non-invasive methods, such as EEG, have the advantage of being cheaper, safer and more practical for patients and researchers [22]. Currently only EEG can support rapid communication with relatively simple and inexpensive equipment that is non-invasive and requires no neurosurgical procedures (such as for ECoG). Hence EEG is favoured by many BCI researchers and is used in this research as a source of neural information [10].

1.5 Brain-Computer Interface as a Solution

Based on the assumption that neural activity can be translated into intended movements, a BCI can interpret the neural motor control signals for the five selected hand movements via EEG [1]. The user's intention to perform a particular type of hand movement can then be realized by actuating a prosthetic or orthotic hand accordingly [1].

Although EEG represents brain activity, there are several challenges associated with extracting relevant information from EEG. These challenges are described in Section 2.3. It is thus necessary to improve on the interpretation of EEG with the purpose of improving prosthetic/orthotic hand functionality. Hence this research investigates the possibility of improved EEG interpretation for five essential hand movements.

1.6 Problem of Interpretation

The incomplete understanding of the neural signals that control hand movements and the need for the improvement of EEG interpretation toward prosthetic/orthotic hand control remain challenging areas in BCI and prosthetic/orthotic hand research

[1][23][12]. Hence this research is directed towards improving on the interpretation of the neural information, encapsulating movement intent, taken from EEG, using a BCI, in order to facilitate efficient, multifunctional control of a prosthetic/orthotic hand.

In terms of the bigger picture, the BCI that controls the prosthetic/orthotic device requires the ability to differentiate between the EEG associated with each movement type in order to execute the user's intention to perform one of the selected movements. Currently, to the best of the author's knowledge, no known BCI research has been undertaken using the combination of WE, WF, FE, FF and the TR and such efforts are deduced to be minimal. Some success, however, has been shown in differentiating EEG for different wrist movements (which include extension, flexion and rotation) [12][24][25]. Current BCI literature is examined more extensively in Chapter 3. The questions thus arise as to whether EEG can be interpreted to differentiate these five hand movements, to what degree is this interpretation possible and whether this interpretation is possible for imagined movements as well? Furthermore, what methods can be used to evaluate this?

1.7 Procedure to Solve the Problem

The research is divided into three sub-investigations:

1. Firstly, the different types of movements will be combined for each hand and differentiation between right and left hand movements will be verified.
2. The possibility of differentiating between groups of wrist and finger movements will be examined in the second investigation.
3. The third investigation examines the possibility of discrimination between the individual five hand movements.

Motivation for the division into these sub-investigations is detailed in Chapter 4.

Considering that the neural control signals for different types of movements on the same hand originate from roughly the same area of the brain (see Section 2.2) [12] and the challenges associated with EEG interpretation (see Section 2.3 for details), the discrimination between the EEG for WE, WF, FE, FF and the TR is a complex task [12]. Independent component analysis (ICA) is a technique that has provided improved performance in the discrimination of EEG associated with wrist movements

and movements of other body parts [25][26][27][28] (shown in Section 3.4). It can be used to isolate signals originating from the motor control areas of the brain [29] and is hypothesised to be suitable for this research, which involves different types of wrist and finger movements.

The designed method is applied to all three investigations for real and imagined movements. ICA is used as a spatial filter to aid feature extraction. Time-frequency (TF) spectral features based on event-related (de)synchronisation (ERD/ERS) (referred to as TFSE) and movement-related cortical potentials (MRCP) (referred to as TFSM) are extracted. It is hypothesised that the combination of features from these two electrophysiological features could improve results [30]. Hence the individual and combined uses of both feature types are investigated and compared. Mahalanobis distance (MD) clustering and artificial neural networks (ANN) are used to classify the extracted EEG features into different classes of movement. The results of the classifiers are compared.

1.8 Conclusion

This chapter has introduced two research fields i.e. prosthetic/orthotic arm control and brain-computer interfaces. The functional limitations of current prosthetic solutions are due to incomplete understanding of the neural signals that control hand movements and it is thus necessary to improve on the interpretation of the neural signals that control essential hand movements. Five essential hand movements are thus selected from a rehabilitation perspective in order to provide basic hand functionality to aid daily activities. The benefits of using an EEG-based BCI to control a prosthetic/orthotic hand in order to return essential hand movement functionality to those who have motor impairments (specifically amputees and victims of strokes and spinal cord injuries) has been described.

The research is directed towards the improvement of EEG interpretation to allow a prosthetic hand to perform these basic movements in real-time. However, no BCI research exploring these movements has been found. Hence it is necessary to first determine the level of possible discrimination of the EEG for these five movements in an offline and synchronous manner. This research is a pilot study to investigate this

possibility in healthy test subjects on a single trial-basis. ICA may be advantageous in the complex task of extracting suitable movement information from EEG. This information is derived from electrophysiological sensorimotor features, i.e. ERD/ERS and MRCP, where the combination of the two feature types may improve results. The research is divided into three investigations to align the research with the literature and to investigate the level of possible discrimination of hand movement type. The investigations aim to answer the following questions: can a synchronous BCI use ICA in conjunction with TFSE and TFSM features to allow single-trial, offline differentiation of EEG patterns for real and imagined 1) left and right hand movements, 2) wrist and finger movements and 3) five types of hand movements viz. WE, WF, FE, FF and the TR? In summary, does the selected method allow improved offline and synchronous EEG interpretation, such that different wrist and finger movements on the same hand can be differentiated?

The next chapter provides some basic background knowledge and relevant terminology pertaining to this research. Thereafter, the novelty of the problem of the research will be shown along with the benefit of solving the problem before it is clearly defined. The design and implementation of the method used is documented and the consequential results are thereafter presented and discussed. Future work is briefly discussed and the research is concluded.

Chapter 2

Background

2.1 Introduction

Brain-computer interface research is a multidisciplinary and interdisciplinary field, which involves and integrates researchers from different fields including neuroscience, engineering, physiology, psychology, computer science, rehabilitation and health-care [10][31]. Thus in order to contextualise the research, some basic background is provided in this chapter. This includes necessary terminology, relevant neural anatomical and physiological knowledge and an overview of brain-computer interfaces.

2.2 Sensorimotor Neuro-Anatomy

The areas of the brain associated with movement are the primary motor cortex (M1), the premotor cortex (PMA) and the supplementary motor cortex (SMA) [32]. They all play different roles in movement control and their locations are shown in Figure 2.1 [32]. Control by these regions can be contralateral or bilateral [32].

As the name suggests, the primary motor cortex is the main area of the brain responsible for motor control, which is apparent from the critical motor deficits that follow its destruction [32]. M1 contralaterally controls basic movements such as flexion of the finger or movement about a single joint [32]. As shown by Figure 2.1, it

occupies a tapering strip in the precentral gyrus, which corresponds to Brodmann's area 4 [32]. It lies anterior to the Rolandic fissure or central sulcus and is also referred to as the Rolandic region [33]. M1 is spatially organised into divisions that are each directly responsible for the control of a specific part of the body [32]. This is referred to as a somatotopic arrangement which can be represented as a distorted image of the human body known as the homunculus [32]. This is shown in Figure 2.2 [32]. Finer motor skills of a particular part of the body, such as the hand, require a larger number of neural connections and hence a larger area on the homunculus of M1 [32]. From Figure 2.2 it is clear that the control areas for the wrist and finger are located in close proximity, while the control regions for the hand, foot and tongue are spatially distant. Electrodes superficial to this region according to the 10-20 system are Cz, C1, C2, C3, C4, C5 and C6, which correspond to electrodes 129, 31, 106, 37, 105, 42 and 104 in the EGI system [34][35][37]. Refer to Figure 5.3 in Section 5.2.1 for the electrode positions of the 128-channel 10-20 and EGI systems

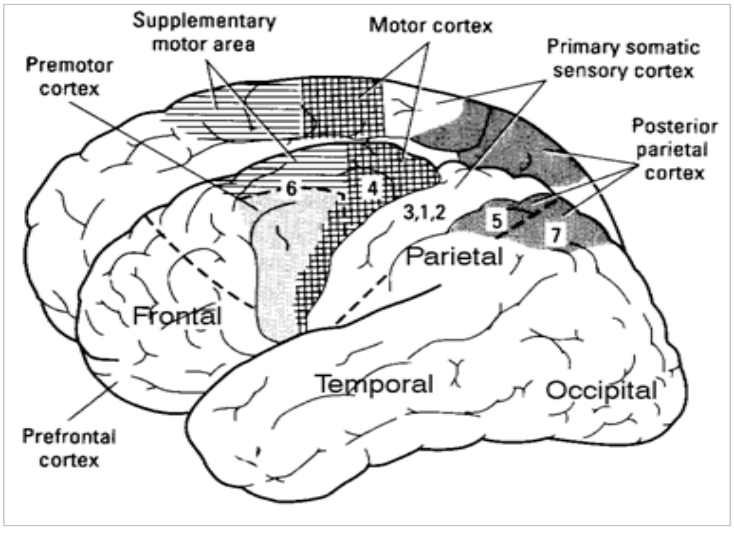

Figure 2.1: Location of motor areas of the cerebral cortex. The numbers are the labels of the Brodmann areas [32].

The premotor cortex plays a role in the planning, selection and execution of movements from external cues [36] (refer to Figure 5.2 for the timing of the external cues used in this research). It is located in Brodmann's area 6 [32] as shown in Figure 2.1. The PMA also contains a homunculus, but the somatotopy is not as specific as for M1 [32]. This has been shown by electrical stimulation, which results in the

movement of a group of muscles with the PMA as opposed to singular muscles with M1 [32]. Electrodes superficial to this region according to the 10-20 system are FC1, FC2, FC3, FC4, FC5 and FC6, while the corresponding EGI electrode numbers are 21, 119, 30, 117, 35 and 112 [34][35][37] (refer to Figure 5.3).

In contrast to the PMA, the SMA activates when performing self-initiated movements, such as movements from memory [36]. The SMA can be divided into the pre-SMA and SMA proper, where the former is more active when learning new movement sequences, while the latter is more active when the movement is automated and performed from memory [36]. The SMA also shows activity during movement preparation [36] and is involved in the performance and imagination of more complex tasks, such as those that require two hands [32]. This is supported by the fact that electrical stimulation of the SMA causes bilateral muscle activation [32]. The SMA is located in Brodmann's area 6, anterior to the foot control region of M1 [32]. This is shown in Figure 2.1. Electrodes superficial to this region according to the 10-20 system are FC1, FC2, and FCz, while the corresponding EGI electrode numbers are 21, 119 and 6 [34][35][37] (refer to Figure 5.3).

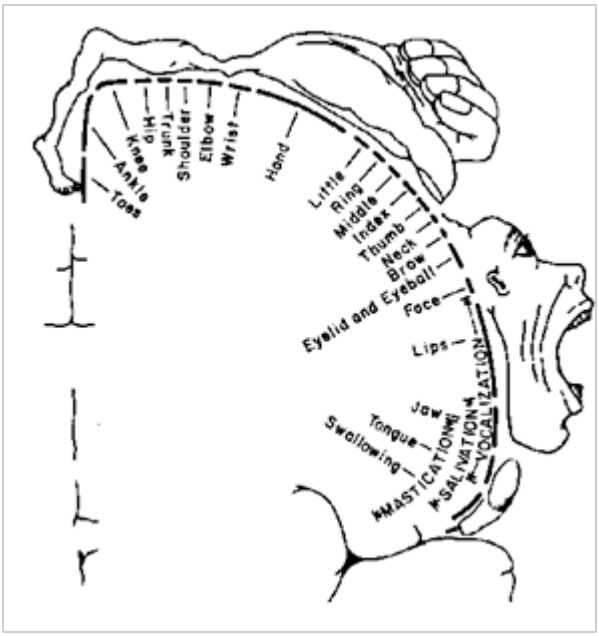

Figure 2.2: Somatotopy of human primary motor cortex. The size of a given part of the homunculus is approximately proportional to the size of the area dedicated to controlling that region [32].

Since this research is based on performed and imagined hand movements, which involve finger and wrist movements, the wrist, hand and finger control regions of M1 are of main interest. This research incorporates a synchronous BCI (see Figure 5.2 and Section 2.5) and aspects of movement intention. The SMA shows an association with intended movements and the PMA with externally-stimulated movements [32][36]. Hence these areas are also considered as sources of movement-control information.

2.3 Electroencephalogram

The electroencephalogram (EEG) is comprised of electrical potentials originating from multiple sources i.e. neuron clusters [16]. The electrical potentials combine to form a superposition of topographical maps on the scalp, which can be measured by scalp electrodes [38]. Electrical signals of interest in the brain can be extracted from the EEG [38]. Since the early 1900's, EEG has been used mainly to investigate neurological disorders and to investigate brain functions [10]. Recent years have shown an interest in the use of EEG to decipher intended movements, however, the task of extracting information containing movement intent is not trivial [10].

The brain presents a complex geometry and involves numerous simultaneously-active neural processes, which are generated by approximately 100 billion central neurons [10][38]. The limited number of EEG measurement sites (even with high resolution EEG, e.g. 128 surface electrodes) results in a considerable mixing of these information sources from all over the head at each electrode [10][38][39]. With ECoG, neural signals are measured directly from the cortical surface of the brain [18]. In contrast, with EEG, neural signals must pass through the high electrical resistance of the scalp and skull, which results in spatial blurring [40]. EEG electrodes are also more widely positioned than ECoG electrodes [21]. All the above contribute to the low spatial resolution of EEG, which in turn contributes to its low SNR [10][38][39].

EEG signals are small (in the μV range), difficult to measure and are easily contaminated by artifacts originating from muscle movement, eye movement and blinks and noise from the mains power supply [10][41]. Consequently it becomes difficult to detect and isolate weak signals (< 10 μV), such as sensorimotor signals,

due to interference by stronger signals (> 30 μV) from artifacts and non-sensorimotor neurons, such as the alpha rhythm from the visual cortex [10]. These interferences also result in a low SNR for EEG [10]. Furthermore, neural signals vary with regard to time, circumstance and the individual, which adds to the challenge of extracting and learning the neural patterns associated with movement control [10].

However, clinical research has increased the understanding of EEG signals and numerous studies have shown relationships between EEG and imagined movements [10][42][43][44]. Inexpensive computer equipment now supports the required computational demands for real-time EEG signal processing [10]. The latter two factors make it possible to use EEG to perform simple functions, such as basic prosthetic/orthotic hand control [10] in a controlled laboratory environment.

2.4 Spatial Filters and Independent Component Analysis

A spatial filter is a technique that combines data from two or more locations (electrodes) in order to enhance the focal activity from spatially local sources and reduce those from widely distributed sources, hence improving the SNR of EEG [16][10]. Spatial filtering techniques include common average referencing (CAR), surface Laplacian (SL), common spatial patterns (CSP), principle component analysis (PCA) and independent component analysis (ICA). Some advantages of ICA are discussed and a brief background on ICA pertaining to its use in BCI is presented.

As in the case of PCA and CSP, ICA determines the weighting of the channels from the data [10], i.e. blind source separation, while CAR and SL combine channels or electrode locations linearly to create a set of weights that is independent of the underlying data [10]. SL emphasizes the radial component of the neural activity from sources located directly below each recording electrode [10]. In comparison, ICA is able to detect radial and tangential sources and thus may be advantageous over SL [10][45].

Defined statistically, ICA is a method aimed to find a linear representation of non-Gaussian data in the form of constituent components, which are as statistically independent as possible [46]. Using ICA, measured signals consisting of a linear

mixture of statistically independent source signals, such as EEG, can be decomposed into their fundamental underlying Independent Components (ICs) thus extracting the original source signals [29][46]. Access to the mixture of neural processes is available in the form of EEG and ICA allows the extraction of the original components of brain activity [46] or estimation thereof. ICA was first applied to EEG by Makeig *et Al* [41] in 1996 and is now widely used in the EEG and BCI research community [29][41]. It is commonly used to remove artifacts, but has also proven useful in separating biologically plausible brain components whose activity patterns relates to behavioural occurrences [41]. In terms of a sensorimotor BCI, ICA can in principle be used as a spatial filter to isolate activity over the sensorimotor cortex [10][29]. ICA can be implemented using a number of algorithms, such as infomax, JADE and FastICA [41][46].

2.5 Brain-Computer Interfaces

Research into the relationship between neural signals and limb movement has led to the development of brain-computer interfaces [1]. By using EEG or other electrophysiological methods, a brain-computer interface (BCI) provides a communication channel from the brain to the external world, circumventing the natural neuro-muscular pathway [10][11]. BCI systems aim to provide a means of communication and control for people who suffer from neuromuscular disorders or motor disabilities, such as spinal cord injuries, brainstem stroke, multiple sclerosis, Amyotrophic lateral sclerosis (ALS) and limb amputations [10][11][16]. BCIs could allow the use of assistive devices such as simple word processors, speech synthesizers, wheelchairs, prosthetics and orthotics in order to improve the quality of life of such individuals [16].

Recent studies have shown the ability to partially decipher movement intent or movement imagination from neural signals [10]. Motor impairments may change the motor cortices of the brain and thus alter the neural activity associated with movement imagination. Turner *et Al* [47] suggests that motor cortex rewiring occurs in the case of spinal cord injuries and to a lesser degree in the case of limb amputations, but that activity in the motor areas is still present. Hence it is possible that people who have lost motor capabilities of their hand through amputation or spinal cord injuries can

imagine hand movements in order to initiate prosthetic/orthotic actuation [11][16]. BCIs are ultimately intended to aid those with motor impairments, yet in this research data was captured from healthy test subjects. Further experiments would need to be undertaken to establish the effectiveness of the proposed system on impaired patients. This is however beyond the scope of this research.

BCIs help users interface with the world using an alternative method and can be dependant or independent [10]. A dependant BCI relies on the activity in the brain's natural output pathways in order to generate neural activity, while an independent BCI relies on the user producing voluntary neural activity to actuate an external device without the use of the brain's natural output pathways [10]. The latter is more suitable for the control of a prosthetic/orthotic hand since the user's voluntary mental intention is used to control the assistive device [10]. BCI analysis can also be done online or offline [10]. In the case of offline analysis, data is recorded from several test subjects and techniques are applied to the data thereafter [10]. Methods that appear promising offline are validated by extensive online testing, where the user's/subject's neural signals are analyzed in real-time [10][12].

BCIs can operate in an asynchronous or synchronous manner [48]. For synchronous or cue-based BCIs the user is instructed when to perform a task and the computer is in control of the timing, whereas in the case of an asynchronous or self-paced BCI, the user decides when to perform the task [48]. Asynchronous BCIs are more complicated than synchronous ones [48]. They need to differentiate between control states (when the user intends to control the BCI) and non-control or idle states (when the user is engaged in other activities not related to the intention to control the BCI, such as thinking or daydreaming) [48]. They also need to decipher between different types of control states in order to actuate the different functions of the external device [48]. A synchronous BCI only needs to perform the latter since the control states are time-locked to and marked by the cues [48] (see Figure 5.2 for an example of external cues). Hence synchronous BCIs are suitable for laboratory investigations (such as those contained in this research) since they allow the exploration of time-related features used to design a suitable feature extraction and translation method [48]. Refer to Sections 5.2.5 and 5.2.6 as well as Appendix B for feature extraction methods. A successful synchronous BCI can then be adapted to an asynchronous BCI, which is

suitable for real world applications [48] such as the control of a prosthetic/orthotic hand in everyday life [49].

The main components of a BCI are shown in Figure 2.3 [16][10]. The signals are captured either by invasive (ECoG) or non-invasive (EEG) methods and thereafter digitized [10]. Refer to Sections 1.4 and 2.3 for more information on these methods. After acquisition, the digitized signals enter the signal enhancement phase to improve the SNR [16]. The signals are pre-processed: they are usually filtered and artifacts that could contaminate the required information are removed [16][10]. Spatial filters are usually applied to enhance the signals originating from the relevant electrophysiological sources [16][10]. Thereafter features are extracted from these sources and the best features are selected to reduce dimensionality [16]. These are the features that ideally capture the user's control commands [10]. The feature translation algorithm classifies the selected features into logical commands that can be passed to the device controller [10]. The device controller actuates the external device, such as a prosthetic/orthotic hand, in order to perform the user's intent [16].

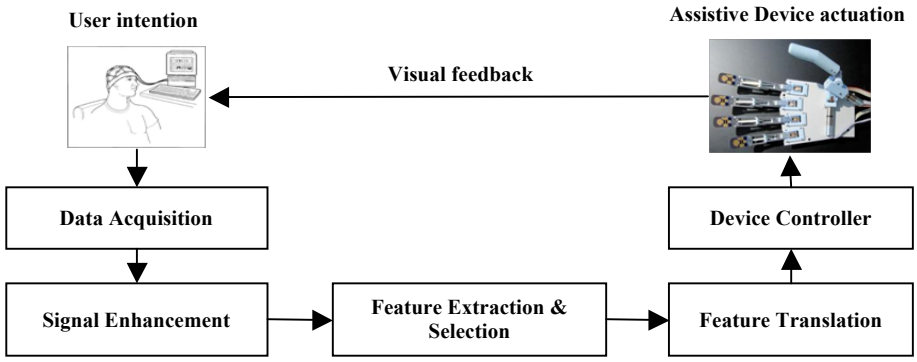

Figure 2.3: Model of a sensorimotor BCI used for communication to a prosthetic hand.

Results and analysis in BCI research are either based on multi-trial or single-trial techniques, where a trial is an EEG time-sequence containing an individual instance of a stimulus or task, such as a single hand movement (see Figure 5.2 as an example) [50][51]. Most of the literature reviewed (in Chapter 3) employs single-trial methods which are more suitable for BCI applications since they facilitate real-time BCI

operation [12][51]. The challenges lie in dealing with the large inter-trial variability in EEG signals and dealing with the fact that the desired patterns are mostly hidden in the background noise [50]. A method to try to reduce the effects of inter-trial variation is to use an average template created from multi-trial results to try to identify the waveform from a single-trial dataset as done in [50] and [52]. This can involve the analysis of event-related potential (ERP) time-series waveforms from individual events [50]. Averaging over many individual trials, which are grouped according to some relevant measure such as movement type, allows the pattern to emerge from the average ERP [41][50][51].

2.6 Electrophysiological Signal Features

BCIs that deal with motor functions or sensory inputs of the body deal with the sensorimotor cortex of the brain. They are thus called sensorimotor BCIs and are suitable for the control of a prosthetic/orthotic hand. The two most distinctive electrophysiological signal features physiologically related to movement performance or movement imagination are sensorimotor rhythms (SMR) or ERD/ERS and movement-related cortical potentials (MRCP) [12]. Hence they are both used in this research. Although MRCP and SMR emanate from the motor cortices of the brain, they show differences in their spatiotemporal patterns and thus represent different and independent aspects of sensorimotor cortical processes [30][53][54]. A brief description of each signal feature type follows.

2.6.1 Event-related desynchronisation and synchronisation

When people are not engaged in processing sensory inputs or producing motor outputs while awake, the sensory and motor cortices produce EEG activity in the 8-12 Hz range [10]. This is called the mu rhythm and has been shown to be present in most adults and related to concurrent sensory or motor processes [10]. The mu rhythm is usually accompanied by the beta rhythm ($13 - 30$ Hz), which can present independent EEG features [10]. Since these sensorimotor rhythms are associated with the brain's normal motor output channels, prominent features are usually extracted from the mu and beta frequency ranges [16][10]. Some studies, however, have also explored the use of SMR from the delta, theta and gamma bands [22][25][55] since

there is evidence of their relevance to movement [56] (some of this is explained further in Section 3.3). This research focuses on sensorimotor rhythms in the mu and beta ranges.

Events, such as sensory stimuli or motor actuation, produce frequency specific changes in the sensorimotor rhythms, which in general consist of increases or decreases in power in these frequencies [56]. These changes are a result of a change in synchrony of the underlying neurons [56]. The rhythms are synchronized when no sensory inputs or motor outputs are being processed [16][10]. Voluntary movement or preparation for movement results in a decrease in the mu and lower beta rhythms, referred to as event-related desynchronisation (ERD) [16][10][57]. It begins in the contralateral rolandic region about 2 s prior to movement onset and becomes bilaterally symmetrical just before movement execution [16][56]. Event-related synchronization (ERS) occurs after movement when the rhythms increase again [16][10][57]. Post-movement beta ERS occurs about 1 s after movement in contralateral M1 [56]. It is a robust oscillatory brain signal with a relatively good signal-to-noise ratio and is prevalent in most test subjects [56]. More importantly, contralateral ERD and ERS occur during imagined movements as well, making them suitable for independent BCIs [10] (see Section 2.5). In terms of controlling a prosthetic/orthotic hand, the user can voluntarily imagine performing a particular hand movement in order to produce the neural ERD and ERS patterns that correspond to that hand movement.

The terms SMR ERD and ERS typically refer to the respective amplitude (and hence power) attenuation and enhancement of EEG rhythms in the mu and beta bands [58] originating from the motor cortex. The use of the terms ERD/ERS in this research refers to the use of mu and beta frequencies, unless otherwise specified. Although event-related trials are time-locked to the event, they can either be phase-locked or non-phase-locked [56][58]. Averaging over all trials, as with an ERP, enhances the phase-locked components, which can mask the non-phase locked components of the EEG rhythms; hence methods of ERD/ERS calculation are available to overcome this [56][58]. There are two methods for calculating the event-related power changes i.e. the classical ERD or power method (P) and the inter-trial variance (ITV), shown by Equations 2.1 and 2.2 respectively [58].

$$P_{(j)} = \frac{1}{N}\sum_{i=1}^{N} x_{f(i,j)}^2 \quad 2.1$$

$$ITV_{(j)} = \frac{1}{N-1}\sum_{i=1}^{N}\left(x_{f(i,j)} - m_{f(i,j)}\right)^2 \quad 2.2$$

For both methods each trial has been bandpass filtered and is denoted by $x_{f(i)}$. N refers to the number of trials, i denotes the trial number, j the sample number and $m_{f(j)}$ is the mean over all bandpassed trials at the j^{th} sample. The power method computes the power change for phase-locked and non-phase-locked components, while only the non-phase-locked are computed using the ITV method [58]. ERD and ERS are defined as the respective percentage change of power decrease and increase relative to a reference or rest period [56]. The ERD at each sample is given by Equation 2.3, where $A_{(j)}$ is either $P_{(j)}$ or $ITV_{(j)}$ and R is the average of $A_{(j)}$ over the reference period [58].

$$ERD_{(j)} = \frac{R - A_{(j)}}{R} \times 100\% \quad 2.3$$

The analysis of ERD/ERS patterns is usually done over multiple trials as shown by equations 2.1 and 2.2. [56][51]. For single trials, the relative changes in power over time within mu and beta frequency sub-bands can be calculated using time-frequency (TF) techniques [16]. TF techniques represent changes in EEG with regard to time and frequency and are used to analyze the time-varying content of EEG [16]. They show improvements over ordinary frequency-based techniques [16] and have been shown to be effective with the analysis of single trial EEG [59]. Some examples of TF techniques used for single-trial EEG analysis include discrete wavelet transforms and discrete Gabor transforms [16][24][25][59].

Commonly used electrode locations for the extraction of ERD/ERS features for hand (and sometimes foot and tongue) movements are C3, C4 and Cz according the 10-20 system, which correspond to regions over M1 (see Section 2.2 for anatomical information and Figure 5.3 for electrode positioning) [44][37]. The corresponding GSN-128 electrode numbers are 37, 105 and 129 [35].

2.6.2 Movement-related Cortical Potentials

Another type of electrophysiological feature emanating from the motor cortex is the movement-related cortical potential (MRCP) and the pre-movement stage is a slow moving potential [24][30][60]. Shibasaki *et Al* [53] suggest that movement characteristics, such as speed, precision and repetition can influence the amplitude and time course of MRCPs. Other studies have linked MRCPs to force parameters in movement [12][61][64]. For further information of these studies refer to Section 3.3.

The pre-movement stage of the MRCP is associated with an event-related negativity referred to as the Bereitschaftspotential (BP) that occurs 1 - 2 s before the onset of movement [10][24][52][60]. According to Shibasaki *et Al* [53], the BP can be divided into two sections, named the early BP and late BP, the latter having a steeper negative slope [24][62]. The early BP starts about 2 s before movement onset in the pre-SMA and SMA proper and thereafter in the PMA with a maximum at the centro-parietal midline [53] (refer to Figure 2.1). It appears bilaterally and without any specific somatotopic organization in the pre-SMA, but with relatively clear somatotopy bilaterally in the PMA and SMA proper [53]. The late BP occurs with precise somatotopy in contralateral M1 and lateral PMA from approximately 400 ms before movement onset [53]. The motor potential (MP) occurs just prior to movement (approximately 10 ms) and is localised with precise somatotopy in the contra-lateral motor cortex (M1) [53]. The pre-motor stage is followed by a rebound after the movement or imagination onset and is referred to as the post-movement potential [24].

Traditional methods for extracting features based on MRCP patterns, particularly for movement disorder analysis in clinical applications, involve time-series analysis [53], where the slope of the BP, the rebound rate, the latency and peak amplitudes can be used to form features [24][54][63]. Such analysis usually involves the detection of typical or atypical patterns in average MRCP ERPs after averaging over 100's of trials [51][53]. Some studies, however, have used time-frequency techniques to extract EEG patterns from MRCP. The discrete wavelet transform was used on MRCP signals to successfully discriminate different levels of torque development in isometric plantar flexion in [64] and [70] (refer to Section 3.3 for more information on

the success of these studies). Vuckovic and Sepulveda [25] used the discrete Gabor transform to extract features for imagined wrist movement classification and found that features in the MRCP frequency range were most prominent.

Electrode locations commonly used for MRCP analysis covers regions between frontal and central sites including Cz, FCz, FC3, FC4, C1, C2, C3 and C4 in the 10-20 system [50][53][64] (see Section 2.2 and Figure 5.3). The corresponding GSN-128 electrode numbers are 129, 6, 30, 112, 31, 106, 37 and 105 [35].

2.7 Conclusion

Some background knowledge on sensorimotor anatomy, EEG, spatial filters, BCIs and sensorimotor electrophysiological sources of information is outlined in this chapter. This is relevant information needed to contextualise the problem to decipher the EEG for different hand movements using a sensorimotor BCI. The next chapter explores relevant BCI literature so as to identify the problem of the research.

Chapter 3

Literature Review

3.1 Introduction

The previous chapter provides an overview of the necessary background knowledge for sensorimotor BCI research. This chapter explores related sensorimotor BCI literature in order to find an area that has not yet been explored. The types of movements explored for interpretation by BCIs are discussed and the combination of WE, WF, FE, FF and the TR are deduced to be novel to BCI literature to the best of the author's knowledge. Due to nature of the problem, techniques such as ICA and ERD/ERS and MRCP feature combination are explored. The way the research complements and extends the literature is explained and possible benefits are discussed.

3.2 Exploring Different Movement Types

The use of a BCI to utilize EEG to extract information from the motor cortex of the brain in order to interpret movement imagination began in the 1990s [65]. This has led to numerous research efforts into the classification or differentiation of different motor tasks. These motor tasks consist of real and imagined movement tasks and can also differ in a kinematic (movement type) or dynamic nature (force or speed).

The discrimination between the EEG associated with right and left hand motor tasks

is common in sensorimotor BCI research. The choice for this type of discrimination is most likely due to the contralateral positioning of the hand control regions of M1 [32], which allows spatial discrimination between the left and right motor cortices. See Figure 2.2 to view the hand control region of M1. Different types of real and imagined, right and left motor tasks have been explored using a variety of techniques to improve classification rates. Pfurtscheller *et Al* [65] first investigated the possibility of right vs. left movement imagination discrimination on a single-trial basis in 1997. The discrimination between right and left imagined middle finger movements was investigated in [28], [42] and [66], while studies such as [59] used the movement of right and left index fingers. The use of right and left self-paced key finger presses was also used in some studies, such as in [28] and [50]. Navarro *et Al* [26] and Khan and Sepulveda [55] investigated the EEG discrimination between right and left wrist movements. Although different variations of hand movements were used by different authors, these problems all involve differentiating between the EEG information associated with the control the right and left hand or parts thereof. According to the classification review by Lotte *et Al* [11], the accuracy of classification (AOC) for right vs. left movement/imagery problems ranges between 60 % and 90 % and averages around 79 %.

Another common objective in sensorimotor BCI research is the discrimination between the execution or imagination of left hand, right hand, foot and tongue movements [44][67]. This can be considered an extension of the right vs. left hand classification problem when looking at the chronological order of publications by Pfurtscheller and associates [37][44][65][68][69][71] and by noting that the locations on M1 for the control of the four appendages are spatially distinct [32] (refer to Figure 2.2). Wang and James [29] used imagined right hand and right foot movements in an EEG classification investigation. Similarly, Blankertz *et Al* [39] used imagined right hand, left hand and right foot motor tasks and Neuper and Pfurtscheller [57] used imagined foot and hand movements in their investigation.

Studies aimed at discriminating various dynamic properties of movements are few [12]. Farina *et Al* [70] classified different levels and rates of torque development for real isometric plantar flexion of the right foot, while do Nascimento and Farina [64] performed a similar study for imagined isometric plantar flexion. The former reported

varying AOC rates between 50 % and 90 %, while the later reported an average maximum AOC rate of 82.6 %. A study by Slobonouv *et Al* [64] examined the interdependency of fingers associated with force-related tasks and showed that musicians exhibit improved control of and interdependency between their ring and index fingers over non-musicians. Logar *et Al* [61] studied the possibility of predicting different gripping forces of the hand using EEG, which was consequently shown to contain enough information for gripping force prediction.

Most current BCIs are effective when discriminating between two different limb effectors [12], but to date not much research has been done to discriminate between the EEG associated with different types of movements on the same hand [12]. Vuckovic and Sepulveda [25] investigated the possibility of classifying between different types of unilateral wrist movements i.e. extension, flexion, pronation and supination. Averaging the results for real and imagined movements, an overall AOC of approximately 72 % was obtained when discriminating between binary combinations of the four movement types. Gu *et Al* [24] investigated the classification between fast and slow variations of wrist extension and rotation and reported AOC rates of 79 % for the best binary combination of the movement tasks. It was the first study to compare classification accuracies in a kinematic and dynamic manner.

Classification of neural signals associated with different kinematic or dynamic movements on the same limb/hand is complex and challenging since these movements activate a similar area in the cortex of the brain (M1) [12][32][72] (refer to Figure 2.2). Successful discrimination of EEG for binary combinations of four different unilateral wrist movements [24][25] suggests that binary classification between other types of hand movements on the same hand (e.g. wrist vs. finger movements), using EEG, is possible.

The problem, however, becomes increasingly more difficult when considering more than two types of movement on the same hand in a multiclass problem since accuracy decreases as the number of classes increases [25][71]. Individual finger movement discrimination using BCIs based on ECoG [20][73][74] suggests that more advanced movement discrimination on the same hand is physiologically possible. This problem is significantly more challenging for EEG-based BCIs due to the noisy nature of EEG

and the difficulty with spatially-specific recordings [10][12] (see Section 2.3 for more challenges associated with EEG). A four-class BCI problem involving wrist movement imagination achieved an AOC of 78 % in one subject [75]. This study, however, classified between right and left wrist extension and wrist flexion i.e. binary classification on different limbs [75]. A multiclass, EEG-based BCI problem, involving five tasks i.e. movement imagination of the left hand, right hand, foot and tongue as well as a mental calculation task, showed an AOC of approximately 68 % in one subject [71]. According to a review on BCI classification by Lotte *at Al* [11], the average accuracies for two other multiclass problems, involving right and left hand movements, foot movements and tongue movements, range between 42 % and 63 % [71][99] (using the AOC). These results, along with the success of [24][25], suggests that it may be possible to discriminate EEG for different unilateral hand movements in a multiclass problem in at least one subject, provided that sufficient spatially-specific information can be extracted. Refer to Sections 2.4 and 3.4 on how ICA may be beneficial in this regard.

To the best of the author's knowledge, the combination of WE, WF, FE, FF and the TR (refer to Section 1.2 for details of these movements) has not been explored in BCI literature [12]. This is possibly due to most BCI studies focusing on inclusively aiding ALS patients, who favour simple communication above the return of hand functionality [76]. As a result, the author is unaware of studies concerned with the right vs. left EEG discrimination of the combination of these movements. Wrist and finger movement/imagery have been used in separated studies [24][25][26][42][50][55][66], but a studies have not been found, which attempt to differentiate between the EEG for finger and wrist movements or imagination [12]. Furthermore, the classification between EEG associated with WE, WF, FE, FF and the TR in a five-class multiclass problem is novel to BCI research to the best of the author's knowledge.

3.3 Exploring Different Sensorimotor Features

In order to allow for differentiation of movements on the same hand, it is necessary to extract as much relevant motor control information from EEG as possible. The uses of

MRCP and SMR or ERD/ERS in the literature are presented and the feasibility of combining the two feature types is discussed.

Studies done by Pfurtscheller and colleagues used ERD and ERS of mu and beta sensorimotor rhythms to distinguish between simple real and imagined motor actions including right hand, left hand, right finger, left finger, foot and tongue movements [10][77]. Consequently, many other studies have used this feature for similar investigations [22][28][29][39][43][78]. This sensorimotor rhythm has allowed online AOC rates around 80 % for right vs. left hand imagery after several training sessions [10][65]. Features related to ERD/ERS are used to distinguish between the EEG associated with right hand, left hand, foot and tongue movements in [44] and [67], where the latter showed AOC rates between 60 % and 90 % in one subject for binary combinations of pairs of ERD/ERS feature sets for the four motor tasks.

Vuckovic and Sepulveda [25] applied the concept of power ratios of ERD and ERS in the mu and beta frequency bands to the SMR in the delta, theta, alpha, beta and gamma ranges in order to investigate the possibility of discrimination between different kinematic wrist movements. Time-frequency features of the SMR were obtained using the discrete Gabor transform [25]. The findings show a dominance of SMR features from the lower delta band, which is the same frequency range for MRCP [25]. Power in the mu and beta bands (ERD/ERS), obtained using a discrete wavelet transform, is also used as part of the feature set for classifying EEG signals for different types and speeds of wrist movements [24].

MRCPs are not used as frequently as ERD/ERS is for discrimination of EEG for the performance or imagination of different limb movements on a single-trial basis. This is probably due to ERD/ERS being more reliable for single-trial analysis [51]. Kohlmorgen *et Al* [50] used the BP portion of MRCPs to create a classifier to differentiate between EEG for right and left self-paced finger presses, where the best AOC achieved was 95 %. In a study by Bai *et Al* [28], different computational methods were explored for movement intention and features related to ERD/ERS and MRCP were used, however it is not clear how well the MRCP-related features performed in isolation and to what extend MRCP contributed toward the classification rate [28]. Studies have been undertaken to use MRCP features for EEG associated

with dynamic movement discrimination [24]. Force-related studies using MRCP for foot movements, finger movements and gripping movements were studied in [64], [63] and [61] respectively, while the rebound rate of MRCP played a key role in discriminating different speeds of movements in [24].

Dornhege *et Al* [30] showed an improvement in classification rate when exploring different methods of combining MRCP and ERD/ERS features for the imagination of right and left finger movements. Promising results in [24] and [25] also showed the value of adding lower frequency or MRCP features to mu and beta ERD/ERS features for different unilateral wrist movements. It is thus hypothesized that the combination of features related to ERD/ERS and MRCP can improve EEG interpretation for other types of hand movements on the same hand; more specifically for WE, WF, FE, FF and the TR.

3.4 Exploring the use of ICA as a Spatial Filter

Section 2.4 presents some background knowledge on ICA and other spatial filters. The spatial filters used in studies investigating wrist movements are explored in this section, since these types of investigations bear the closest resemblance to this study. The advantages of the use of ICA in this research are then discussed.

Considering BCI research involving wrist movements, Vuckovic and Sepulveda [25] and Navarro *et Al* [26] used ICA; Gu *et Al* [24] used SL and Khan and Sepulveda [55] used CSP. Since Vuckovic and Sepulveda [25] discriminated EEG for only kinematic movements on the same hand, ICA could be most suitable for this research, which involves a similar problem. The superiority of ICA over raw EEG for the classification of EEG for right vs. left wrist movement was shown in [26].

With regard to other types of movements, Pfurtscheller and colleagues as well as other BCI researcher used SL to aid the extraction of features based on ERD/ERS [30][42][54][56][65]. However, when exploring different computational methods for classifying EEG between voluntary right and left finger key strokes, Bai *et Al* [28] reported superior performance of ICA over raw EEG, PCA, SL and CSP. Brunner *et Al* [27] compared the performances of different ICA algorithms to each other and to

other spatial filters. Here, for EEG discrimination between right hand, left hand, foot and tongue movements, the ICA infomax algorithm performed best, with CSP coming in second [27]. Hence ICA may be superior to SL in terms of extracting maximum information from local sources (see Section 2.4).

ICA has shown usefulness in extracting spatial features for different kinds of wrist movements [25][26] and has shown to provide more accurate classification results than other spatial filters in some studies involving other motor tasks [28][27]. ICA can also provide subject-specific spatial filters, which is advantageous since EEG patterns and hence the specific source location of motor control may differ subtly between individuals [10][29]. ICA can in theory also distinguish between spatially overlapping sources [10]. This makes it suitable for the discrimination of different kinds of hand movements on the same hand, whose control originates from sources located close together on M1 [32][39] (see Figure 2.2).

3.5 Conclusion

The exploration of relevant BCI literature reveals that the auhor is not aware of any EEG research done involving the combination of the basic hand movements of WE, WF, FE, FF and the TR. Consequently the use of EEG to detect the difference between right and left hand combinations of all five movements, between wrist and finger movements and between the individual five movements is deduced to be novel. This chapter has also shown that the use of ICA and the combination of MRCP and (mu and beta) ERD/ERS features are most suitable to handle the complexity of this research. The question of improving EEG interpretation to differentiate between different types of hand movements/imagery, using suitable techniques, is clearly defined in the next chapter.

Chapter 4

Problem Statement

4.1 Introduction

The previous chapter identified a problem within BCI research that has not yet been explored. This chapter clearly defines the purpose of this research aimed to address this problem and highlights the possible impacts of a solution.

The aim of this dissertation is to investigate the possibility of using EEG to decipher between the neural motor signals that control different types of essential hand movements i.e. WE, WF, FE, FF and the TR. The combination of TF spectral information from two types of electrophysiological features [30] is used in conjunction with ICA [41] to improve EEG interpretation. It is also desired to investigate the possibility of improved EEG interpretation for real and imagined movements. The question is: can the use of ICA along with features related to ERD/ERS and MRCP (TFSE and TFSM features) be used to differentiate between the EEG for different types of real and imagined unilateral hand movements using data recorded synchronously from healthy test subjects and processed offline on a single-trial basis?

In order to answer the latter, the research is divided into three sub-investigations as outlined in Section 1.6. The rest of this chapter defines the purposes and aims of each

investigation and highlights their impacts. Success criteria and the overall value of the research are outlined.

4.2 Right vs. Left Hand Movement Investigation (RLI)

The ability to classify between right and left hand movements is an important intermediate step towards classifying more advanced movement types on the same hand for two reasons. Firstly, differentiating between left and right hand movements is a simpler task since the spatial differences between the neural patterns for right and left hand movements are more distinct than between those for different types of unilateral movements [12][32][39] (refer to Sections 2.2 and 3.2). Secondly the results obtained for right vs. left classification for real and imagined movements can be compared to those in the literature (refer to Section 3.2). Consistencies with the literature would indicate that the data and method are satisfactory and that they can be used to attempt to classify different types of hand movements on the same hand.

The purpose of this investigation, which will be referred to as the right vs. left investigation (RLI), is to determine the ability of the designed method to classify between EEG for right and left (real and imagined) hand movements using ICA along with TFSE and TFSM features. Based on the average of the results for similar studies in the literature (refer to Section 3.2), the investigation will be successful if an average result close to 80 % classification accuracy is obtained for both real and imagined movements [11][42][43][65]. This can be achieved using TFSE or TFSM features or preferably using the combination of features [30].

4.3 Wrist vs. Finger Movement Investigation (WFMI)

The five basic types of movements consist of two wrist movements and three finger movements (see Section 1.2). Relative to the challenging task of multiclass unilateral hand movement discrimination using EEG (refer to Section 3.2 for details of these challenges), the binary classification between EEG associated with wrist and finger movements is a simpler task. The ability to differentiate between the movement of the wrist and the movement of the fingers will provide insight into the ability to extract separable information from neighbouring hand control regions of the cortex [12][32]

(refer to Figure 2.2). The purpose of this investigation, which is referred to as the wrist vs. finger movement investigation (WFMI), is to examine the possibility of classifying between the EEG for wrist and finger, real and imagined, movements on the same hand using ICA in conjunction with TFSE and TFSM features.

The focus of the investigation is not to obtain the best classification rates possible but rather to evaluate the level of possible discrimination. Hence success is considered to be the achievement of an average classification accuracy close to 70 % using TFSE or TFSM features or preferably using the combination of features. This criterion is chosen based on the expectation of poorer results than that of the RLI and on the average result of a similar binary classification study [25] (refer to Section 3.2).

4.4 Five Movement Differentiation Investigation (FMDI)

The purpose of this investigation, which is referred to as the five movement differentiation investigation (FMDI), is to determine if it is possible to classify between EEG associated with the real and imagined movements of WE, WF, FE, FF and the TR using ICA to enhance TFSE and TFSM features. This investigation contributes toward increasing the number of classes for hand motor task classification problems in BCI research and also adds new types of hand movements which may be explored in future BCI studies [12].

As with the WFMI, the focus of the investigation is not to optimise classification, but to evaluate the level of possible discrimination of EEG for the five hand movements. Success is considered to be the achievement of classification accuracy between 65 % and 75 % in at least one subject for either hand, using any feature type for either real or imagined movements. This criterion is based on the results of a five-class multiclass BCI problem mentioned in Section 3.2 [71]. Considering that results vary between subjects [10][71], accurate classification in at least one subject is an indication that classification of the selected five movements is possible on some level.

4.5 Conclusion

A complete positive result entails the success of all three investigations. This implies that the designed method allows for improved offline EEG interpretation for a sensorimotor BCI to the point where the neural motor control signals for five essential hand movements can be differentiated on a synchronous, single-trial basis. The success of only the first two investigations implies that the designed method only provides improved EEG interpretation to the degree where the movement control of different major parts of the hand i.e. the wrist and fingers, can be distinguished. In this case, however, the method is not suited to individual movement differentiation and a different approach should be investigated to solve this. It does however show that more advanced unilateral movement identification is possible and in that sense still answers the overall question of the research positively. The success of only the first investigation implies that the method is equivalent to existing methods in differentiating between right and left hand motor control signals obtained from EEG, yet does not allow any improved EEG interpretation in terms of distinguishing between different types of movements on the same hand. In this case more research needs to be done to find a method to improve EEG interpretation and the result of the research will be defined as negative.

The WFMI and the FMDI could contribute toward respectively increasing and improving the class number and flexibility of motor tasks in BCI research [12]. They also add knowledge to the attempt to find a method that will allow the control signals of individual hand movements to be distinguished. This may lead to further advances in neurally controlled assistive devices.

This chapter clearly defines the overall objective of the research and the question that needs to be answered. The problem of answering the question is split into three investigations and the purpose and impact of each are detailed. Success criteria are defined and the benefit of the research is discussed. The next chapter details the design and implementation of the method to perform the investigations.

Chapter 5

Methodology

5.1 Introduction

This chapter presents the design and implementation of the methodologies used to investigate all three problems described in the previous chapter. The method is designed to differentiate between different types of unilateral hand movements, but its effectiveness is first evaluated using the RLI (as explained in Section 4.2). The method is thereafter applied to the WFMI and the FMDI to determine its ability to differentiate between the neural control information for different types of hand movements using information taken from EEG.

The backbone of the methodology and the techniques used therein are common to all the investigations; however the details of the procedures within each section of the methodology differ slightly between the investigations. The details of these differences are discussed within the description of each section of the method, which makes up the rest of this chapter.

5.2 Design and Implementation of Method

The general method applied to all three investigations is described by Figure 5.1 [16][10][25]. EEG was captured and pre-processed, the result of which yielded two sets of bandpass-filtered data, mu/beta band data (for ERD/ERS) and delta band data

(for MRCP) [10][24]. The bandpass-filtered data were arranged in accordance with the type of investigation and flowed through the rest of the method in parallel. ICA was then run and the best ICs were chosen using visual inspection [41][80]. This is explained in more detail in Section 5.2.4. TF spectral features based on ERD/ERS and MRCP (TFSE and TFSM features respectively) were then extracted [25][28][30][70] and the best features were selected using the Bhattacharyya distance [67]. MD clustering and ANN methods were used to classify the reduced feature set [11]. Classification was done using TFSE and TFSM features individually and thereafter on the combination of the two types of features [30]. MATLAB and two of its open-source toolboxes, EEGLAB [41] and Netlab [79], were used to process the data and to implement the techniques and algorithms.

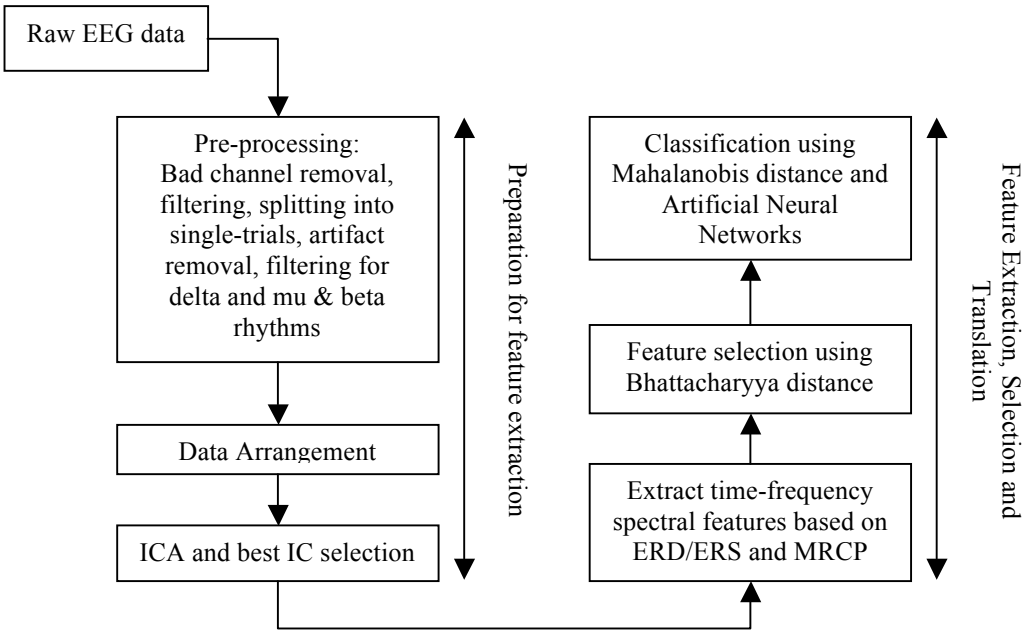

Figure 5.1: Overall process flow of method

The general method is customised for each investigation to accommodate for their differences. The main differences are as follows:

1. The RLI and the WFMI are two class classification problems, while the FMDI is a five-class multiclass classification problem.

2. The RLI compares movements on the right hand to movements on the left, while the WFMI and the FMDI consider data for right and left hand movements independently.
3. For the RLI, one class consisted of the grouping of all five types of movements for the right hand, while the other class grouped all types of movements for the left hand. For the WFMI, WE and WF were grouped to form one class, while FE, FF and the TR are grouped to formed the other class. Each of the five movement types formed a class in the FMDI.

Hence each stage in the method was adapted to accommodate for these differences, while keeping the function and basic structure of each stage common.

5.2.1 Experimental Procedure and Data Acquisition

Following ethics approval from the University of Cape Town, data was captured from five healthy, male, untrained volunteers in their early twenties. Data recording for BCI research is demanding on test subjects [11][28][67] whose EEG exhibits a large inter-subject variance [10] and are thus usually examined individually [24][25][43][67]. Hence the numbers of subjects are usually few and range approximately between three and twelve subjects [22][24][25][67][59][61]. This research examines each subject individually (also refer to the latter portion of Section 3.4), hence the use of five test subjects was thus deemed suitable.

The subjects were seated in a comfortable chair facing a computer screen [24][25][67], which was used along with custom E-prime software to queue the movements [81]. The hand and forearm in use were rested on an armrest while the subjects' EEG were measured [25][80]. Each subject was asked to perform real and imagined repetitions of the 5 movement types for each hand (starting with the right hand). Repetitions were grouped into sets of 20 such that each set consisted of one movement type, which is similar to the grouping of movements into sets of 15 in [25]. For each hand, the subjects performed 10 sets of movements: 5 for real movements and 5 for imagined movements. In summary each test subject had: movement type (5) × Left/Right hand (2) × real/imagined (2) × repetitions (20) = 400 trials.

The type of movement for each set was shown to the subjects on the computer screen prior to the commencement of the set. E-prime was used to mark the queues on the recorded EEG data as events [81]. Before the start of the each movement set, subjects were allowed to practice the movements [25]. There were short breaks between sets and the repetitions for each set were performed continually, while the EEG was recorded [25]. The trials were controlled by instructions shown on the computer screen, the timeline of which is shown in Figure 5.2 [25][67]. Subjects were instructed to prepare for the current movement/imagination of the set (S1); thereafter they were instructed to commence the movement/imagination, which was sustained (S2) until the instruction to stop was given [25][55][67]. A short relaxation period (S3) preceded the instruction to prepare for the next repetition. The timing of each period was based on the experimental setups in [25] and [67]. The duration of the preparation period (S1) allows for the visualisation of the BP (which can precede movement onset by up to 2 s) [53] and of pre-movement ERD (which can occur 1 – 2 s before movement) [16][10]. A sustained movement (S2) requires more concentration from the test subject, which may improve EEG patterns for imagined movements and also allows sufficient time to extract relevant features during movement performance/imagination [67]. S3 was kept to a minimum to allow more trials to be performed before the subject began to fatigue [11][26].

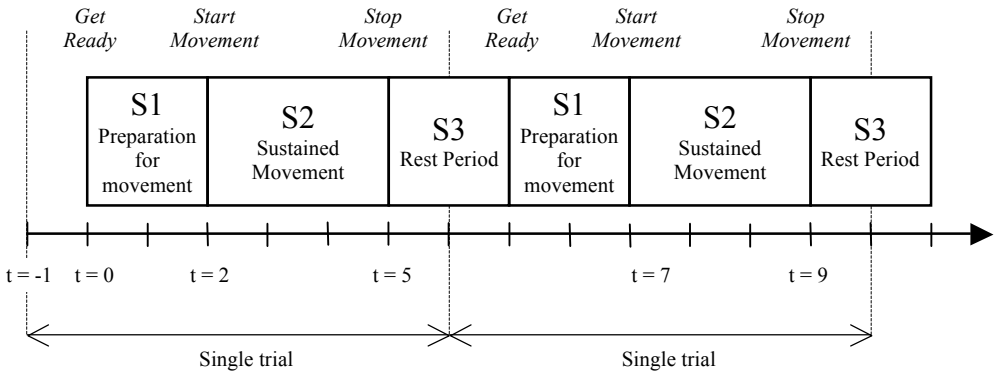

Figure 5.2: Time sequence and instructions for a single trial

A subject's EEG may vary during the recording session since they may become physically settled or alternatively restless over time [10]. The progression of the experiment allows more practice and can consequently improve the performance of

the test subject [10]. If the movement sets are performed in the same order for each subject, an unwanted pattern may be embedded into the data simply due to EEG variance with time. To avoid this, the order of the sets was randomised [55].

Subjects were asked not to blink, swallow, move their eyes, adjust their bodies or clear their throats during S1 and S2, but rather during S3, so as to reduce artifact contamination during the movement preparation and movement performance phases [28][67]. Subjects were observed to ensure that they did not perform any real hand movements when they were required to imagine hand movements and any undesired movement performance or behaviour by the subjects, such as the shifting of the body, was noted [67].

An EGI system (System 200) that consisted of 128 high-impedance scalp electrodes forming the Geodesic Sensor Net 128 (GSN 128), along with Geodesic EEG System and Net Station Software was used [82]. The electrode layout is shown in Figure 5.3 [82][83][84]. The electrodes consisted of Ag/sAg-Cl pellets that are attached to sponges, which were soaked in an electrolyte solution of potassium chloride and make contact with the scalp [84]. The 129^{th} electrode formed the reference electrode and was placed centrally at the top of the scalp, corresponding to Cz in the 10-20 EEG electrode placement system [35] (see Figure 5.3). Electrode impedance was kept below 50 kΩ as per EGI specifications for this high impedance system [84].

5.2.2 Pre-Processing

EEGLAB was used to handle the pre-processing [41]. Some channels had to be removed for some subjects' data due to excessive noise corruption [41]. The number of channels removed for each subject is summarized in Table 5.1. It was found that the left hand data for subjects 1 and 4 was greatly insufficient and was disregarded [25]. A high pass filter at 0.5 Hz was applied to remove DC (direct current) shifts, while a low pass filter removed frequencies above 90 Hz since the data was sampled at 200 Hz by the EGI system [25][67]. A 50 Hz Notch filter was also applied to remove noise from the mains power line [25][85]. MRCP frequencies range between 0 and 3 Hz, hence the lowpass filter may have removed some very slow moving components of the MRCP [24]. However, Vuckovic and Sepulveda [25] showed a

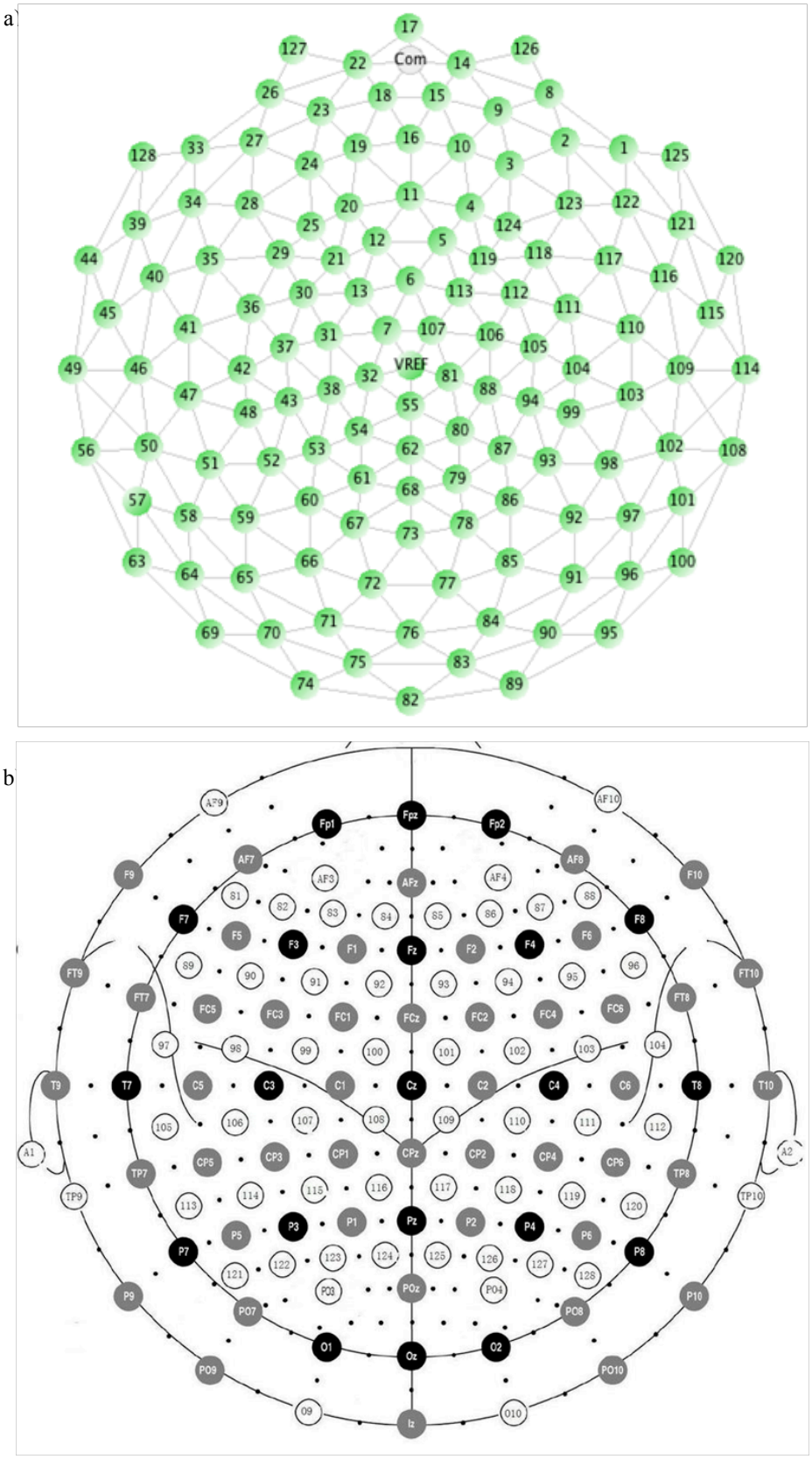

Figure 5.3: Electrode positions of the 128 electrode a) EGI GSN 128 system and the b) 10 – 20 international system [83][84].

dominance of features from frequencies between 0.5 and 2 Hz during imagined unilateral wrist movement classification. Kauhanen *et Al* [86] achieved classification accuracies up to 91 % for right vs. left imaginary index finger movements using features from the 0.5 – 3 Hz frequency band. Furthermore, the presence of the BP is still apparent after applying the lowpass filter (refer to Figure 5.4 as an example).

Table 5.1: Summary of the number of bad channels and bad trials that were removed.

	Removed Channels		**Removed Trials**	
	RH	LH	RH	LH
Subject 1	0	N/A	2	N/A
Subject 2	0	4	12	5
Subject 3	1	1	8	11
Subject 4	0	N/A	0	N/A
Subject 5	0	0	5	5

Data was then divided into 7 s trials [25][67], from t = -1s to t = 6 s, placing t = 0 at the *Get Ready* event shown in Figure 5.2. This was done so that the continuous signals are not split in the crucial areas of S1 and S2 [25]. Trials were manually inspected for voltage spikes and severe distortions across multiple channels and bad trials were consequently removed [41][67]. The numbers of bad trials removed for each subject are summarized in Table 5.1. The trials were baseline corrected using the interval from t = -1 to t = 0 s in order to align the rest state with the zero volt level [25][30][85].

The Automatic Artifact Removal (AAR) toolbox [87] for EEGLAB was used to remove artifacts, which includes electrooculogram (EOG) from eye-blinks and eye movements, and EMG from tongue, face, neck and shoulder movements [10]. EOG and EMG artifacts were removed using spatial filtering and blind source separation (BSS) [87]. EMG removal and EOG removal are particularly important since they share common frequencies with mu/beta rhythms and MRCP respectively [10]. The single-trial data was decomposed into spatial components representing information sources within the brain [87]. Thereafter, artifactual components were automatically removed using suitable criteria for each artifact type [87]. Criteria for EOG artifacts

were based on the fact that EOG components have high amplitudes relative to EEG, have few low-frequency sub-components and occur spatially near the front of the head [87][88]. Criteria for EMG artifacts are based on the fact that they occur in shorter bursts and their average power exceeds that of average EEG according to a ratio based on the typical power values of EMG and EEG [87][88]. The data was then reconstructed from the reduced component set. The effectiveness of the AAR approach was verified by using ICA (*infomax* algorithm) and visual inspection. The ICs before and after artifact removal were extracted and inspected to make sure that artifactual ICs had been removed using AAR and that non-artifactual EEG data was predominantly unchanged [41]. A Blind source separation technique in the form of Canonical Correlation Analysis (which is part of the AAR toolbox) was most effective in removing EOG and EMG artifacts [87].

A bandpass filter between 8 – 30 Hz was applied to isolate the mu and beta data (for ERD/ERS analysis) [24], while a lowpass filter with a 3 Hz cut-off was used to isolate delta band data (for MRCP analysis) [24].

5.2.3 Data Arrangement

EEG patterns and hence the timing, origin and spatial pattern of the sensorimotor activity differs between individuals [59], between different frequencies and feature types [30], between right and left hands [43][44] and between real and imagined data [25][67]. Hence, the two sets of bandpass-filtered data were rearranged into datasets by separating real and imagined movements and either grouping or separating right and left movements depending on the investigation type. This arrangement enabled ICA to extract spatially-specific components (see Section 5.2.4). The details of the data arrangement for each investigation are shown in Table 5.2. All five types of movements for both hands were grouped for the RLI. For the WFMI and FMDI, the five movements were grouped for each hand. The grouping allowed the same ICA weighting to be applied to all the classes in each investigation (refer to Section 2.4 for additional information on ICA channel weighting).

Datasets were created for each subject (for reasons explained in Section 5.2.1) where sufficient data is available. Multiple subjects' data were combined where possible in

order to investigate the inter-trial variability. Data per subject per movement was limited for the FMDI (100 trials per dataset); hence the use of a few features and simple classifier architecture was essential in this investigation [11]. It was not possible to perform the RLI for subjects 1 and 4 since their LH data was insufficient. The same datasets were used for the WFMI and FMDI since the same data splits were required for both. The movement types were grouped differently for these two investigations in the classification phase, which is explained in Section 5.2.8. In summary the RLI used 16 datasets and the WFMI and FMDI used 40 datasets.

Table 5.2: Data arrangement for each investigation, where 'RL' denotes a single dataset with right and left movements combined, 'RH' a single dataset with right hand movements only and 'LH' a single dataset with left hand movements only. In contrast to 'RL', 'RH, LH' in a cell represents two datasets, such that the right and left hand movements are separated

Investigation Type	Bandpass filter type	Movement Type	Subject 1	Subject 2	Subject 3	Subject 4	Subject 5	Subjects 2, 3 & 5 combined	Subjects 1 - 5 combined
RLI	Mu/beta	Real	-	RL	RL	-	RL	RL	-
		Imaginary	-	RL	RL	-	RL	RL	-
	delta	Real	-	RL	RL	-	RL	RL	-
		Imaginary	-	RL	RL	-	RL	RL	-
WFMI and FMDI	Mu/beta	Real	RH	RH, LH	RH, LH	RH	RH, LH	LH	RH
		Imaginary	RH	RH, LH	RH, LH	RH	RH, LH	LH	RH
	delta	Real	RH	RH, LH	RH, LH	RH	RH, LH	LH	RH
		Imaginary	RH	RH, LH	RH, LH	RH	RH, LH	LH	RH

5.2.4 Source Localisation using ICA as a Spatial Filter

Background on ICA and spatial filters are given in Section 2.4, while studies showing the advantageous use of ICA as a spatial filter are examined in Section 3.4. ICA was run on each dataset described in the previous sub-section using EEGLAB's automatic implementation of the *infomax* ICA algorithm: *runica* [41]. This was to decompose the EEG into individual localised sources of potentials. In order to accommodate for the variability of EEG patterns (as explained in the previous sub-section), the potentials or ICs emanating from relevant motor areas (see Section 2.2) were visually and uniquely selected and isolated for each dataset. Hence a spatial filter specific to each dataset was attained [29].

Several ICs representing motor activity were selected [25][80]. This approach is advantageous since the inter-subject variability of EEG makes it difficult to predict which electrodes provide relevant information [59]. The use of multiple ICs may also help to capture the information from different regions of the motor areas (see Section 2.2), which may activate during different stages of movement [59]. Spatial focusing was aided by the use of a high density EEG system (128 channels) to provide a better resolution for IC activity [41] (note the small localised activity in Figure 5.4 d). Motor IC selection also reduced the dimensionality of the data and filtered contamination from non-sensorimotor potentials in the brain [41][80].

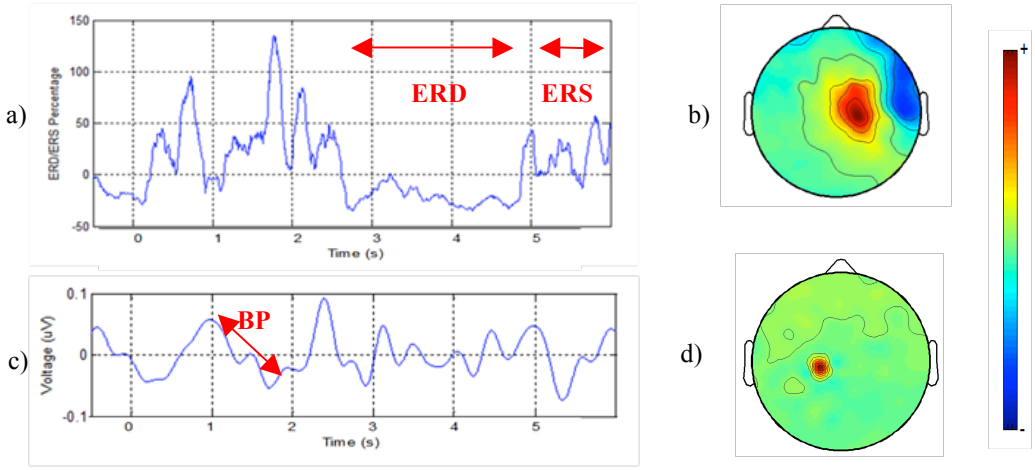

Figure 5.4: Examples of selected ICs for the RLI based on the visual inspection of scalp, ERP and ITV plots. a) shows the average ITV ERD/ERS pattern in the mu and beta frequencies for an IC from subject 2 and b) shows the corresponding IC scalp plot. ERD occurs after 2.5 s and ERS after 4.8 s in a), which respectively corresponds to sustained movement in S2 and relaxation at the commencement of S3 (refer to Figure 5.2). c) shows the average MRCP ERP pattern for an IC from subject 3 and d) shows the corresponding IC scalp plot. The BP between 1 and 2 s, which corresponds to movement preparation during S1, is clear. Positive activity in the hand control region of M1 is clear in b) and d) with a much sharper resolution in d).

The criteria for IC selection were based mainly on viewing localised contralateral, ipsilateral or bilateral activity in the region of M1 that controls the hand, but activity in the SMA and PMA was also considered [30][37][59] (see Section 2.2 for more information). Ipsilateral components were considered since they may have represented part of the bilateral activity of the electrophysiological features (see Section 2.6). For mu and beta filtered data, the average ERD/ERS pattern was calculated using the ITV method (see Section 2.6.1) and this was used to aid IC selection. The desired pattern consisted of the presence of ERD just prior to and/or

during S2 followed by ERS after the movement has ceased i.e. when S2 ends and S3 starts [56]. ICs whose event-related patterns differed greatly from the above were discarded even if their activity was localized over the appropriate hand control areas. For delta-band filtered data, IC selection was also based on the presence of the Bereitschaftspotential in the average ERPs. Examples of the desired ERD/ERS and average MRCP ERP patterns, upon which the selection criteria were based, are shown in Figure 5.4 along with their associated scalp plots. The scalp plots of all the visually selected ICs for all datasets are shown in Appendix A as well as their ITV ERD/ERS or average MRCP ERP patterns. The number of visually selected ICs differed between the subjects and Table 5.3 summarises the range of selected ICs within each investigation.

Table 5.3: Number of selected ICs, total features and optimum number of selected features

	RLI		**WFMI**		**FMDI**	
	ERD/ERS	MRCP	ERD/ERS	MRCP	ERD/ERS	MRCP
Number selected ICs	6 - 8	4 - 15	8 - 12	3 - 12	8 - 12	3 - 12
Total number of features	1176 - 1568	84 - 315	1568 - 2352	63 - 252	1568 - 2352	63 - 252
Optimum Number of selected features	5	7	18	17	8	8

5.2.5 Time-Frequency Spectral Feature Extraction for ERD/ERS

As explained in Section 2.6.1, TF representations of the ERD/ERS patterns from sensorimotor neural signals can be used to form a set of features [16]. A simple TF technique has shown success in extracting features from pre-recorded audio such as music and audio advertisements [89]. Both music and EEG are non-stationary signals; hence the technique was used in this study to extract features based on ERD/ERS patterns [16][89].

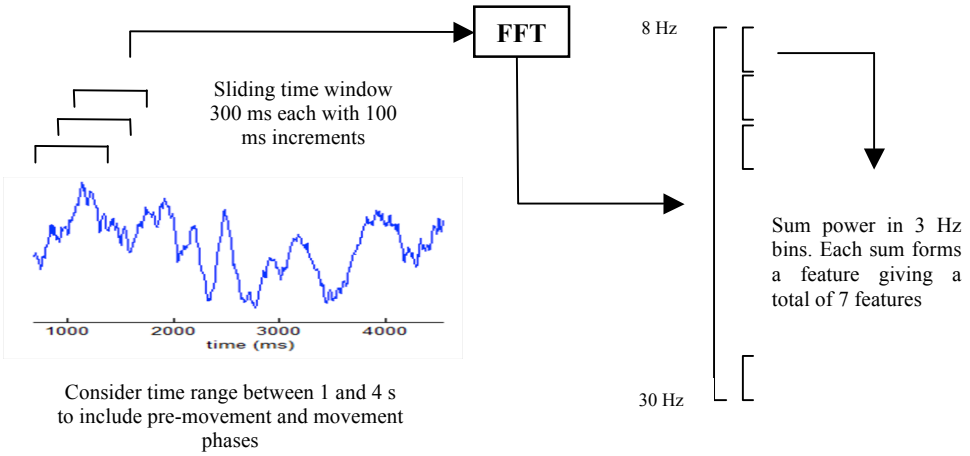

Figure 5.5: Flow of TFSE feature extraction algorithm

The TF technique is explained graphically in Figure 5.5 and was used to extract power spectral features from the selected ICs. It was used to capture the changes in power over time for different frequencies and thus captures the event-related power synchronisations and desynchronisations for each trial [16][24]. The time range from t = 1 s to t = 4 s was considered in order to include pre-movement (S1) and movement or movement-imagination (S2) phases (refer to Figure 5.2) [24][25][28][67]. An overlapping sliding window of 300 ms was then applied in increments of 100 ms (similar window sizes are used in [25] and [28]). The power spectrum for each window was calculated using a fast Fourier transform (FFT) [28][89]. The resulting frequency spectrum was then split into 7 bands of 3 Hz each (similar frequency splits were used in [25], [28] and [67]) and the sum of the powers within each band formed a feature [89]. 28 time windows were extracted over the time range considered, with 7 power band features each. This was done for each IC resulting in a large number of features per dataset equal to (number of ICs) × 28 × 7. The range of the total number of features for each investigation is shown in Table 5.3.

5.2.6 Time-Frequency Spectral Feature Extraction for MRCP

A method of feature extraction based on traditional time-domain analysis of MRCP (refer to Section 2.6.2) was attempted but proved unsuccessful. Refer to Appendix B for details of this method. Hence an alternate approach involving TF analysis was

adopted since some studies have used TF techniques for MRCP as explained in Section 2.6.2.

A TF technique similar to that used for the extraction of TFSE features is used to extract power features from the selected ICs for delta-filtered data and is shown in Figure 5.6. The time range between t = 0.6 s to t = 2.9 s (most of S1 and beginning of S2 in Figure 5.2) was considering. This time range was chosen considering the estimated time of occurrence of the Bereitschaftspotential, motor potential and rebound rate (see Section 2.6.2). Although the timing and amplitudes of these occurrences were not used as features, they affect the TF characteristics of the signals, which may in turn allow class discrimination. As with TFSE feature extraction, an overlapping sliding window of 300 ms was then applied in increments of 100 ms and the power spectrum for each window was calculated using a FFT [25][28][67][89]. Since the frequency range of MRCP signals was limited to 3 Hz [24] (see Section 5.2.2), only one frequency band was used, wherein the sum of the power was calculated. 21 time windows were extracted over the time range considered, with 1 power band feature each. This was done for each IC and the total number of features is given by (number of ICs) × 21 × 1. Since the numbers of ICs for each investigation and dataset differed, the range of the total number of features associated with each investigation is summarized in Table 5.3.

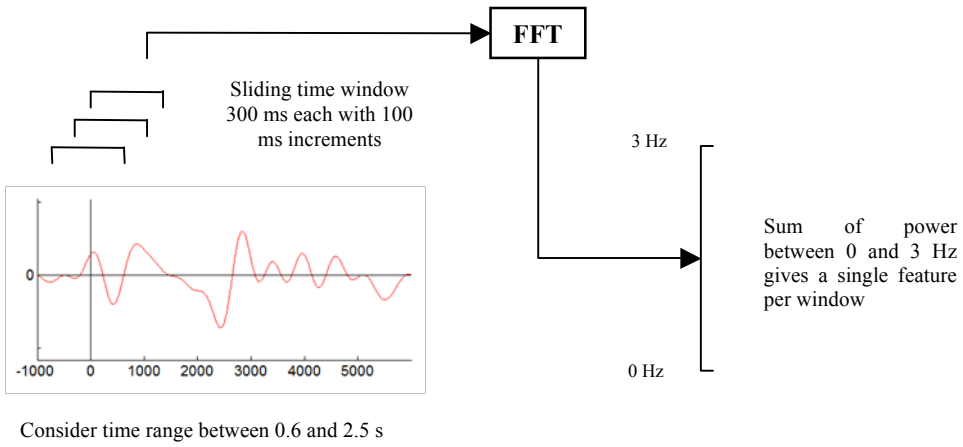

Figure 5.6: Flow of TFSM feature extraction algorithm

5.2.7 Feature Selection

The TFSE and TFSM feature sets were very large and the dimensionality needed to be reduced to simplify the classification problem and allow the classifier to perform optimally [16]. At the same time, key information needed to be retained [16]. The Bhattacharyya distance (BD) was used to reduce the TFSE and TFSM feature sets to much smaller feature sets, which the classifiers could handle [67][28]. The TFSE and TFSM feature sets were also concatenated to form a combined dataset (referred to as COMB) and the BD was used to reduce this dataset as well. This also reduced any duplicated movement information that was contained in both feature sets.

The BD can be used to measure the separability of classes for univariate feature sets [28]. Hence it measures how well a single feature can differentiate between two classes and can thus be used to find those features, from a multivariate feature set, that individually capture the differences between the classes best [28]. It is related to the Bhattacharyya coefficient (BC) which measures the closeness of two statistical populations or sample sets by considering the overlap of their respective probability distributions [90][91]. The more the probability distributions for each classes' sample populations overlap, the larger the BC will be calculated to be according to equation 5.1 [91]. The BD can be calculated from the BC according to equation 5.2 and decreases as the BC increases [91]. Variables *a* and *b* represent the probability distributions of the two classes concerned, while *x* is the variable describing the values of the samples.

$$BC(a,b) = \int a(x)b \int x dx \tag{5.1}$$

$$BD(a,b) = -\ln\big(BC(a,b)\big) \tag{5.2}$$

For two class classifier problems such as the RLI and WFMI, the BD was simply calculated for each feature using all trials concerned and those with the largest BDs were selected to form a small subset of features [28]. For multiclass problems such as the FMDI, the 2-class feature selection method was extended by considering each binary combination of classes and calculating the BD for each pair. A matrix was created containing the BD for each class pair for each feature. For the FMDI, which

contains 5 classes, the matrix was a 10 by N matrix, where N is the total number of features and 10 is the number of possible pairings of the 5 classes. For each of the 10 pairs of classes, the BDs over all features were sorted in descending order. A weighted average were then applied across all 10 sets of sorted BDs to select the features that had the highest BDs for all classes considered.

The number of selected features used for classification was varied iteratively for TFSE, TFSM and COMB feature sets and the classification accuracies (measured using the ACA method described in Section 5.2.8.4) using MD clustering were examined for all datasets and investigations [59][66][80]. Section 5.2.8.2 explains the advantages of the use of MD clustering. The change in accuracy with respect to feature number is averaged over all datasets within each investigation and plotted in Figure 5.7 [80]. The optimum number of features for each investigation is summarized in Table 5.3 and it is shown that low dimensionality is provided in all cases.

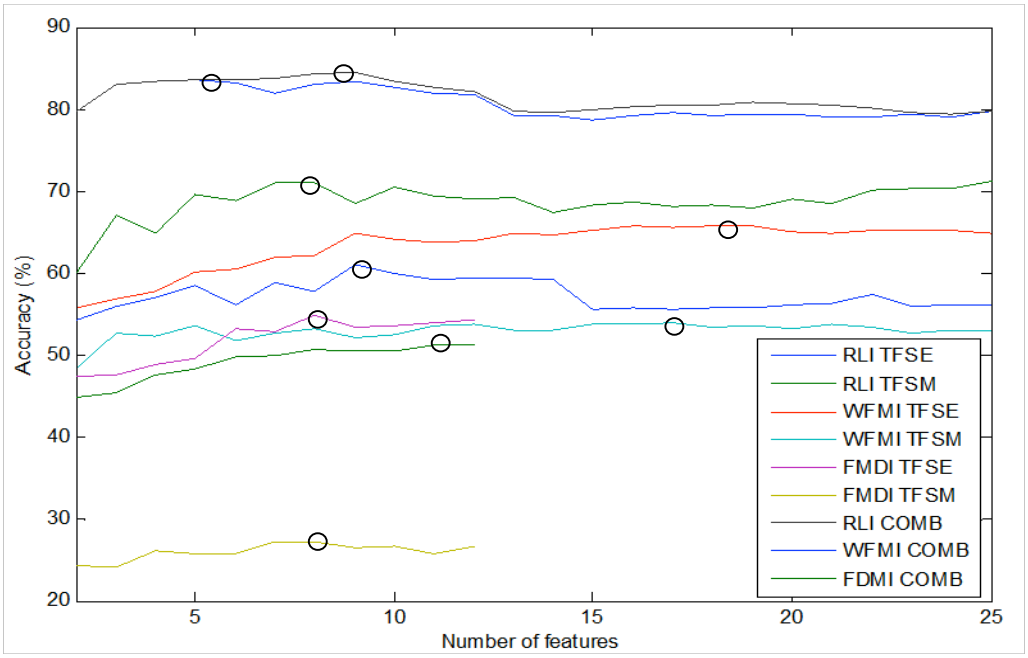

Figure 5.7: Change in accuracy with respect to the number of selected features for all investigations and feature types. The number of features producing the best accuracy (ACA) for each case is circled. A maximum of 25 BD-selected features were tested for the RLI and WFMI and 12 for the FMDI. This is to limit dimensionality and reduce classifier complexity in the former case and to accommodate for the limited data in the latter case (since more training data is needed for more input features [97]).

Feature selection was then performed for each dataset (see Section 5.2.3) since the features holding crucial movement-control information that can separate the classes can differ between subjects, between right and left hands and between real and imaginary movements [65]. The number of features selected for each dataset depends on the investigation it is associated with.

5.2.8 Classification

The MD was used to first remove outliers and thereafter MD and ANN techniques were used to attempt to translate the selected features into a class representing a single type or a grouped type of movement. Classification was done for each dataset and investigation on a single-trial basis. The MD clustering method provided an objective first view at the classification accuracy and the ANN method attempted to validate and improve the results. The method of calculating the classification accuracy is explained and this method was applied to both classification methods to yield the results for all three investigations.

5.2.8.1 Mahalanobis Distance Outlier Removal

Outlier removal is an important task in data mining and involves identifying, from the sample population, those samples/observations that deviate from the expected or general range and consequently removing or accommodating them [92][93]. The extreme values of these samples could be due to the erroneous recording of data [93] or the origination from a different mechanism [94] and could thus incorrectly skew the results of the data analysis [92][93]. Since the data was obtained from EEG, outliers were most likely due to noisy bursts or recording errors [11] and were thus dealt with by removing them from the population [16].

The MD can be used to find multivariate outliers [95] by finding those samples that lie far away from the mean of a population [92][93]. To identify the outliers, the MD from the feature vector of each trial to the mean of the feature vectors for all the trials was calculated, thus forming a set of MDs for all trials [95]. The standard deviation for all the MDs was then calculated. If the MD for a given feature vector from a single trial was greater than 3 times the standard deviation, that vector was defined as an outlier and removed [25]. Thus a feature vector from a single-trial was considered

an outlier only if it was very different from the feature vectors for the total population [92][93]. In this way outliers were removed before classification.

5.2.8.2 Mahalanobis Distance Clustering

A MD-based classifier is simple and robust and despite its good performance in BCI research, including multiclass problems, has not been widely used therein [11]. It is based on the MD, which can be used as a multivariate method of measurement between objects and is appropriate since it takes into account the correlation in the data [95]. It is also suitable for use with a few features [66] and is an objective means of classification not susceptible to overtraining as ANNs are [11]. It can be used to find the dissimilarity between multivariate feature vectors from different classes [95] and in that way determine if the chosen features capture the separateness of the classes. The squared MD d_i^2 between the i^{th} vector of dataset x and the mean of dataset y can be calculated using equation 5.3, where μ_Y is the mean of dataset y, C_Y^{-1} is the inverse covariance matrix of dataset y and T is the transpose operator [66].

$$d_i^2 = (x_i - \mu_Y)^T C_Y^{-1}(x^i - \mu_Y) \quad 5.3$$

Figure 5.8 shows classification by MD clustering diagrammatically using the example of the problem to classify between right and left hand movements, but only using 2 features for classification so as to allow feature representation on a 2D graph. When considering a single-trial for classification, the MDs from that observation/trial to the means of all the classes are calculated [66]. The mean of a class represents the centre of the cluster for that class. If the MD between the single-trial's feature vector x_i and the mean feature vector of its class μ_x is smaller than the MDs between that single-trial vector and the mean vectors of the other class(es), then it can be concluded that x_i belongs to class x and that classification is successful for that single-trial.

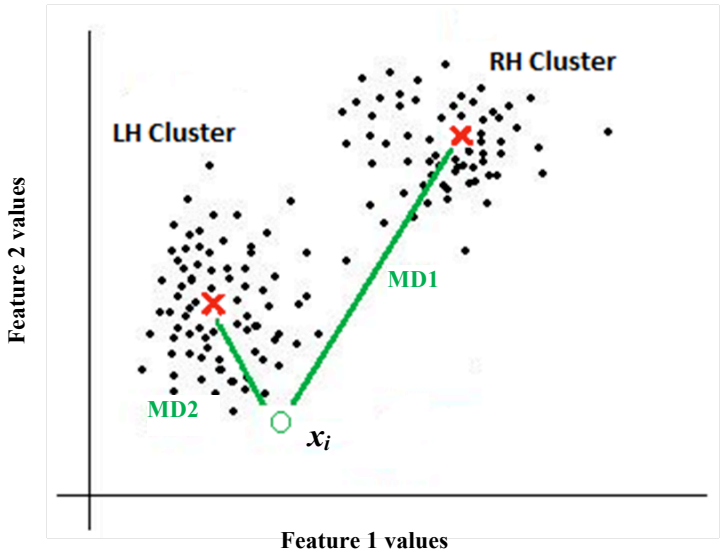

Figure 5.8: Illustration of Mahalanobis distance clustering between 2 classes. Each trial is represented by a small solid dot, while the crosses are the means of the clusters/classes. The hollow circle (x_i) is the trial to be classified, while lines represent the distances to each cluster mean. In this scenario x_i is classified as belonging to the LH Cluster, since MD1 > MD2.

The trial to be classified was not used in the calculation of the mean and covariances of the clusters/classes so that it did not impact on the mean and covariance of the class to which it did in fact belong. Hence, for each trial, and the means, covariances and MDs were calculated based on all other trials. This allowed all trials to be used for testing and eliminated the need to split the data into training and testing datasets for this type of classification. This is advantageous since data is limited in BCI research [11]. In this way classification using MD clustering was performed on all datasets for all investigations and the classification accuracy was thereafter calculated.

5.2.8.3 Neural Network Classification

An ANN can approximate almost any function, given enough neurons, and can classify any number of classes making them flexible and adaptable to many problems [11][96]. A multilayer perceptron (MLP) ANN consists of neurons arranged in several layers i.e. an input layer, one or more hidden layers and an output layer [11]. MLP ANNs have thus been used for a variety of BCI problems including binary and multiclass classifications scenarios [11]. They are however sensitive to overtraining especially with noisy data such as EEG [11]. In this research, MLP ANNs used the

selected features to predict the movement-type class for single-trials. They were implemented using the Netlab toolbox for MATLAB [79]. From this point on the MLP ANNs used in this research are referred to only as ANNs.

Outliers were removed from the reduced feature set using the MD as explained in Section 5.2.8.1. Each dataset was then randomly divided into training and testing data in a 7:3 ratio [67]. The classes were represented as numerical outputs since ANNs require a mapping to a numerical output. For the RLI, a single binary output was used for all associated ANNs, where *1* and *0* corresponded to right and left respectively [96]. Similarly for the two-class problem in the WFMI, a single binary output was used, where *1* and *0* corresponded to wrist and finger movements respectively. 3 binary outputs were used to represent the 5 classes in the FMDI, where the combinations of *001*, *010, 011*, *100* and *101* respectively represented WE, WF, FE, FF and TR [96][97].

The structures of the ANNs are summarized in Table 5.4 and depend on the type of investigation. The numbers of nodes in the hidden layer were chosen by iteratively varying the number of hidden nodes to select that which yielded the smallest classification error [96][97]. A subset of the training data, the validation data, was used to test the performance of each ANN structure when evaluating the optimum number of hidden nodes [96][97]. Hence curves comparing accuracy against the number of hidden nodes were generated for all datasets within each investigation, where the maximum number of hidden nodes was limited to 30 to prevent the ANN becoming too complex [96]. The number of hidden nodes used for each investigation and feature type was calculated by averaging the accuracy curves across all related datasets.

Thus ANNs were structured according to the type of investigation and feature type and trained, using the training data, for all datasets [25][96]. Each ANN was then tested by using each trial in the testing dataset to compare the class predicted by the ANN to the trial's actual class [25][96]. The accuracy was evaluated using cross validation, where the testing and training data were randomly separated three times and the accuracy each time is calculated. The three results were averaged to yield the accuracy [25].

Table 5.4: Summary of optimum ANN structures for each investigation.

	RLI			WFMI			FMDI		
	TFSE	TFSM	COMB	TFSE	TFSM	COMB	TFSE	TFSM	COMB
Number of input nodes	5	7	9	18	17	9	8	8	11
Number of hidden nodes	6	15	11	24	24	17	15	16	16
Number of output nodes	1	1	1	1	1	1	3	3	3

5.2.8.4 Accuracy Calculation

In clinical applications, the statistics most often used to evaluate the accuracy of diagnostic tests are sensitivity and specificity [98]. Sensitivity describes the likelihood of a positive test result if a patient has a disease, while specificity indicates the likelihood of a negative result if the patient does not have the disease [98]. They have the advantage of allowing the comparison of the diagnostic potential of different clinical tests [98] and since BCI research is very much linked with medical research, the use of these statistical measures, as done in [43], is advantageous. Sensitivity and specificity are calculated using equations 5.4 and 5.5 respectively, where TN, TP, FN and FP represent true negative, true positive, false negative and false positive respectively [43][98].

$$Sensitivity = \frac{TP}{TP+FN} \quad 5.4$$

$$Specificity = \frac{TN}{TN+FP} \quad 5.5$$

Sensitivity and specificity can be generalized if one considers all cases where the patient has a disease as belonging to class 1 and all those who do not have the disease as belonging to class 2. If one considers right vs. left hand classification and labels right hand movements as class 1 and left hand movements as class 2, selectivity and specificity will respectively indicate the percentage of right and left hand movements that are correctly classified. This applies similarly to wrist vs. finger movement

classification or any other binary classification problem. Hence both sensitivity and specificity measure the accuracy rate within a single class.

This idea can be extended to multiclass problems where the accuracy rate within each class is measured using Equation 5.6, where A_i indicates the accuracy in class i, C_i the number of correctly classified cases from class i and F_i the number of falsely classified cases belonging to the same class. The overall accuracy can then be calculated by finding the average of the sensitivity and selectivity or by the average of the all accuracies per class. Equation 5.7 shows this, where N refers to the number of classes and A_i to the accuracy for each class. In this research, this measure of classification accuracy is referred to as the average of class accuracy (ACA).

$$A_i = \frac{C_i}{C_i + F_i} \tag{5.6}$$

$$ACA = \frac{1}{N}\sum_{i=1}^{N} A_i \tag{5.7}$$

Hence the classification accuracies of for all investigations and datasets, using both classifiers, were evaluated using the ACA as shown by equation 5.7. Accuracies for other studies mentioned in this research (mostly in Chapter 3) used the measure of the AOC. They both essentially evaluate the overall percentage of trials that are correctly classified and are thus comparable provided that the number of trials for each class is similar.

5.3 Conclusion

A method aimed at improving the interpretation of EEG using a sensorimotor BCI is presented in this chapter. It is designed to allow the differentiation of EEG for different types of unilateral hand movements, but its general structure was applied to all three investigations. The customization of the general method to suit each investigation is detailed for each stage of the method. The experimental setup, the data acquisition stage and the pre-processing stage are explained. The method uses ICA as a spatial filter to aid the extraction of TFSE and TFSM features, which are used individually and in combination. Smaller subsets of features are selected using the BD and are then classified using MD-clustering and ANNs. The method to

evaluate the accuracy of classification for all investigations is also described and the accuracy results are presented in the next chapter.

Chapter 6

Results

6.1 Introduction

This chapter presents the results of the implementation of the method described in the previous chapter. The results of all three investigations are presented and involve the presentation and analysis of: 1) the time-frequency characteristics of the features that are selected using the BD, and 2) the classification accuracies.

The selected features differ for each dataset (see Section 5.2.7). Hence, within each investigation, the selected features are plotted for left and right hands, real and imagined movements, and TFSE and TFSM features on an individual subject basis i.e. for each dataset described in Section 5.2.3. This was done by combining the selected features from all the ICs associated with that dataset since the selected features could originate from multiple ICs. The TF positions of the selected features from all ICs are represented on a single TF plot for each subject's real and imagined data. These selected features were then summed for all individual subjects in order to highlight those features that are selected more frequently.

The classification accuracy is labelled as *Accuracy* in all the figures in this chapter and was calculated using the ACA method described in Section 5.2.8.4. For each investigation, the classification accuracies for the real and imaginary, RH and LH

datasets for each subject are plotted and the average accuracies across all subjects are tabulated. This is done for TFSE, TFSM and COMB features. The datasets containing data from all the subjects (those labelled *AllSubjects* in the plots in this chapter), are not included in the calculation of the average accuracy, since they do not represent data from a single subject and will thus distort the mean accuracy across the subjects. Their use is explained in Section 5.2.3. In all plots, *Imag* represents data for imaginary movements.

6.2 Right vs. Left Hand Movement Investigation (RLI)

6.2.1 Selected Features

The TF distributions of the selected TFSE and TFSM features for each subjects' data for the RLI are shown in Figure 6.1 and Figure 6.2 respectively. Figure 6.3 shows the summation of the selected features for all individual subjects. As explained in Section 5.2.3, only data for subjects 2, 3 and 5 can be used in the RLI. Right and left hand data are combined. The time scales for all plots are consistent with the timing diagram in Figure 5.2, which can be found in Section 5.2.1.

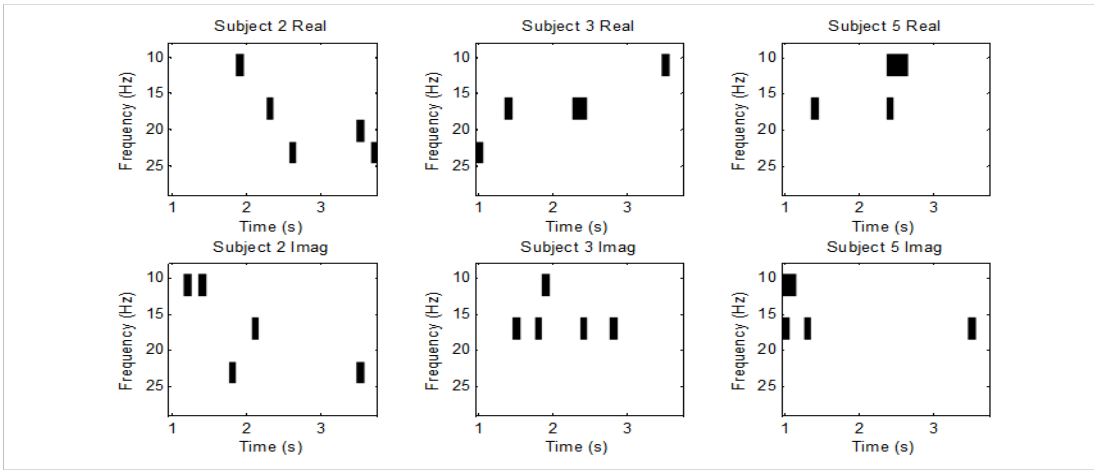

Figure 6.1: TF distributions of BD selected TFSE features for the RLI. Selected features are shown in black and shown for each subject's data for real and imagined movements. *Imag* represents data for imaginary movements.

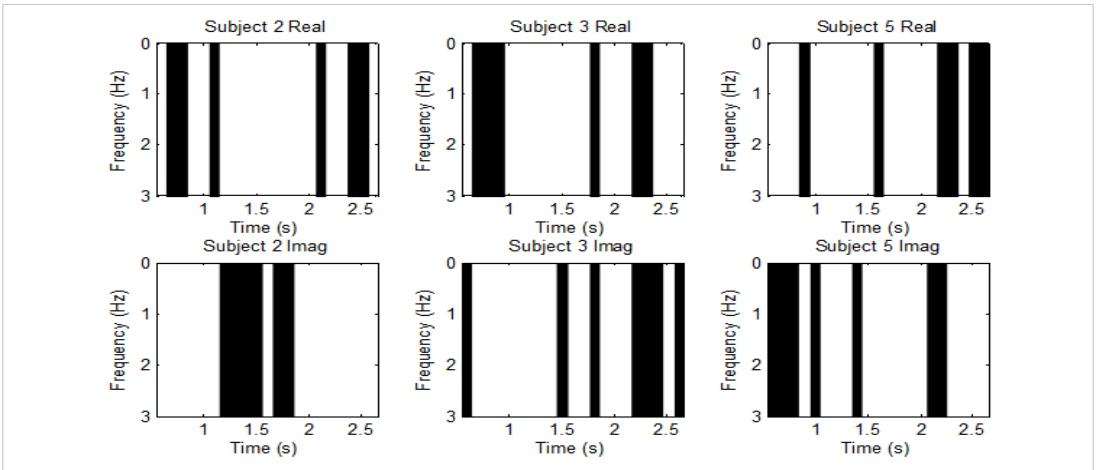

Figure 6.2: TF distributions of BD selected TFSM features for the RLI. Selected features are shown in black and shown for each subject's data for real and imagined movements.

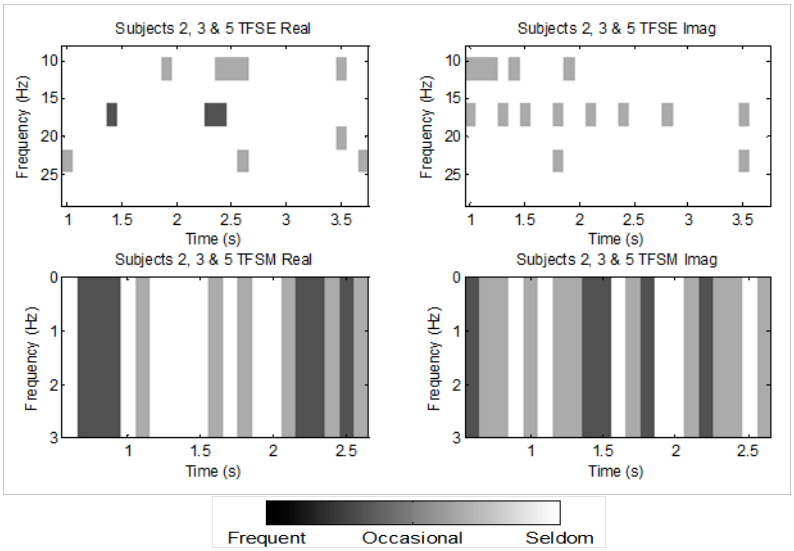

Figure 6.3: TF distributions of BD selected TFSE and TFSM features for the RLI, which have been summed for all individual subjects' data for real and imagined movements. The greyscale indicates the frequency of occurrence of a feature amongst all subjects i.e. black for features occurring in all subjects, and white for features occurring in no subjects.

6.2.2 Accuracy

The classification accuracies for the RLI, based on TFSE, TFSM and COMB features, are shown in Figure 6.4, Figure 6.5 and Figure 6.6 respectively. Accuracies for each individual subject and for the combination of subjects are shown in these plots. Table 6.1 summarises the average classification accuracy across all individual subjects used in the RLI.

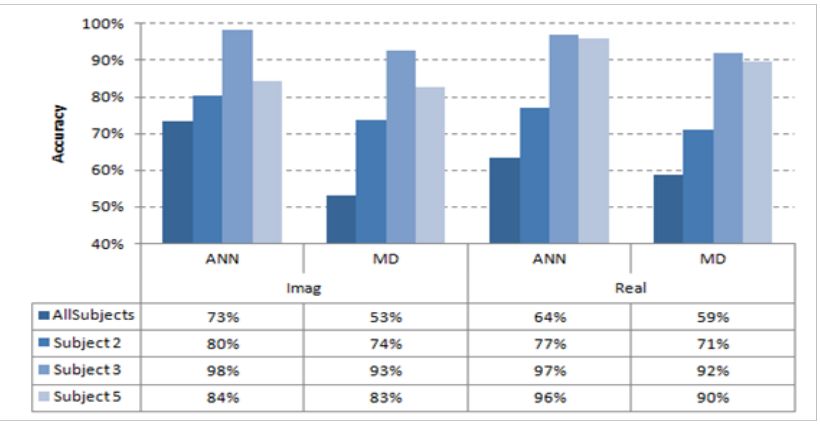

	Imag		Real	
AllSubjects	73%	53%	64%	59%
Subject 2	80%	74%	77%	71%
Subject 3	98%	93%	97%	92%
Subject 5	84%	83%	96%	90%

Figure 6.4: Accuracy for individual and combined subjects for TFSE features in the RLI using 2 different classifiers i.e. ANN and MD.

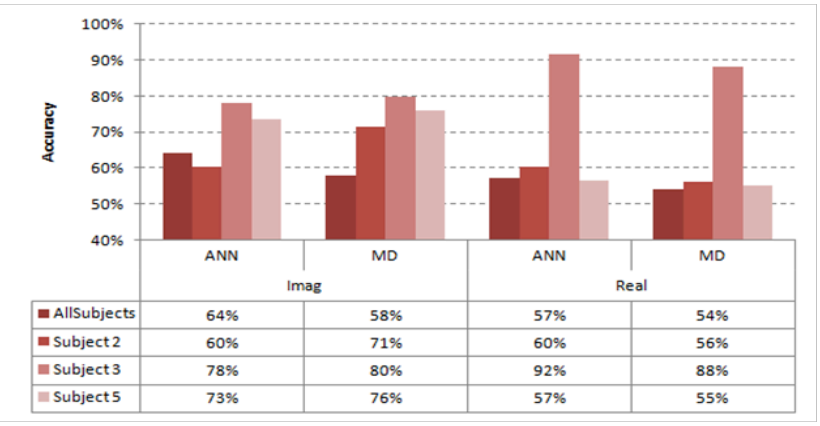

	Imag		Real	
AllSubjects	64%	58%	57%	54%
Subject 2	60%	71%	60%	56%
Subject 3	78%	80%	92%	88%
Subject 5	73%	76%	57%	55%

Figure 6.5: Accuracy for individual and combined subjects for TFSM features in the RLI using 2 different classifiers i.e. ANN and MD.

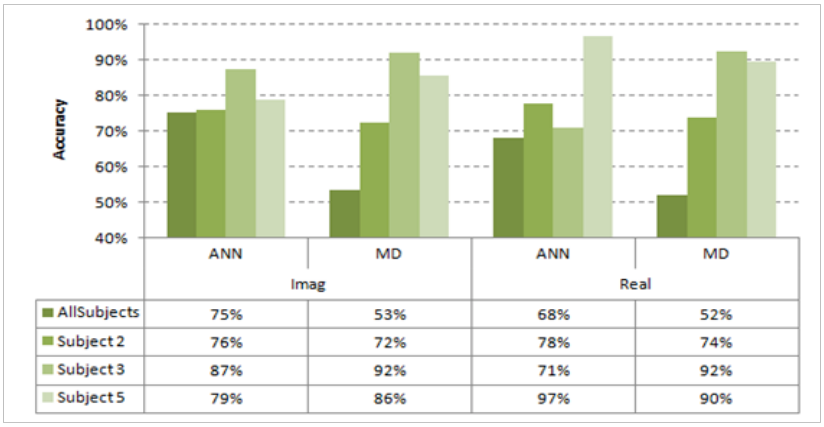

	Imag		Real	
AllSubjects	75%	53%	68%	52%
Subject 2	76%	72%	78%	74%
Subject 3	87%	92%	71%	92%
Subject 5	79%	86%	97%	90%

Figure 6.6: Accuracy for individual and combined subjects for COMB features in the RLI using 2 different classifiers i.e. ANN and MD.

Table 6.1: Summary of average classification accuracies and standard deviations for the RLI (%)

	TFSE		TFSM		COMB		Average of all Feature Types	
	MD	ANN	MD	ANN	MD	ANN	MD	ANN
Real								
Average of all individual subjects	84	90	66	69	85	82	78.7	80.4
Average of all individual subjects and both classifiers	87 ± 11		68 ± 17		84 ± 11		79.5 ± 15.1	
Imaginary								
Average of all individual subjects	83	88	76	71	83	81	80.7	79.7
Average of all individual subjects and both classifiers	85 ± 9		73 ± 7		82 ± 8		80.2 ± 9.1	
Average of Real and Imaginary								
Average of all individual subjects	84	89	71	70	84	81	79.7	80.0
Average of all individual subjects and both classifiers	86 ± 9		71 ± 13		83 ± 9		79.9 ± 12.3	

6.3 Wrist vs. Finger Movement Investigation (WFMI)

6.3.1 Selected Features

The TF distributions of the selected TFSE and TFSM features for each subjects' data for the WFMI are shown in Figure 6.7 and Figure 6.8 respectively. Figure 6.9 shows the summation of the selected features for all individual subjects. Feature selection for each subject's right and left hand data is shown. As explained in Section 5.2.3, the left hand data for subjects 1 and 4 is not available. The time scale for all plots is consistent with the timing diagram in Figure 5.2 which can be found in Section 5.2.1.

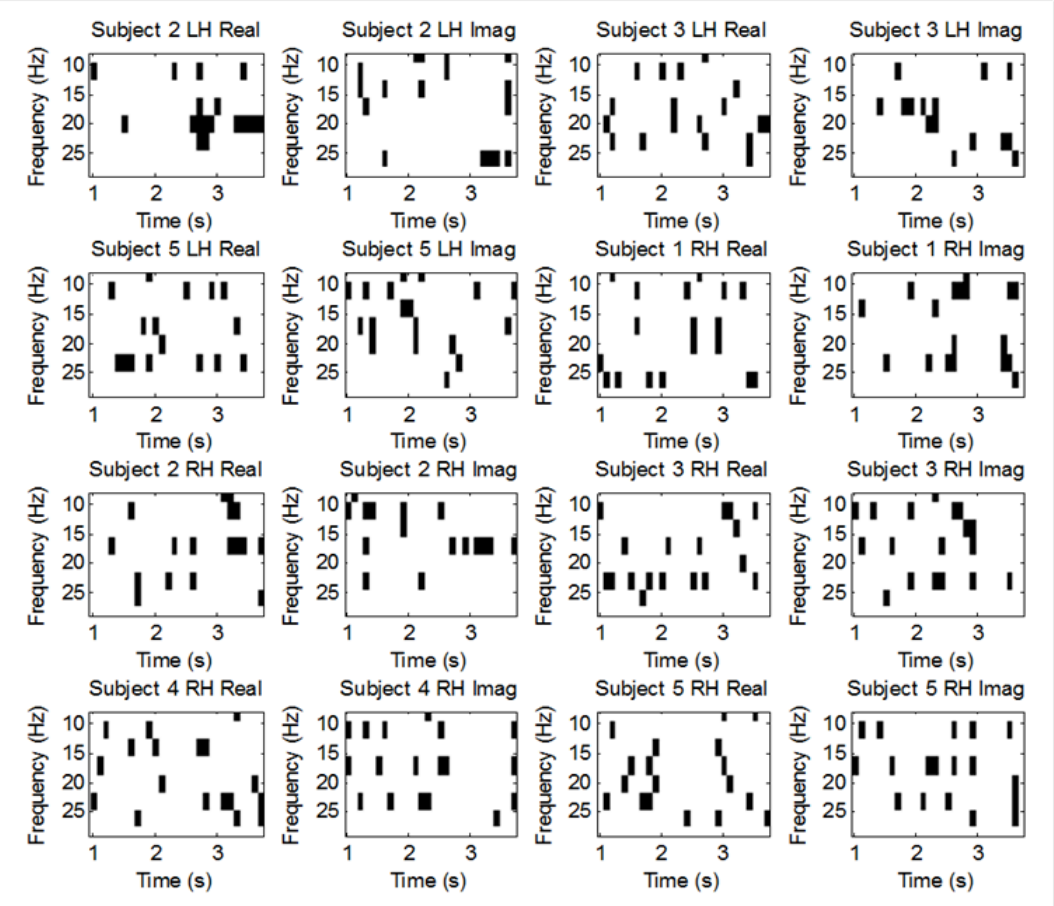

Figure 6.7: TF distributions of BD selected TFSE features for the WFMI. Selected features are shown in black and shown for each subject's data for real and imagined movements. *Imag* represents data for imaginary movements.

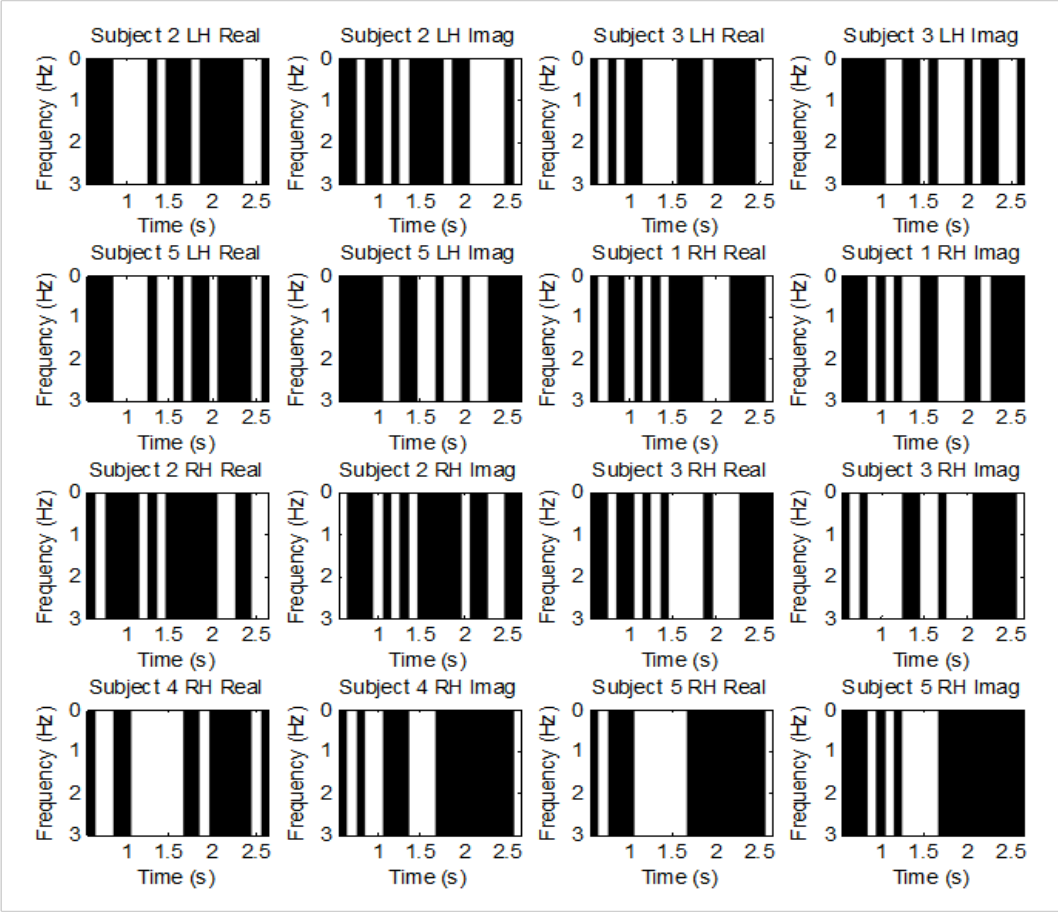

Figure 6.8: TF distributions of BD selected TFSM features for the WFMI. Selected features are shown in black and shown for each subject's data for real and imagined movements.

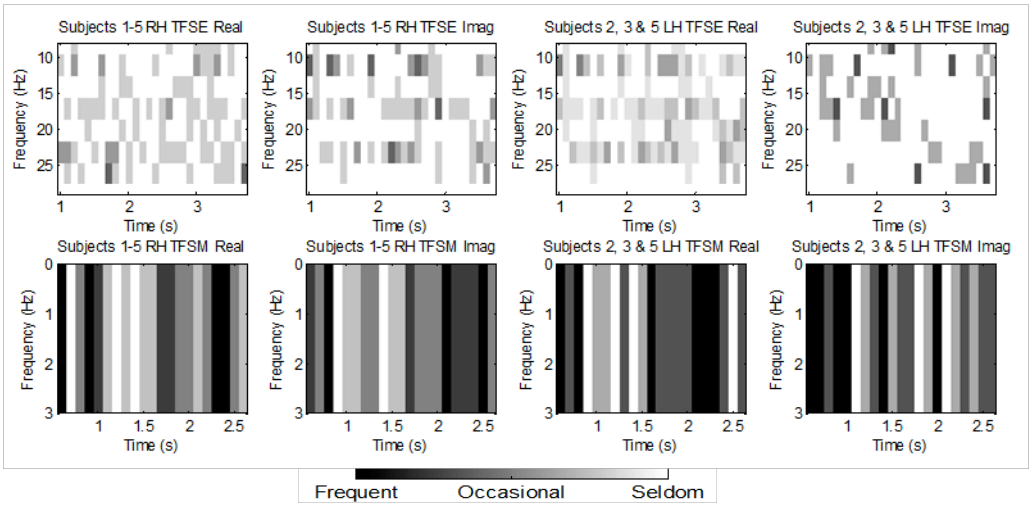

Figure 6.9: TF distributions of BD selected TFSE and TFSM features for the WFMI, which have been summed for all individual subjects' data for real and imagined movements. The greyscale indicates the frequency of occurrence of a feature amongst subjects i.e. black for features occurring in all subjects, and white for features occurring in no subjects.

6.3.2 Accuracy

The classification accuracies for the WFMI, based on TFSE, TFSM and COMB features are shown in Figure 6.10, Figure 6.11 and Figure 6.12 respectively. Accuracies for each individual subject and for the combination of subjects are shown. Table 6.2 summarises the average classification accuracy across all individual subjects used in the WFMI.

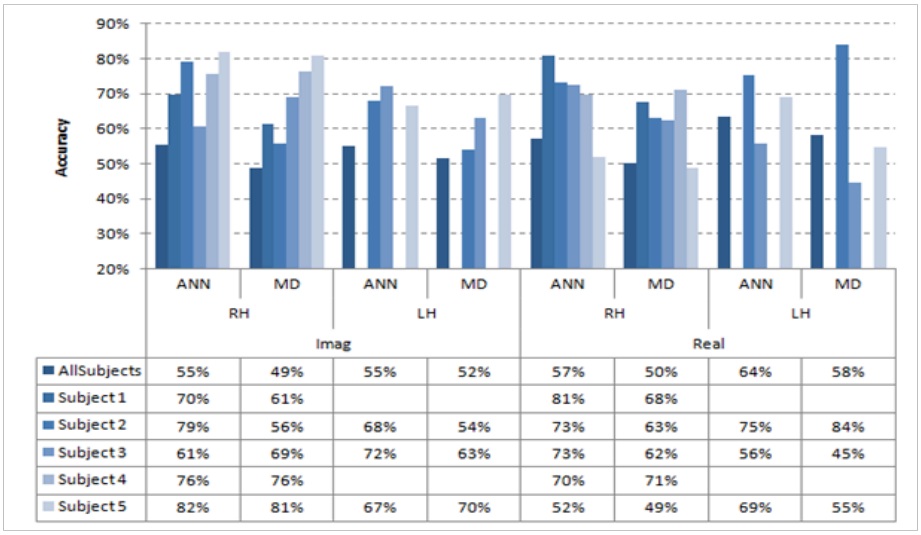

	Imag RH ANN	Imag RH MD	Imag LH ANN	Imag LH MD	Real RH ANN	Real RH MD	Real LH ANN	Real LH MD
AllSubjects	55%	49%	55%	52%	57%	50%	64%	58%
Subject 1	70%	61%			81%	68%		
Subject 2	79%	56%	68%	54%	73%	63%	75%	84%
Subject 3	61%	69%	72%	63%	73%	62%	56%	45%
Subject 4	76%	76%			70%	71%		
Subject 5	82%	81%	67%	70%	52%	49%	69%	55%

Figure 6.10: Accuracy for individual and combined subjects for TFSE features in the WFMI using 2 different classifiers i.e. ANN and MD.

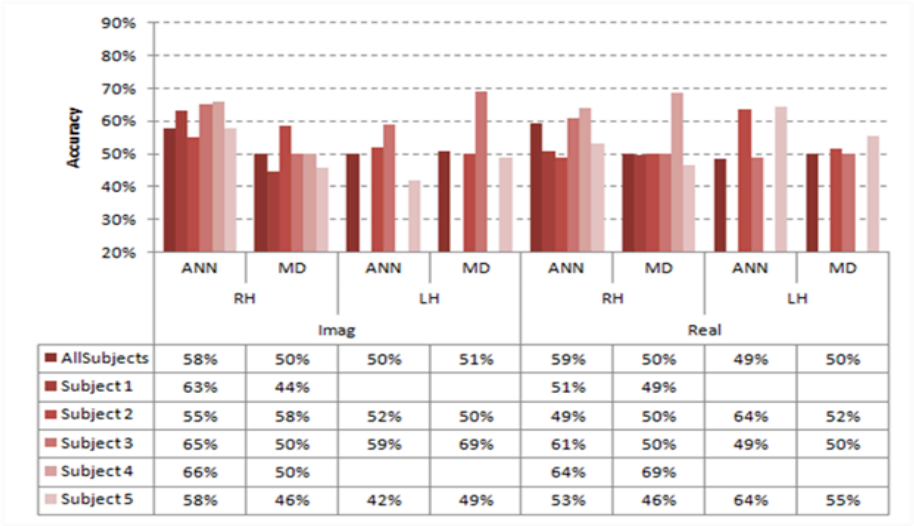

	Imag RH ANN	Imag RH MD	Imag LH ANN	Imag LH MD	Real RH ANN	Real RH MD	Real LH ANN	Real LH MD
AllSubjects	58%	50%	50%	51%	59%	50%	49%	50%
Subject 1	63%	44%			51%	49%		
Subject 2	55%	58%	52%	50%	49%	50%	64%	52%
Subject 3	65%	50%	59%	69%	61%	50%	49%	50%
Subject 4	66%	50%			64%	69%		
Subject 5	58%	46%	42%	49%	53%	46%	64%	55%

Figure 6.11: Accuracy for individual and combined subjects for TFSM features in the WFMI using 2 different classifiers i.e. ANN and MD.

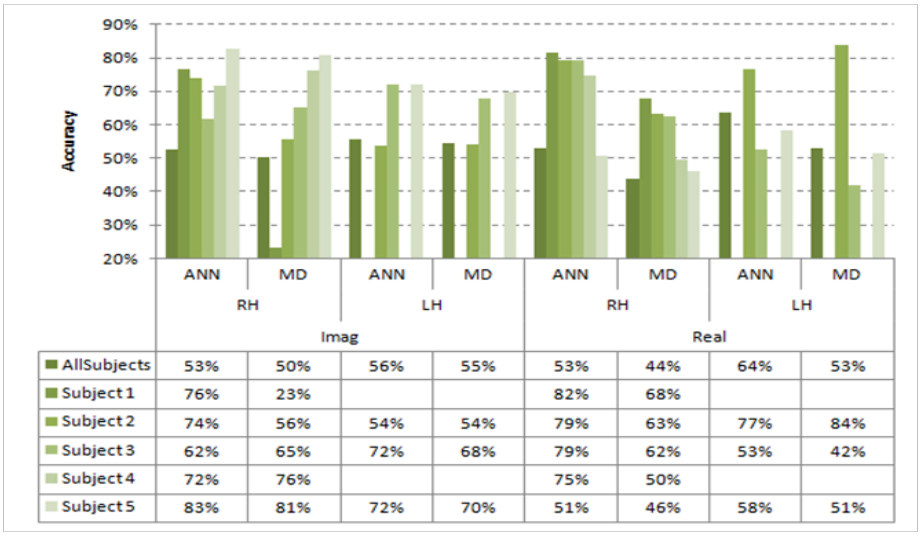

	Imag RH ANN	Imag RH MD	Imag LH ANN	Imag LH MD	Real RH ANN	Real RH MD	Real LH ANN	Real LH MD
AllSubjects	53%	50%	56%	55%	53%	44%	64%	53%
Subject1	76%	23%			82%	68%		
Subject2	74%	56%	54%	54%	79%	63%	77%	84%
Subject3	62%	65%	72%	68%	79%	62%	53%	42%
Subject4	72%	76%			75%	50%		
Subject5	83%	81%	72%	70%	51%	46%	58%	51%

Figure 6.12: Accuracy for individual and combined subjects for COMB features in the WFMI using 2 different classifiers i.e. ANN and MD.

Table 6.2: Summary of average classification accuracies and standard deviations for the WFMI (%)

	TFSE		TFSM		COMB		Average of all Feature Types	
	MD	**ANN**	**MD**	**ANN**	**MD**	**ANN**	**MD**	**ANN**
Real								
Average of all individual subjects	64	70	54	57	58	71	58.6	65.9
Average of all individual subjects and both classifiers	63 ± 9		56 ± 7		60 ± 12		59.8 ± 10.6	
Imaginary								
Average of all individual subjects	67	72	51	59	59	71	59.0	67.3
Average of all individual subjects and both classifiers	69 ± 7		55 ± 7		65 ± 16		63.2 ± 12.4	
Average of Real and Imaginary								
Average of all individual subjects	65	71	53	58	59	71	58.8	66.6
Average of all individual subjects and both classifiers	66 ± 8		55 ± 7		63 ± 14		61.5 ± 11	

6.4 Five Movement Differentiation Investigation (FMDI)

6.4.1 Selected Features

The TF distributions of the selected TFSE and TFSM features for each subjects' data for the FMDI are shown in Figure 6.13, and Figure 6.14 respectively. Figure 6.15 shows the summation of the selected features for all individual subjects. Feature selection for each subject's right and left hand data is shown. As explained in Section 5.2.3, the left hand data for subjects 1 and 4 is not available. The time scale for all plots is consistent with the timing diagram in Figure 5.2 which can be found in Section 5.2.1.

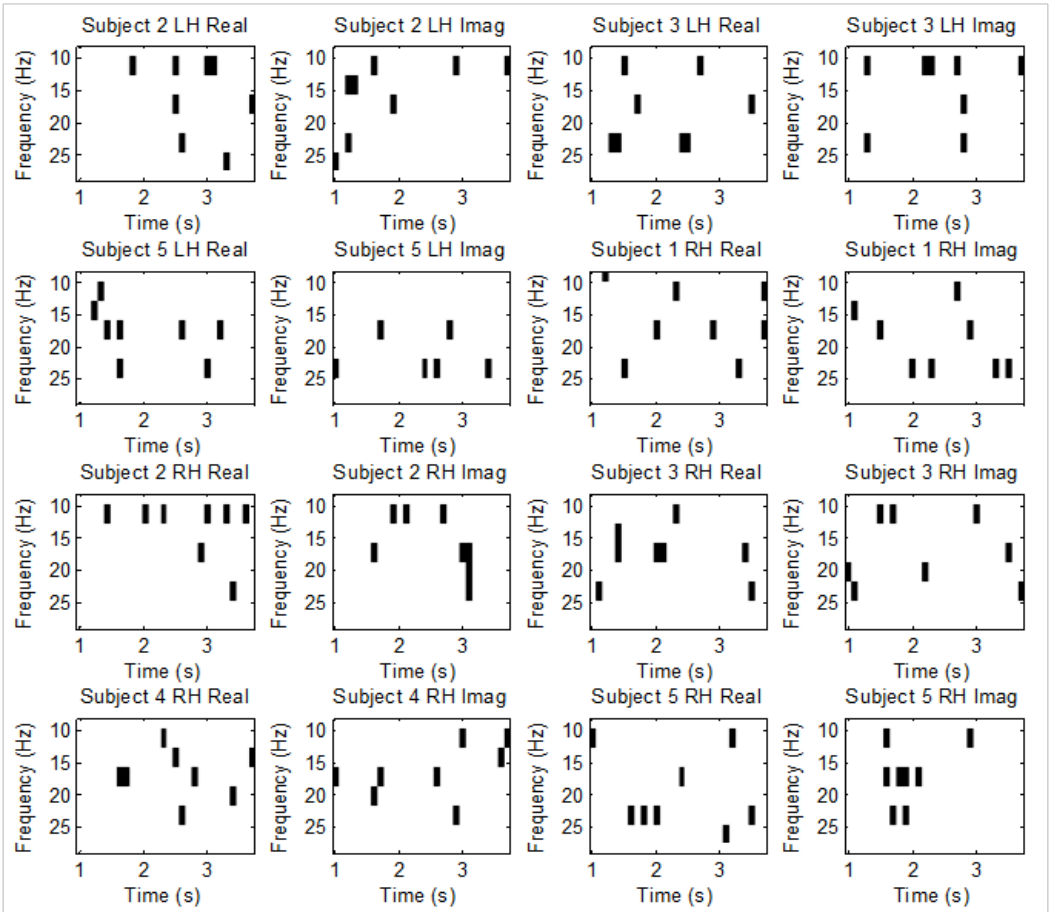

Figure 6.13: TF distributions of BD selected TFSE features for the FMDI. Selected features are shown in black and shown for each subject's data for real and imagined movements. *Imag* represents data for imaginary movements.

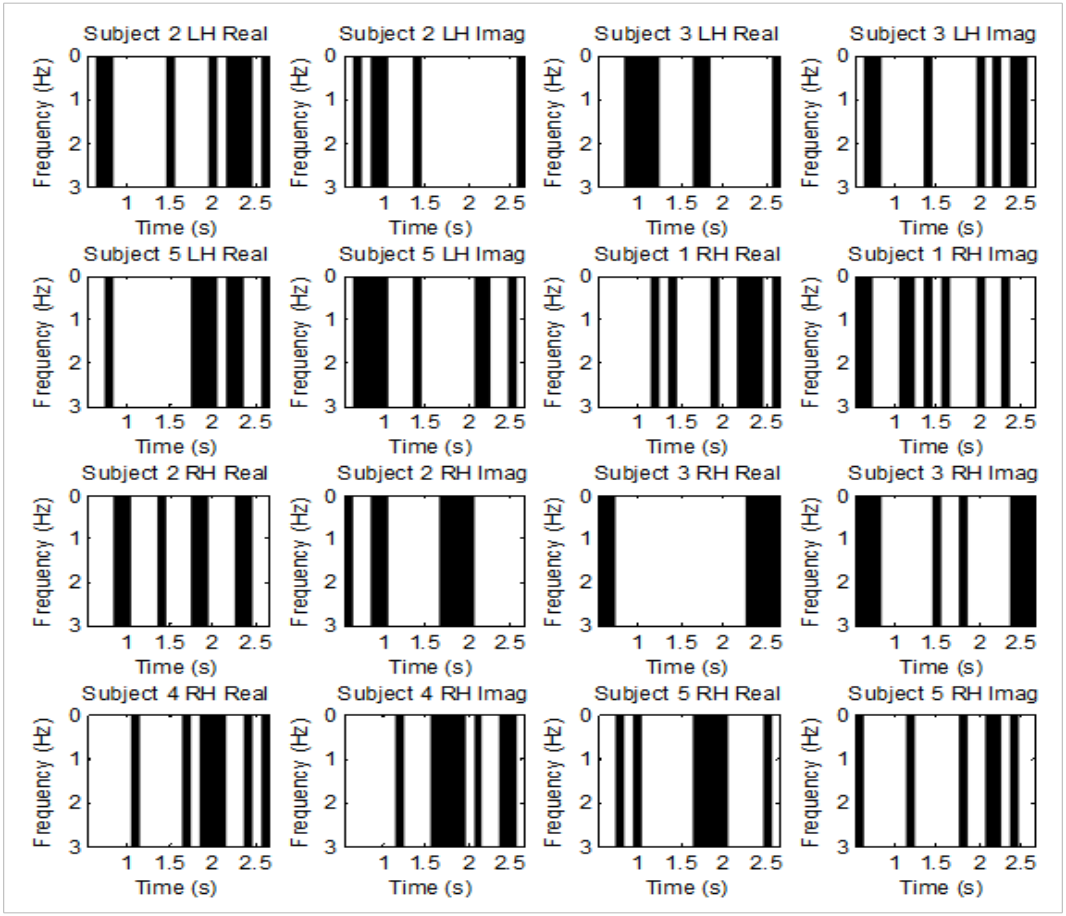

Figure 6.14: TF distributions of BD selected TFSM features for the FMDI. Selected features are shown in black and shown for each subject's data for real and imagined movements.

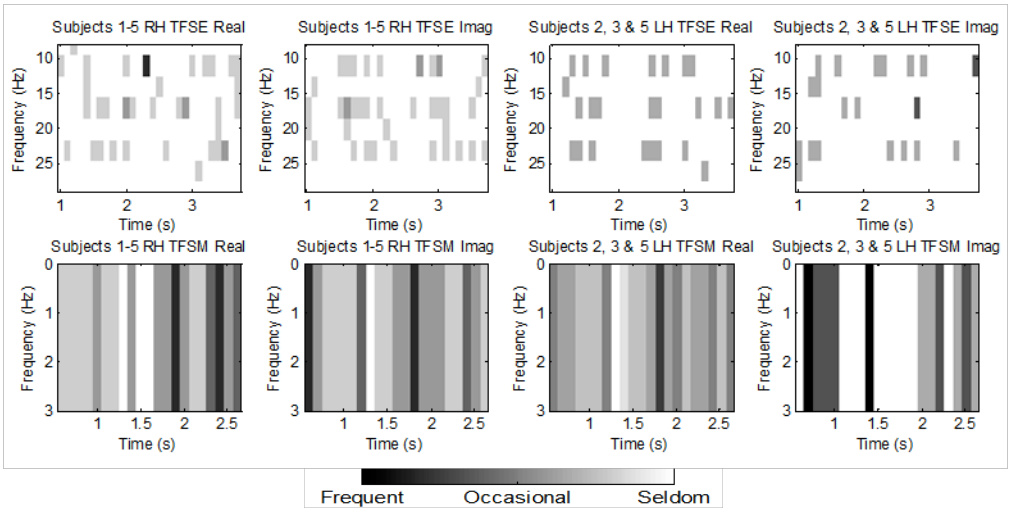

Figure 6.15: Time-frequency distributions of BD selected TFSE and TFSM features for the FMDI, which have been summed for all individual subjects' data for real and imagined movements. The greyscale indicates the frequency of occurrence of a feature amongst subjects i.e. black for features occurring in all subjects, and white for features occurring in no subjects.

6.4.2 Accuracy

The classification accuracies for the FMDI, based on TFSE, TFSM and COMB features, are shown in Figure 6.16, Figure 6.17 and Figure 6.18 respectively. Accuracies for each individual subject and for the combination of subjects are shown. Table 6.3 summarises the average classification accuracy across all individual subjects used in the FMDI.

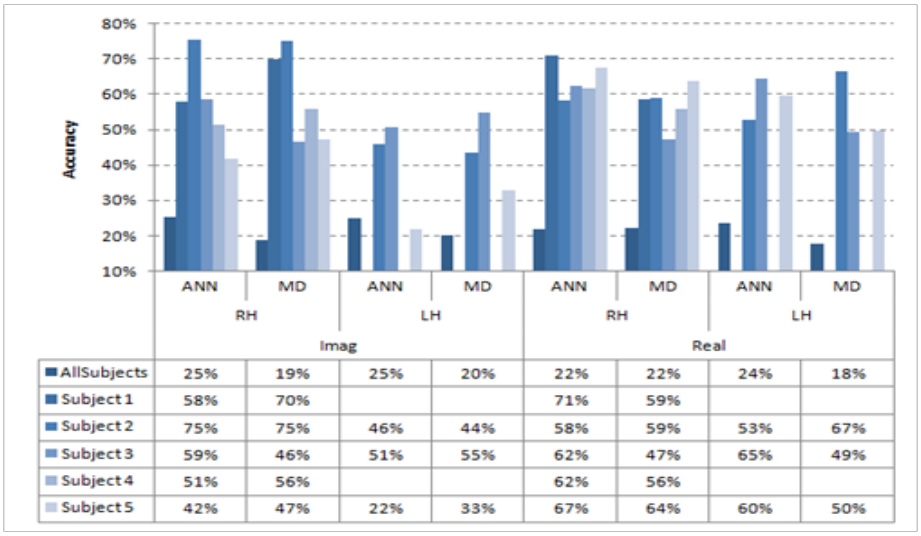

	Imag RH ANN	Imag RH MD	Imag LH ANN	Imag LH MD	Real RH ANN	Real RH MD	Real LH ANN	Real LH MD
AllSubjects	25%	19%	25%	20%	22%	22%	24%	18%
Subject 1	58%	70%			71%	59%		
Subject 2	75%	75%	46%	44%	58%	59%	53%	67%
Subject 3	59%	46%	51%	55%	62%	47%	65%	49%
Subject 4	51%	56%			62%	56%		
Subject 5	42%	47%	22%	33%	67%	64%	60%	50%

Figure 6.16: Accuracy for individual and combined subjects for TFSE features in the FMDI using 2 different classifiers i.e. ANN and MD.

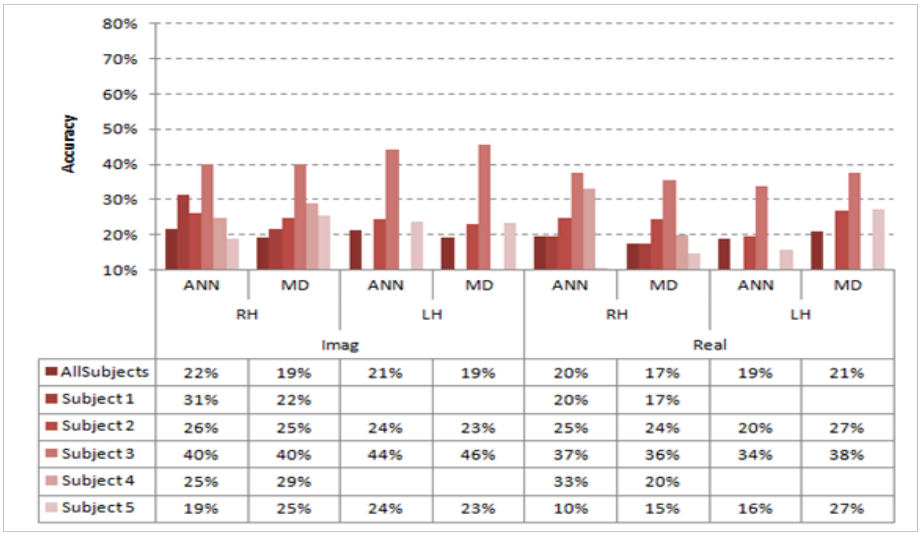

	Imag RH ANN	Imag RH MD	Imag LH ANN	Imag LH MD	Real RH ANN	Real RH MD	Real LH ANN	Real LH MD
AllSubjects	22%	19%	21%	19%	20%	17%	19%	21%
Subject 1	31%	22%			20%	17%		
Subject 2	26%	25%	24%	23%	25%	24%	20%	27%
Subject 3	40%	40%	44%	46%	37%	36%	34%	38%
Subject 4	25%	29%			33%	20%		
Subject 5	19%	25%	24%	23%	10%	15%	16%	27%

Figure 6.17: Accuracy for individual and combined subjects for TFSM features in the FMDI using 2 different classifiers i.e. ANN and MD.

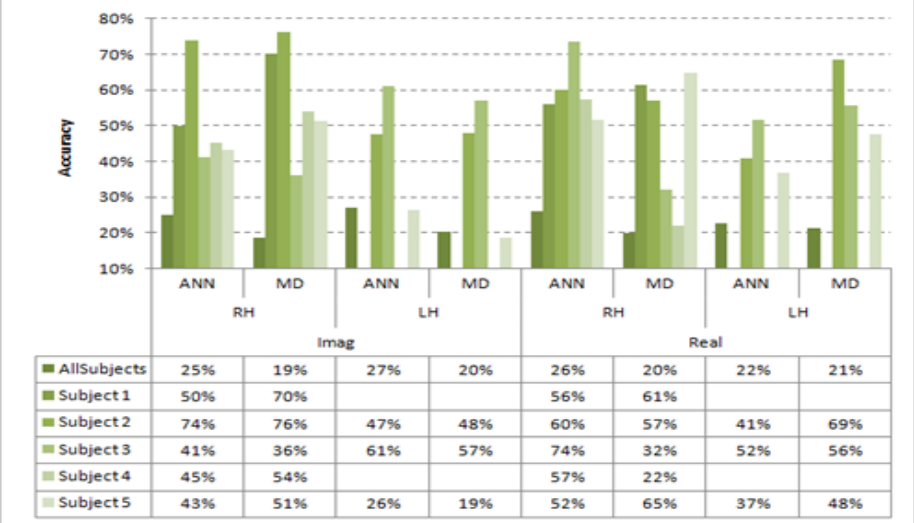

	ANN	MD	ANN	MD	ANN	MD	ANN	MD
AllSubjects	25%	19%	27%	20%	26%	20%	22%	21%
Subject 1	50%	70%			56%	61%		
Subject 2	74%	76%	47%	48%	60%	57%	41%	69%
Subject 3	41%	36%	61%	57%	74%	32%	52%	56%
Subject 4	45%	54%			57%	22%		
Subject 5	43%	51%	26%	19%	52%	65%	37%	48%

Figure 6.18: Accuracy for individual and combined subjects for COMB features in the FMDI using 2 different classifiers i.e. ANN and MD.

Table 6.3: Summary of average classification accuracies and standard deviations for the FMDI (%)

	TFSE		TFSM		COMB		Average of all Feature Types	
	MD	ANN	MD	ANN	MD	ANN	MD	ANN
Real								
Average of all individual subjects	57	63	24	25	49	54	43.3	47.3
Average of all individual subjects and both classifiers	51 ± 6		25 ± 8		44 ± 13		40.0 ± 17.8	
Imaginary								
Average of all individual subjects	55	51	28	29	54	48	45.7	42.9
Average of all individual subjects and both classifiers	53 ± 11		29 ± 8		51 ± 11		44.3 ± 14.9	
Average of Real and Imaginary								
Average of all individual subjects	56	57	26	27	51	51	44.5	45.1
Average of all individual subjects and both classifiers	52 ± 9		27 ± 8		48 ± 12		42.1 ± 16	

6.5 Conclusions

The results of the implementation of the method for all three investigations are presented in this chapter. For each investigation, the time-frequency distributions of the features selected using the BD are plotted, followed by the classification accuracies, which are shown for individual subjects and on average. The next chapter discusses the results in relation to the purpose of the research.

Chapter 7

Discussion

7.1 Introduction

This chapter discusses the results presented in the previous chapter. For each investigation the following are discussed: 1) the time-frequency characteristics of the selected features, 2) the success of the investigation in relation to its purpose and success criteria (which were defined in Chapter 4) and 3) the inter-subject variability.

The time scales of the plots of the selected features shown in Chapter 6 are consistent with the timing of the trials shown in Figure 5.2. The trials are time-locked to the movement stimuli or cues as explained in Section 5.2.1 and not to movement onset. Hence the exact times of commencement and completion of the performance or imagination of a movement in any given trial cannot be clearly defined, since a test subject will most likely not respond immediately to a cue. A fraction of a second delay between the computer's cue and the subject's response is created and most likely varies from trial to trial.

Movement onset is thus estimated to occur between 2.1 and 2.7 s and on average at approximately 2.3 s (these estimates are based on inspection of the subjects' ERPs and ITV ERD/ERS patterns; some of which are shown in Appendix A). Similarly, the commencement of the performance or imagination of muscle relaxation is estimated

to occur on average around 5.3 s such that complete relaxation is estimated to be attained around 5.6 s.

Movement preparation in the motor cortices is estimated to commence between 0.3 and 1.3 s, but on average around 0.8 s (refer to Section 2.6). Based on these assumptions, the early BP could commence from 0.3 s on average and the late BP from around 1.9 s (refer to Section 2.6.2 for details on the BP). The feature extraction method uses a time window of 0.3 s and has a resolution of 0.1 s (see Sections 5.2.5 and 5.2.6) which may blur the boundary between the pre-movement, movement performance/imagination and movement completion phases. Hence the estimations of the different movement phases are guidelines used to determine whether the selected features are extracted from the movement preparation, or movement performance/imagination phase.

For each investigation, the time and frequency characteristic of the TFSE and TFSM features are examined for individual subject's data and on average. The selected TFSE features are categorised into four groups i.e. mu pre-movement (MPM), beta pre-movement (BPM), mu movement performance/imagination (MMPI) and beta movement performance/imagination (BMPI). This is done based on typical ERD/ERS patterns described in the literature [56] (and explained in more detail in Section 2.6.1). This research maximises the information needed to classify between different types of hand movements on the same hand and thus includes both pre-movement and movement performance/imagination features [24][25][67]. Movement preparation or pre-movement features become increasingly valuable for a real time system in order to prevent delays between movement intentions and BCI responses [67]. TFSM features are grouped into early BP, late BP and movement-onset phases [63].

7.2 Right vs. Left Hand Movement Investigation (RLI)

7.2.1 Analysis of Selected Features

Figure 6.3 shows that MPM features occur more frequently for imagined movements than for real movements. This is verified in Figure 6.1, where MPM features are absent in 2 out of 3 subjects for real data, while are prevalent in all subjects for

imagined data. BPM features also appear more frequently in imagined data than in real data as shown in Figure 6.3. Figure 6.1 shows that BPM features are present in subjects 3 and 5 for real movements, while they are present in all 3 subjects for imagined movements. On the other hand, MMPI features are absent for all imagined movements for all subjects (see Figure 6.1), but shows some prevalence for real movements (see Figure 6.3).

As shown by Figure 6.3, features from imagined movements are largely from the pre-movement phase, while many features for real movements come from the time of estimated movement onset. Real movement BMPI features also show some commonality amongst subjects in the lower beta range (15 – 18 Hz) close to the estimated movement onset. These BMPI features are common to both real and imagined movements. Furthermore BMPI features are common in all subjects for real and imagined data, although their specific timing and frequencies differ between subjects and between real and imagined data.

TFSM features that appear in the time range estimated to correspond to the early BP are common in all subjects for real and imagined data, as shown in Figure 6.2. Figure 6.3 shows that fewer features occur within the estimated time of the late BP in real movements when compared to imagined movements. Conversely more features from the estimated movement onset phase are prevalent for real movements than for imagined movements.

A few points can be deduced from the above observations:

- In this research, for the investigation between right and left hand movements, the mu (and to a smaller extent beta) frequency range plays a more important role in movement preparation for imagined movements than in real movements, while the mu frequency range plays a more important role in movement performance than in movement imagination.
- In this investigation, imagined movements favour pre-movement TFSE features, while real movements favour TFSM and TFSE features close to movement onset.
- Activity in the beta frequencies during movement imagination and performance shows commonality and a large prevalence in this investigation.

The relevance of these deductions in relation to similar literature and to future work is discussed in Section 7.5.2.

7.2.2 Accuracy Analysis

The average accuracies for the RLI are summarised in Table 6.1. The success criterion mentioned in Section 4.2 requires an average classification rate of 80 %. Both the MD and ANN classifiers meet this criterion for real and imagined movements when using TFSE or COMB features, but not when using TFSM features alone. TFSE features provide the best results with an overall average of 86 %, followed by COMB features with an overall average of 83 %, and thereafter TFSM features with an overall average of 71 %. Reasons for this order are discussed later in this chapter in Section 7.5.2. Navarro *et Al* [26] report an average accuracy of 77 % when using features obtained from the theta, mu and beta frequency ranges, in conjunction with ICA, to discriminate between the EEG for right and left groups of different performed and imagined wrist movements. In a similar study, Khan and Sepulveda [55] obtain a classification accuracy of 89 % when discriminating between the right and left EEG for different kinds of imagined wrist movements individually. (These studies do not detail which measure of accuracy is used, hence the use of AOC is assumed since it is common [11]). This investigation obtains a similar average result when using ANN classifiers and TFSE features for imagined movements (88 %). Thus the results for the RLI meet its success criterion and match the best results obtained in recent similar studies. This suggests the suitability of the method to allow the investigation of EEG discrimination of different types of unilateral hand movements.

As shown in Table 6.1, the ANN classifier performs better than the MD clustering classifier in some cases but not in others. The results show that the ANN classifiers are well suited to TFSE features and this combination provides the best results in the investigation (average of 89 %). MD clustering is more suited to TFSM features and to COMB features. For real movements, the ANN classifiers perform slightly better than the MD clustering (80.4 % vs. 78.7 % respectively), while the converse is true for imagined movements (79.7 % vs. 80.7 % respectively). The results for TFSM imagined movements are better than for TFSM real movements (73 % vs. 68 %

respectively), while results for real movements when using TFSE or COMB features are slightly better than for imagined movements (87 % vs. 85 % and 84 % vs. 82 % respectively). Overall, the average results for real and imagined movements are similar (79.5 % vs. 80.2 % respectively). The comparison between real and imagined movements is discussed further in Section 7.5.4.

7.2.3 Inter-Subject Variability

In this investigation, the highest accuracy for an individual subject occurs for subject 3's imaginary movements (98 % using an ANN as shown in Figure 6.4) and is obtained using TFSE features. The lowest corresponding accuracy occurs for subject 2's real movements (71 % using MD clustering). This presents a large difference of approximately 40 % over real and imagined movements for TFSE. Average standard deviations, over real and imagined movements, of 9 % and 13 % are shown in Table 6.1 for TFSE and TFSM features respectively. The overall standard deviation for real movements is greater than that for imagined movements; 17 % vs. 7 % respectively for TFSM and 11 % vs. 9 % respectively for TFSE. Figure 6.4 shows classification accuracies between 53 % and 73 % for TFSE data for grouped subjects (labelled as *AllSubjects*), while Figure 6.5 shows corresponding accuracies between 54 % and 64 % using TFSM features. These results are not much better than the odds of random selection in a binary problem (50 %). This indicates very little commonality between subjects and along with the above-mentioned points, indicates a large inter-subject variance.

7.3 Wrist vs. Finger Movement Investigation (WFMI)

7.3.1 Analysis of Selected Features

According to Figure 6.9, the TFSE features for the WMFI are in general more evenly distributed than those for the RLI, which is most likely due to the use of more selected features (18 vs. 5) and more test subjects (5 vs. 3 for RH only). However, for imagined LH movements, the features are grouped into two regions i.e. before movement onset below mid beta frequencies (< 20 Hz) and toward the late stage of movement performance/imagination in the upper beta frequencies (> 20 Hz). The features for real movements for the RH also appear slightly more scattered than for

the RH imagined movements. Figure 6.9 also shows a higher prevalence of MPM features for RH imagined movements than for RH real movements; however this is not as clear for the LH. A higher prevalence of BPM features is shown in real movements in comparison to imagined movements and this is clearer for the left hand than for the right. Figure 6.9 also shows a higher prevalence of MMPI features in LH real movements than LH imaginary movements. BMPI features are common to right and left, real and imagined movements. As shown in Figure 6.7, groupings of BMPI features are clear for all of subject 2's data, for subject 4's RH real movements, subject 1's RH imaginary movements, subject 5's RH imagined movements and for subject 3's LH real and imagined movements.

TFSM features from the estimated region of the early BP are common to right and left, real and imagined movements, but occur more frequently for LH imagined movements, as shown in Figure 6.9. In contrast, TFSM features associated with the estimated time of movement onset appear more frequently in real than imagined movements. No pattern is clear for late BP features, but clusters of these features are shown in Figure 6.8 for the RH, real and imagined movements, for subject 2 and subject 5.

In summary, a few points can be deduced from the above observations:

- Pre-movement features pay a bigger role in imagined movement classification than in real movement classification. This is seen, in this investigation, in the pre-movement features for TFSM and mu TFSE, but not in beta TFSE. LH TFSE, and right and left hand TFSM analysis suggests that features extracted during or after movement onset play a more prominent role in movement performance than in movement imagination.
- Activity in the beta frequencies during movement imagination and performance shows commonality and a large prevalence (shown by numerous clusters of features) in this investigation.

The relevance of these deductions in relation to literature and to future work is discussed in Section 7.5.2.

7.3.2 Accuracy Analysis

The average accuracies for the WFMI are summarised in Table 6.2. The success criterion described in Section 4.3 requires average classification accuracy close to 70 %. TFSE or COMB features meet this criterion for real and imagined movements when using ANN classifiers, since they provide average classification accuracies between 70 % and 72 %. TFSE features provide the best results with an overall average of 66 %, followed by COMB feature types with an overall average of 63 %, and thereafter TFSM features with an overall average of 55 %. Reasons for this order are discussed later in this chapter in Section 7.5.2. Considering that this investigation involves a binary classification problem, TFSM features do not provide much better classification than selection by chance i.e. 50 %. The results of this investigation can be compared to other BCI binary classification problems involving discriminating EEG for different unilateral hand movements. The closest study is that by Vuckovic and Sepulveda [25], which achieved an accuracy of 73 % for real movements when averaged across all subjects and all six wrist movement pairs investigated. A corresponding average result of 71 % was achieved for imagined movements (also see Section 3.2). When using TFSE features and ANN classifiers, this investigation achieved similar average results of 70 % and 72 % for real and imagined movements respectively. Thus, the WFMI meets its success criterion and its results match those obtained in recent similar studies. Hence, the method using an ANN classifier and ICA as a spatial filter to aid the extraction of TFSE can discriminate between EEG for wrist and finger movements on the same hand for real and imagined movements.

As shown in Table 6.2, the ANN classifier performs better than the MD clustering in most cases in this investigation. The results show that the ANN classifiers outperform the MD clustering for all three sets of features and for real and imagined movements. The ANN results averaged over real and imagined movements for TFSE features are practically identical to those for COMB features (both 71 %), while the TFSE features outperform the COMB features (65 % vs. 59 % respectively) when using MD clustering. This is most likely due to the ability of the ANN to zero the TFSM input features (which hold little class discriminative capability and provide no improvement to classification) from the combined features set and perform classification based effectively on only TFSE features [97]. With MD clustering it is not possible to

eliminate the effects of the TFSM features in the combined feature set since all features are used to calculate the MD. Thus, the TFSM features may confuse the classifier and reduce accuracy.

Overall, the average accuracies for imagined movements are higher than those for real movements (63.9 % vs. 59.8 % respectively as shown in Table 6.2). The comparison between real and imagined movements is discussed further in Section 7.5.4.

7.3.3 Inter-Subject Variability

The inter-subject variability is gauged using results for TFSE features only. TFSM features performed poorly in this investigation, as shown in Figure 6.11 and Table 6.2, and this influences the COMB features (as explained further in Section 7.5.2).

The lowest result for an individual subject using TFSE features occurs for subject 3's LH real movements (56 % for ANN and 45 % for MD as shown in Figure 6.10). The highest corresponding accuracy occurs for subject 2's LH real movements (84 % using MD clustering). This presents are large difference of approximately 40 %. An average standard deviation of 8 % is shown in Table 6.2 for TFSE features for real and imagined movements. The standard deviation for real movements is greater than that for imagined movements; 9 % vs. 7 % respectively (refer to Section 7.5.4 for further discussion). Figure 6.10 shows classification accuracies between 49 % and 64 % for data for grouped subjects (labelled as *AllSubjects*), which are not much better the odds of random selection in a binary problem (50 %). This indicates very little commonality between subjects and along with the above-mentioned points indicates a large inter-subject variance.

7.4 Five Movement Differentiation Investigation (FMDI)

7.4.1 Analysis of Selected Features

Since the FMDI involves a significantly more complex problem than the WFMI (see Sections 3.2 and 4.3), it would intuitively require more features for classification. However, the optimum number of selected features for the FMDI is less than that of the WFMI. This is most likely due to the maximum number of features being limited

due to limited data for the FMDI (refer to Section 5.2.7 for details on feature selection). Hence, the TF plots (Figure 6.13, Figure 6.14 and Figure 6.15) for the selected features for the FMDI appear simpler. As shown in Figure 6.15, the features are evenly distributed with little commonality amongst the test subjects.

MPM features are apparent for most subjects' real and imagined movements as shown in Figure 6.13. These features appear more frequently for RH imagined movements than for RH real movements, as shown in Figure 6.15; however the same is not clear for the LH. One feature is common for all RH real movements and occurs around 10 Hz close to movement onset. BPM features are very prevalent in all the subject's movements, but no clear difference can be discerned between real and imagined movements. Figure 6.13 shows a prevalence of MMPI features in all plots except for subject 5's LH. According to Figure 6.15, the prevalence of MMPI features appears similar for real and imagined movements for both hands. A common MMPI feature for LH imagined movements is shown around 4 s at 10 Hz. BMPI features occur more frequently in LH real movements than in LH imaginary movements, but the opposite is seen in RH movements. They are prevalent in all plots except two and are frequent for both hands for real and imagined movements.

TFSM features related to the early BP are found in most subjects' data, as shown in Figure 6.14, and are more prevalent in imagined movements than in real movements for both hands. Late BP features are less prevalent than early BP features and are almost completely absent for LH imagined movements, as shown in Figure 6.15. Features associated with the estimation of movement onset are more prevalent in real movements than imagined ones for both hands (shown in Figure 6.15) and are common to all subjects' data (shown in Figure 6.14).

Since there are only a few instances where successful classification is obtained in this investigation (which are attributed to TFSE features as discussed in Section 7.4.2), the selected TFSE features are analyzed for these cases. According to Figure 6.10, classification accuracies around 70 % were obtained for real movements for subject 2's LH, subject 1's RH and subject 5's RH; and for imagined movements for subject 1's RH and subject 2's RH. However, there is little commonality amongst these cases

in terms of feature selection, besides the prevalence of BMPI features. The TF characteristics of these features still differ in each case.

In summary a couple of points can be deduced from the above observations:

- Pre-movement features pay a bigger role in imagined movement classification than in real movement classification. This is seen, in this investigation, in the pre-movement features for TFSM and mu TFSE, but not in beta TFSE.
- Activity in the beta frequencies during movement imagination and performance shows commonality and a large prevalence in this investigation.

The relevance of these deductions in relation to literature and to future work is discussed in Section 7.5.2.

7.4.2 Accuracy Analysis

As shown in Figure 6.16 and Figure 6.18, the success criterion described in Section 4.4 is met in the following six cases for either TFSE features or COMB features or both: subject 2 RH imaginary (MD and ANN), subject 1 RH real (ANN only), subject 1 RH imaginary (MD only), subject 2 LH real (MD only) and subject 3 LH real (ANN only). These individual classification accuracies range from 76 % to 67 %, with 4 cases obtaining accuracies of 70 % or more, for either or both feature types mentioned above. Subject 1 showed success for real and imagined movements. Despite these few successful cases, the average accuracies are low as shown in Table 6.3.

TFSE features provide the best results with an overall average of 52 %, followed by COMB features with an overall average of 48 %, and thereafter TFSM features with an overall average of 27 %. Reasons for this order are discussed later in this chapter in Section 7.5.2. Considering that this investigation involves a 5-class classification problem, TFSM features do not provide much better classification than selection by chance i.e. 20 %. The results of this investigation can be compared to other BCI multiclass problems, although most of these problems are 4-class classification problems and do not involve movements on the same limb (refer to Section 3.2). Hence, they do not present all the challenges of the FMDI, yet provide the closest comparison. An average accuracy of 63 % is obtained in this investigation when using ANN classifiers and TFSE features for real movements, however, the best result for

imagined movements is 55 % when using TFSE features with the MD classifier. These results are comparable to the results of other multiclass BCI problems (refer to Section 3.2).

As shown in Table 6.3, the ANN classifier performs better than the MD clustering for real movements, while MD clustering is preferred for imagined movements. For all three feature sets, MD and ANN classifiers show similar results. Averaged over all feature types and for real and imagined movements, the classifiers performances are very similar (44.5 % for MD vs. 45.1 % for ANN). The overall average results for imagined movements are better than those for real movements (44.3 % vs. 40.0 %). However, the best results are obtained for real movements (63 %). This implies a smaller variance for imagined movements, which is also shown by the comparisons of the standard deviations in Section 7.4.3.

The results for the FMDI meet its success criterion and are similar to results obtained in other multiclass BCI problems, despite the FMDI holding more challenges. Hence, the method using ICA as a spatial filter to aid the extraction of TFSE features has shown the ability to discriminate between EEG for WE, WF, FE, FF and the TR on the same hand for real and imagined movements in a few subjects. This shows the possibility of improved offline EEG interpretation for a sensorimotor BCI to the degree where the neural motor control signals for five basic hand movements can be differentiated on a synchronous, single-trial basis. The method, however, does not provide consistent results and was not successful for all the subjects' data. This implies that the method is not sufficient to allow consistent accurate classification.

7.4.3 Inter-Subject Variability

As with the WFMI (refer to Section 7.3.3), the inter-subject variability is gauged using results for TFSE features only. The lowest result for an individual subject using TFSE features occurs for subject 5's LH imaginary movements (22 % for ANN and 33 % for MD as shown in Figure 6.16). The highest accuracy corresponding accuracy occurs for subject 2's LH imaginary movements (75 % for both classifiers). This presents are large difference of approximately 50 % and emphasises and the inconsistency shown by the other results in this investigation (shown in Figure 6.16

and Figure 6.18). A standard deviation of 11 % is shown in Table 6.3. Imagined movements show an overall smaller standard deviation relative to that for real movements (14.9 % vs. 17.8 %). Figure 6.16 shows classification accuracies between 19 % and 25 % for data for grouped subjects (labelled as *AllSubjects*), which are basically the odds of random selection (20 %). This indicates very little commonality between subjects. The above-mentioned points indicate a large inter-subject variance.

7.5 Overall Discussion for all Investigations

7.5.1 Overall Accuracy

Considering the detailed discussions of the results presented in Sections 7.2.2, 7.3.2 and 7.4.2, the accuracy of the research is summarized below:

1. All investigations show success for real and imagined movements.
2. For the RLI, success is obtained when using TFSE or COMB features along with either MD or ANN classifiers.
3. For the WFMI, success is obtained when using TFSE or COMB features along with ANN classifiers only.
4. For FMDI, success is obtained when using TFSE or COMB features along with either MD or ANN classifiers.
5. The best average results, across real and imagined movements for all subjects, are obtained using the combination of TFSE features and ANN classifiers i.e. 89 %, 71 % and 57 % for the RLI, WFMI and FMDI respectively.
6. TFSE and ANNs provided accuracies ranging between 76 % and 67 % (for either real or imagined movements) in three subjects in the FMDI.
7. Despite the success of the FMDI, its low average result along with the large variability in its results (see Section 7.4.3) shows that its method needs to be improved to provide higher, consistent classification accuracies.
8. The results of all three investigations are comparable to their respective similar BCI studies.
9. The MD clustering classifiers are superior to ANN classifiers for imagined movements in some cases i.e. in the RLI using TFSM and COMB features, and in the FMDI using TFSE and COMB features.

10. COMB features are almost completely dependent on the TFSE features for successful classification, as explained in Section 7.5.2.

As explained in Section 4.5, these results imply that the designed method, using ICA along with TFSE features and ANN classifiers provides a positive solution to the problem of the research. The method is suitable for real and imagined movements and is more reliable and consistent for right vs. left and wrist vs. finger movement EEG classification.

It should be noted that some EMG experiements with common hand movements i.e. WE, WF, FE and FF achieved average classification accuracies over 90 % [7][9]. These studies involved multiclass classification problems with between 6 and 8 classes of hand movements [7][9]. Extensive subject training and real-time classification was used in [9] and it is thus not directly comparable to this research. Nevertheless, the results of these EMG studies highlight the differences in the current capabilities of EEG and EMG methods for prosthetic/orthotic hand control and empahsises the need for increased EEG-based research.

7.5.2 Overall use of Features

For all three investigations, the commonly selected TFSE features originated from the beta frequency range during movement performance or movement imagination (details are discussed in Sections 7.2.1, 7.3.1 and 7.4.1). Classic ERD/ERS patterns deal more with the mu range [56], but other frequency ranges may hold discriminative information for more advanced hand movements [25][55][100]. Promising results for wrist movements have been shown using the delta [25] and gamma bands [55] and this research shows some promise using the beta band. Vuckovic and Sepulveda [25] refers to another study, involving four types of wrist movement, where the largest variation between two wrist movements in general originated from the 12 – 30 Hz frequency band. An online, asynchronous BCI investigation allowed the partial restoration of the grasp function in a tetraplegic patient using beta activity [49]. Bai *et Al* [100] also found that EEG features from beta band activity provided the largest class discrimination in a sensorimotor BCI. It was suggested that the EEG beta rhythm can support a reliable, high performance BCI for both healthy test subjects

and patients with neurological disorders [100]. The results of this research support the latter notion for healthy subjects.

It was expected that COMB features would provide the best results since MRCP and ERD/ERS features would provide complimentary information to improve classification results [30] (refer to Section 2.6) . However, this is not the case as explained in Sections 7.2.2, 7.3.2 and 7.4.2. For all three investigations the best results were obtained using TFSE features, followed COMB features and then TFSM features.

Dornhege *et Al* [30] explored different methods of combining MRCP and ERD/ERS features and found that the simple concatenation of the two feature sets added little benefit over the use of single feature types. In this research, simple concatenation of the two feature types is used (refer to Section 5.2.7), which explains why in most cases COMB features do not perform better than TFSE features. TFSM features carry significantly less class discriminative information than TFSE features, as shown by their relatively poorer results in all three investigations. Hence their combination with TFSE features using concatenation does not provide additional discriminative information. Instead they may contradict the TFSE information and confuse the classifiers, thus reducing the accuracies for COMB features. In the WFMI, the ANN managed to eliminate the effects of the MRCP features in most cases [97], allowing the COMB features to perform close to the ERD/ERS features. In order to improve results, combination methods based on the assumption that ERD/ERS and MRCP are independent should be used [30]. An example would be to use a classifier for each feature type and combine the outputs of each classifier [16][30].

The TFSM feature extraction method was designed and tested in the RLI and the features' performances were satisfactory in this investigation (71 % overall accuracy mentioned in Section 7.2.2). However, they did not perform as well as the TFSE features. When the feature extraction method was applied to the WFMI and the FMDI, the TFSM features extracted proved ineffective. This can be attributed to MRCP patterns not easily appearing on single-trial basis and only emerging in an ERP after averaging over many trials [51]. Although ERD/ERS patterns also emerge clearly only after averaging over many trials, they are more reliable for single-trial

analysis [51]. Gu *et Al* [24] also reported that the early BP, late BP and peak negativity of MRCP (see Section 2.6.2) did not differ much for different kinematic movements on the same hand. This research involves five different kinematic movements (see Section 1.2); hence features related to MRCP cannot clearly distinguish them. Research suggests that MRCP favours dynamic movement discrimination, while ERD/ERS favours kinematic movement discrimination, [63][64] (refer to Section 3.2). This also explains the better results obtained for features related to ERD/ERS in this research. Hence feature combination is useful when classifying between different dynamic and kinematic movements as shown by [24].

In summary, this research shows a dominance of features originating from beta sensorimotor rhythms and some studies have reported similar results [100]. In order for feature combination of ERD/ERS and MRCP to improve classification results, especially for complex problems such as multiclass problems or movement discrimination on the same limb, two areas should be addressed: 1) the improvement of the MRCP feature extraction method in order to add valuable class discriminative information and 2) the improvement of the feature combination method that takes advantage of the independence of the feature types [30].

7.5.3 Inter-Subject Variability and ICA

As shown in Sections 7.2.3, 7.3.3 and 7.4.3, all three investigations show large inter-subject variability. This is based on the:

- high standard deviations,
- large differences between the highest and lowest accuracies,
- limited commonality in the TF characteristics of the selected features and
- low accuracies for the datasets grouping data for all subjects.

The subjects' performances also vary from one investigation to the next. For example, subject 3 holds the highest accuracy in the RLI (98 %), but obtains the worst TFSE result in the WFMI (45 %). The results for RH, LH, real and imagined movements are also not consistent within individual subjects. This is expected since ERD/ERS and other EEG patterns differ for real and imagined movements [67] and for right and left hand movements [30][39][65][66][67].

This EEG inter-subject variability exists since the following varies from one individual to the next: the exact position and size of M1, the amount of cortical activity and the electrode placement when measuring EEG [67]. Other factors may also contribute towards the EEG variance between test subjects [10]. It becomes difficult to develop a system capable of learning the EEG patterns for different individuals due to this large inter-subject variance [10]. Hence a BCI used to control a prosthetic/orthotic hand needs to be adapted to each user [10][65].

In this research ICA, along with visual inspection (see Section 5.2.4) is used to separate the EEG into independent sources that are most likely to represent motor control activity. This approach is different to those used in other studies involving ICA and different types of hand movements, where ICs from all over the head can potentially yield features [25][26][67]. It is beneficial since it ensures that non-sensorimotor activities (such as the visual alpha rhythm) are not used for classification [16][65]. It is also not affected by skewed electrode placement and varying M1 positioning to the degree that other spatial filters, such as SL, may be [10][45][67]. The success of the WFMI shows the ability to differentiate between EEG for wrist and finger movements, whose control regions on the cortex are adjacent [32] (see Figure 2.2). Furthermore, the success of the FMDI shows that separable information from overlapping neural sources was provided in some cases [10], since some movements, such as WE and WF are controlled by the same part of M1 (see Figure 2.2). This demonstrates the spatial resolution provided by the combination of high resolution (128 channels) EEG measurement and ICA [41].

The success of all three investigations suggests that the approach using ICA, along with visual IC selection based on a priori knowledge, is valuable. Such an approach can be used to create subject-specific BCIs [29] (see Section 3.4), which can also accommodate for changes in sensorimotor patterns as a result of motor impairment (see Section 2.5) [47][52].

7.5.4 Real vs. Imaginary

Differences between the results of real and imagined movements are discussed in terms of selected features, overall accuracy and inter-subject variability within each

investigation (Sections 7.2, 7.3 and 7.4). Common issues are discussed in this section in order to draw conclusions on the EEG interpretation of real and imagined movements in this research.

The RLI and WFMI show that features generated during movement performance are more prevalent than those generated during movement imagination. This is most likely due to EEG activity being greater during movement performance than during movement imagination [67][77]. Also, the RLI, WFMI and to a smaller extent, the FMDI, show that pre-movement features are more prevalent in imagined movements than in real movements. Morash *et Al* [67] found that preparatory ERD/ERS was better with predicting movement imagery than with predicting movement performance. A possible explanation could be that EEG activity is stronger during preparation for movement imagination than that for movement performance, since movement imagination requires more concentration [101]. However, more research needs to be done to investigate this result and to understand the underlying neural mechanisms involved in the preparation of motor imagery and performance [67].

Overall, the BCI performed slightly better for imagined movements than for real movements. This is shown by higher overall average accuracies for imagined movements in the WFMI and FMDI. This is contrary to the expectation that real movement classification would outperform imagined movement classification, since motor imagery involves less M1 activation than movement [67][77] and many studies reported better results for motor execution than motor imagery [67][77]. However, some studies reported similar results for real and imagined movements [25]. A possible explanation for the unexpected result in this research is that all the test subjects were university students who were familiar with motor imagery. Consequently their concentration levels and imaginative skills may have been above average, which may have increased the classification accuracy for imagined movements [101]. Subjects who participated in the study in [24] reported an ease of imagining movements such as WE since it is used in everyday life. Hence the use of WE, WF, FE, FF and the TR in everyday life may have made the motor imagery tasks easier for the test subjects, thus enhancing their sensorimotor EEG patterns, despite having no training. This may also have contributed to imagined movement classification outperforming that for real movements.

In all three investigations, imagined movements show smaller standard deviations than real movements, showing more consistency in the former case (see Sections 7.2.3, 7.3.3 and 7.4.3). Vuckovic and Sepulveda [25] also reported more consistency with imagined movements than with real movements. A possible reason is that from trial to trial, real movements may vary slightly in terms of speed, force and direction, while movement imagination may not bear these slight trial-to-trial variations. It may also have to do with differences in the inter-subject variability for real and imagined movements. Reasons for this are unknown and need to be explored [25].

The BCI method used in this research is able to classify imagined and performed hand movements with the similar accuracies (in some cases slightly better). All three investigations are successful for real and imagined movements. It should be noted that this movement imagery will differ for people who have motor impairments (such as amputations and spinal cord injuries) [47][52] and the method used in this research may need to be adjusted accordingly.

7.6 Significance of Findings

Successful results for the WFMI imply that EEG can be used to extract separable neural information from neighbouring areas of the motor cortex (shown in Section 2.2) [12]. Some successful results for FMDI show that it is possible to use EEG to discriminate the neural signals for different real and imagined hand movements on the same hand in a multiclass problem. The research shows that improved EEG interpretation is possible for the essential hand movements of WE, WF, FE, FF and the TR. The research contributes towards improving the flexibility of BCI motor imagery and increasing the number of separable movement classes that a BCI can handle [12]. However, there is a tradeoff between the number of separable classes (which can relate to degrees of freedom) and the accuracy of the system; therefore a balance should be found [25]. The research also introduces a unique combination of movements to BCI research (to the best of the author's knowledge), which may be explored in future BCI studies (see Section 7.7). Some of these movements have not been found in BCI literature (FE and the TR) and may stimulate the exploration of

other basic hand movements, such as adduction and abduction, or different combinations of basic hand movements [2][3][5][12].

The research suggests that ICA may be very valuable in improving the spatial resolution and interpretation of EEG as explained in Section 7.5.3. Training test subjects and tailoring the BCI and the combination of techniques to each test subject could significantly improve results [10][39]. This may allow the development of a real-time BCI capable of using motor imagery to control a multifunctional prosthetic hand for an amputee or an orthotic hand for the victim of a stroke or spinal cord injury [6][10][13][12]. This may provide a safer and more affordable alternative to neurally controlled prosthetics/orthotics solutions that rely on invasive recordings such as ECoG [10] (see Section 1.4).

7.7 Limitations of Method and Future Work

More work is needed to improve on the accuracy and consistency of the offline, synchronous, single-trial EEG discrimination of WE, WF, FE, FF and the TR (as explained in Section 7.5.1). A few shortcomings were identified during the research process and should be corrected in future work. Future work is suggested to validate and expand on the results obtained in this research.

The experimental procedure should be modified slightly. Firstly, the length of each trial should be lengthened from 7 s to approximately 10 s [25][27][28][55] (refer to Section 5.2.1). The movement preparation phase should be increased from 2 s to 3 s to comfortably accommodate the 2 s of neural preparatory activity that precedes movement onset [16]. The rest time should also be increased to approximately 4 s [25] to allow a longer period from which to calculate a reference or rest state and to clearly differentiate movement from non-movement. Secondly, more data should be collected in terms of the number of healthy test subjects and the number of trials per subject [25][67]. The number of trials per subject is more important since analysis should be done on an individual subject basis (as explained in Section 5.2.1). EMG can also be used to mark the onset of performed movements so that analysis based on movement onset can be done, instead of having to estimate movement onset [28]. It can also be used to verify that no muscle activation occurs during movement

imagination [24]. The use of a 256 electrode EEG measurement system may improve the spatial resolution further [41][102].

Another method of to extract MRCP-related features should be explored, which could possibly combine time-domain and spectral features [24]. The full MRCP frequency should be explored as well as features from other frequency bands, such as gamma and theta [55][25][86] (see Section 2.6). Another method of feature combination, such as the use of group classifiers, should also be explored [11][30] (refer to Section 7.5.2). The combination of MD and ANN classifiers can also be applied to each feature type individually to possibly improve results [11]. Support vector machines have shown success in BCI investigations and should also be explored [11].

Similar studies should be performed to validate the results of this research [12] and to verify the possibility of EEG discrimination for WE, WF, FE, FF and the TR. Similar investigations to the RLI, WFMI and FMDI should be conducted using other spatial filters such as CAR, SL and CSP to evaluate the effectiveness of ICA in this application [24][26][28][55] (refer to Sections 2.4 and 3.4 for supplementary information on spatial filters).

Other BCI studies involving the five (wrist and finger) movements used in this research can also be done to expand on the knowledge of these movements [12]. Work should be done to develop a system that can discriminate EEG for the five essential hand movements or for wrist and finger movements in real-time [65][12] (see Section 2.5). This would most likely involve training a single healthy test subject and tailoring the BCI to suit their EEG patterns [10][12][65]. In doing so, the complexity of the algorithms and techniques used in the method should be considered [12]. A similar study could aim to develop an asynchronous BCI that can differentiate between hand movement imagery on the same hand [48] (see Section 2.5). Another follow up study may add force and speed parameters to kinematic wrist and finger movements and use feature combination to discriminate the EEG for different kinematic and dynamic wrist and finger movements [24][61] (also refer to Section 3.2). Another study may involve exploring the possibility of EEG discrimination between imagined wrist and finger movements in a stroke victim or an amputee [49][100] (see Section 2.5).

7.8 Conclusion

The results within each investigation and the overall results of the research are discussed in this chapter. The investigations and the research are discussed in terms of the features used, the inter-subject variability and the accuracies of the results. The differences in the results for real and imagined movements are also discussed. Conclusions on the success of each investigation and on the research as a whole are drawn and the significance of the findings of the research is mentioned. Corrections to the method and future work are suggested. The next chapter concludes the research.

Chapter 8

Conclusion

8.1 Introduction

In conclusion, this chapter summarizes the objectives, methods and results of the research as well as the main deductions from the discussion in the previous chapter.

8.2 Research Summary

The research is directed towards improved EEG interpretation in a sensorimotor BCI for the control of prosthetic/orthotic hand, in order to allow the user more degrees of freedom and improved functionality. In order to provide hand functionality that will allow such users to perform basic daily activities, five essential hand movements are selected i.e. wrist extension, wrist flexion, finger extension, finger flexion and the tripod pinch. The author is unaware of any BCI literature concerned with the combination of these movements and such research is deduced to be minimal. Hence it is necessary to explore the possibility of differentiating the neural control signals for these movements using EEG, as an intermediate step. Hence, this research addresses this general problem in part by investigating the possibility of EEG discrimination for five essential hand movements (real and imagined) in healthy subjects in an offline, synchronous manner on a single trial basis.

The study was divided into three sub-investigations; which all used ICA to aid the extraction of TFSE and TFSM features; the BD to select the best features and reduce the dimensionality of the extracted features; and MD clustering and ANNs to classify the TFSE and TFSM features, individually and in combination. The first investigation explored the use of the above-mentioned techniques to differentiate between the EEG associated with right and left hand groupings of the five movement types. This evaluated the performance of the method by comparing the results with those of other right vs. left BCI studies in the literature. The second investigation attempted to classify between EEG patterns for wrist and finger movement groupings of the selected movements on the same hand, while the third investigation explored the possibility of differentiating the EEG for each movement type on the same hand. The second and third investigations explored the possibility of EEG classification for more advanced hand movements on the same hand.

The method provided similar average results for real and imagined movements in most cases, although the results for imagined movements were more consistent. ANN and MD-based classifiers provided similar results overall, with the ANNs outperforming the MD clustering in the WFMI. The results also show that the combination of TFSE and TFSM features did not improve the classification accuracy. The combination of TFSE features and ANNs provided the best results, with average classification accuracies of 89 %, 71 % and 57 % for the RLI, WFMI and FMDI respectively as well as respective highest classification accuracies of 98 %, 84 % and 75 %. TFSM features provided satisfactory classification for the RLI but not for the WFMI and FMDI. Significant class-discriminative information originates from beta sensorimotor activity, which is consistent with the findings of other BCI studies.

The results show that all three investigations were successful. Hence the designed method shows the possibility of improved offline EEG interpretation in a sensorimotor BCI. This was shown by differentiating the neural motor control signals for five essential hand movements in a few healthy test subjects on a single-trial basis. The method also allows EEG interpretation such that the movement control of different major parts of the hand i.e. the wrist and fingers, can be distinguished. The method can also provide equivalent differentiation of right and left hand motor control signals obtained from EEG in relation to existing methods. However, more

work needs to be done to improve on the accuracy and consistency of the method when differentiating the individual five movements. All of the above holds for real and imagined movements for healthy subjects.

The research provides a platform for future EEG-based BCI work involving the combination of WE, WF, FE, FF and the TR. This research affirms the value of ICA in terms of improving EEG spatial filtering in this regard. Future work should be done to validate, improve on and comprehensively explain the results obtained in this research, especially for the FMDI. The experimental procedure, the extraction of features related to MRCP and the method of feature combination should be improved. Studies can also be undertaken to expand on the use of the five essential hand movements.

8.3 Conclusion

This chapter concludes the research aimed towards improving EEG interpretation in a sensorimotor BCI for the control of a prosthetic or orthotic hand. Such a system can greatly improve the quality of life for those who have suffered amputations, strokes or spinal cord injuries. This can be achieved by allowing such individuals to perform simple daily tasks by controlling a prosthetic or orthotic hand using only their minds.

Appendix A

Scalp Plots and Graphs for Visually Selected ICs

A.1 Scalp plots

A.1.1 Scalp plots for the RLI

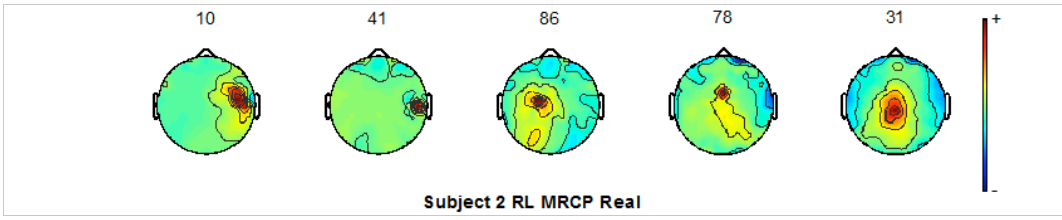

Figure A.1: Scalp plots of all visually selected ICs for subject 2's real, right and left hand (RL), MRCP filtered data.

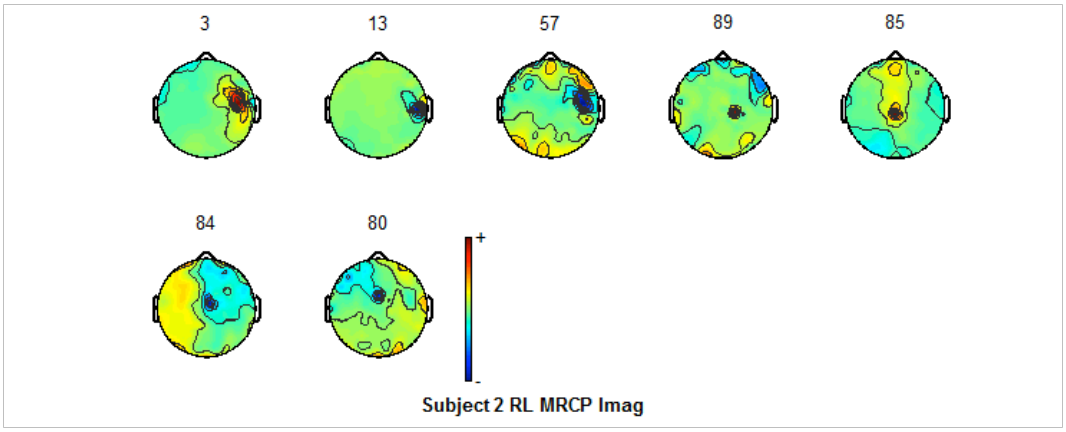

Figure A.2: Scalp plots of all visually selected ICs for subject 2's imaginary, right and left hand (RL), MRCP filtered data.

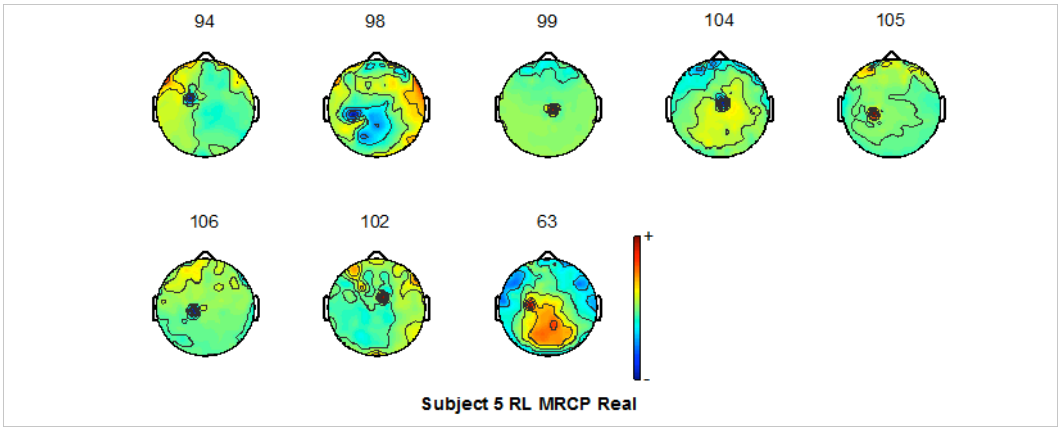

Figure A.3: Scalp plots of all visually selected ICs for subject 5's real, right and left hand (RL), MRCP filtered data.

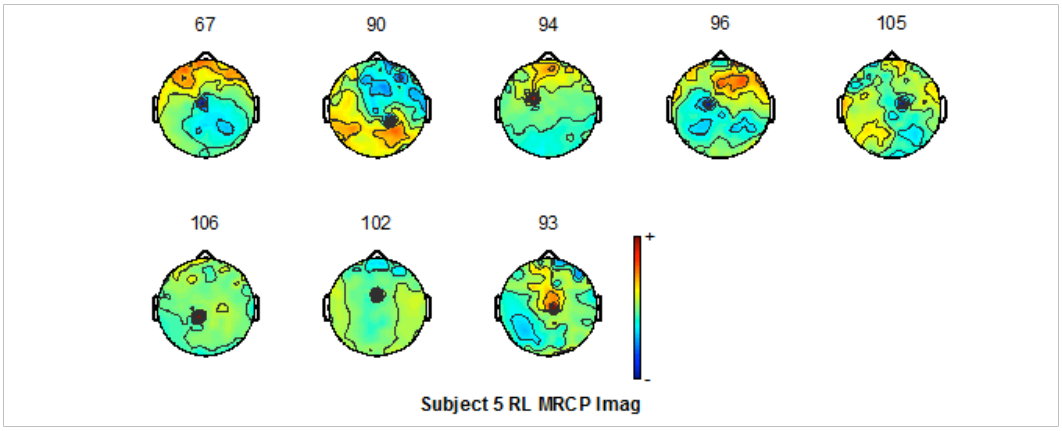

Figure A.4: Scalp plots of all visually selected ICs for subject 5's imaginary, right and left hand (RL), MRCP filtered data.

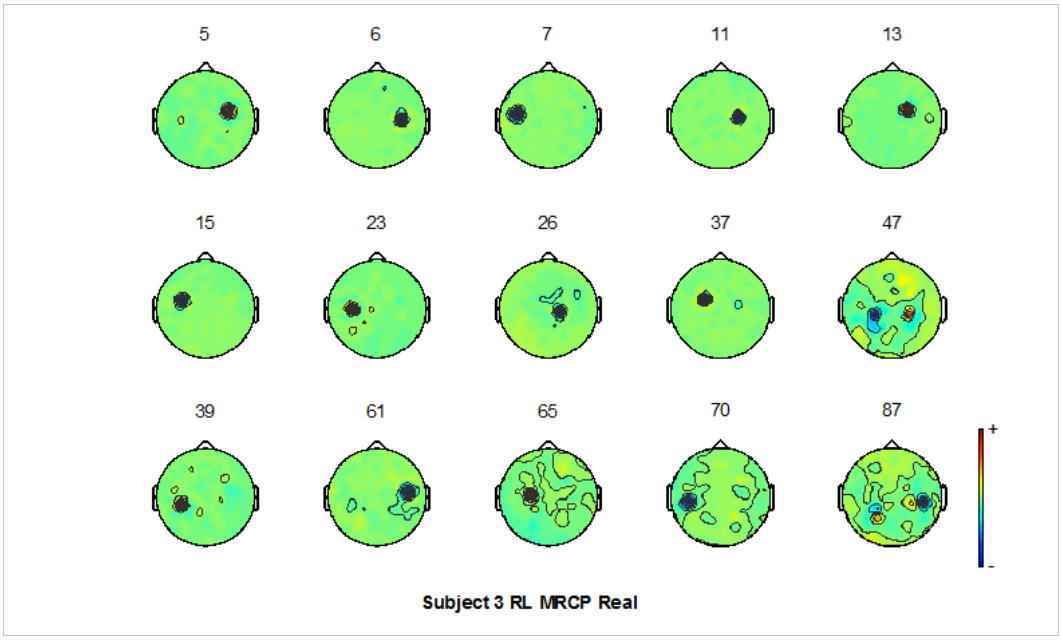

Figure A.5: Scalp plots of all visually selected ICs for subject 3's real, right and left hand (RL), MRCP filtered data.

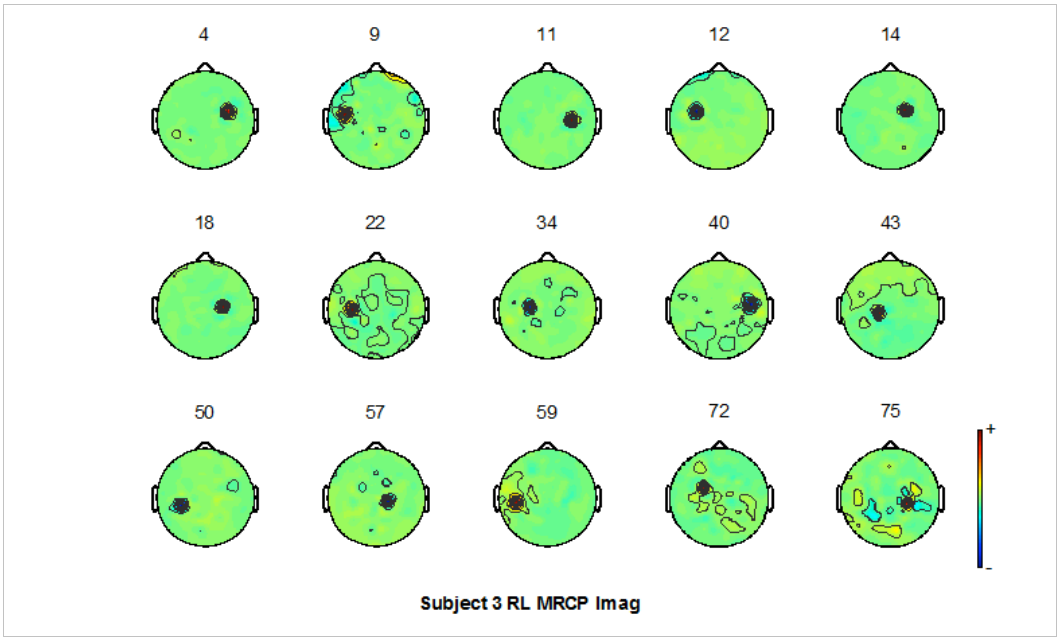

Figure A.6: Scalp plots of all visually selected ICs for subject 3's imaginary, right and left hand (RL), MRCP filtered data.

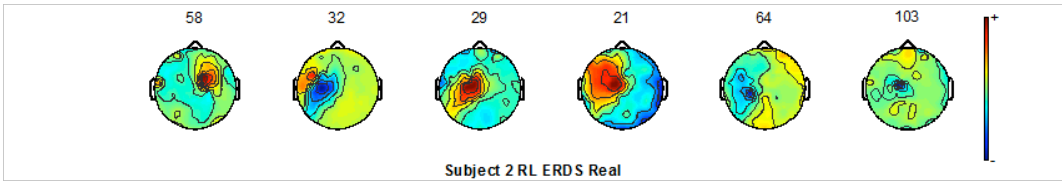

Figure A.7: Scalp plots of all visually selected ICs for subject 2's real, right and left hand (RL), mu and beta (ERD/ERS) filtered data.

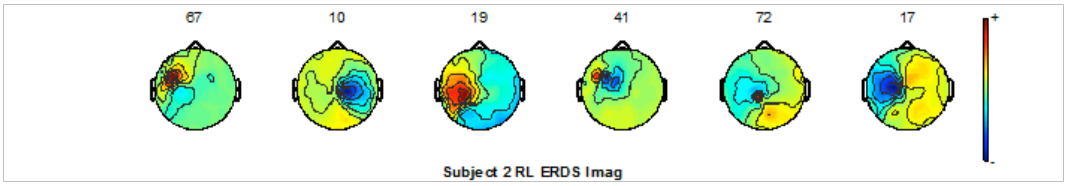

Figure A.8: Scalp plots of all visually selected ICs for subject 2's imaginary, right and left hand (RL), mu and beta (ERD/ERS) filtered data.

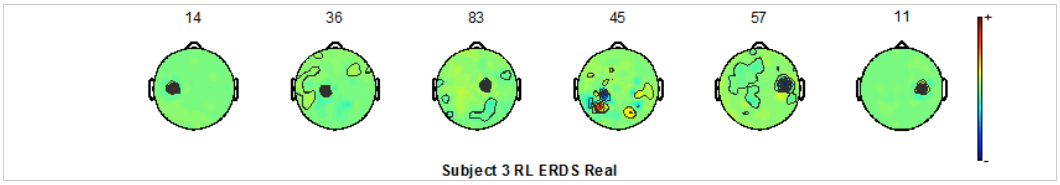

Figure A.9: Scalp plots of all visually selected ICs for subject 3's imaginary, right and left hand (RL), mu and beta (ERD/ERS) filtered data.

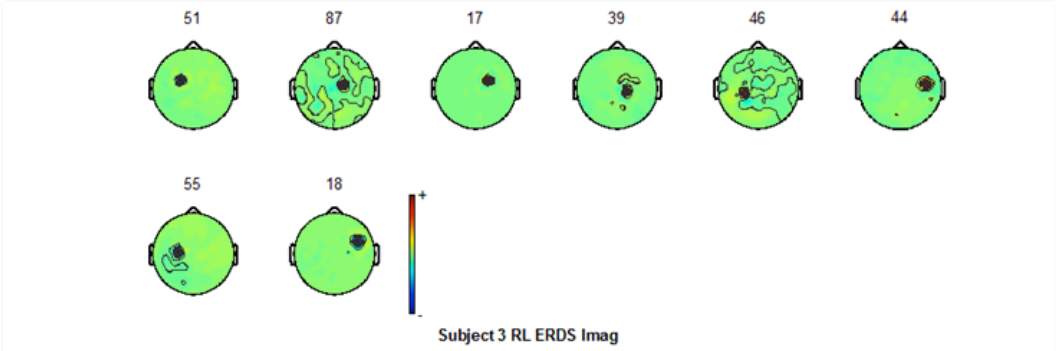

Figure A.10: Scalp plots of all visually selected ICs for subject 3's imaginary, right and left hand (RL), mu and beta (ERD/ERS) filtered data.

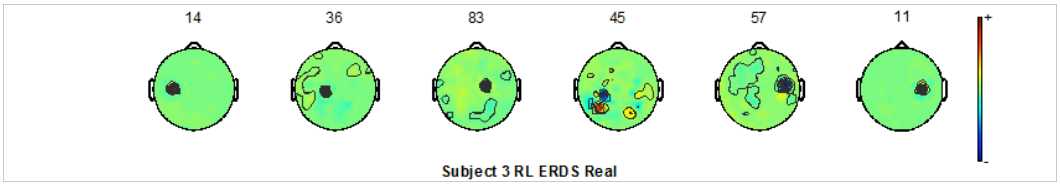

Figure A.11: Scalp plots of all visually selected ICs for subject 3's imaginary, right and left hand (RL), mu and beta (ERD/ERS) filtered data.

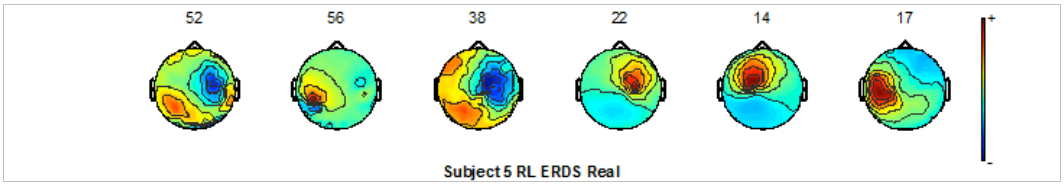

Figure A.12: Scalp plots of all visually selected ICs for subject 5's real, right and left hand (RL), mu and beta (ERD/ERS) filtered data.

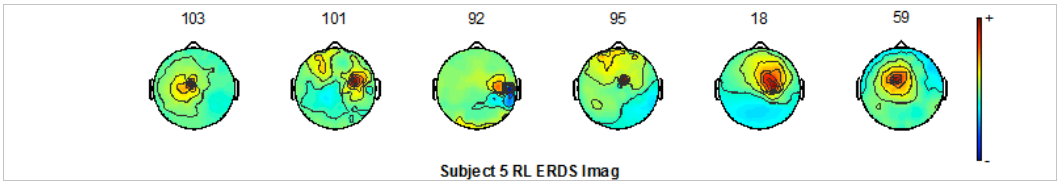

Figure A.13: Scalp plots of all visually selected ICs for subject 5's imaginary, right and left hand (RL), mu and beta (ERD/ERS) filtered data.

A.1.2 Scalp Plots for WFMI and FMDI

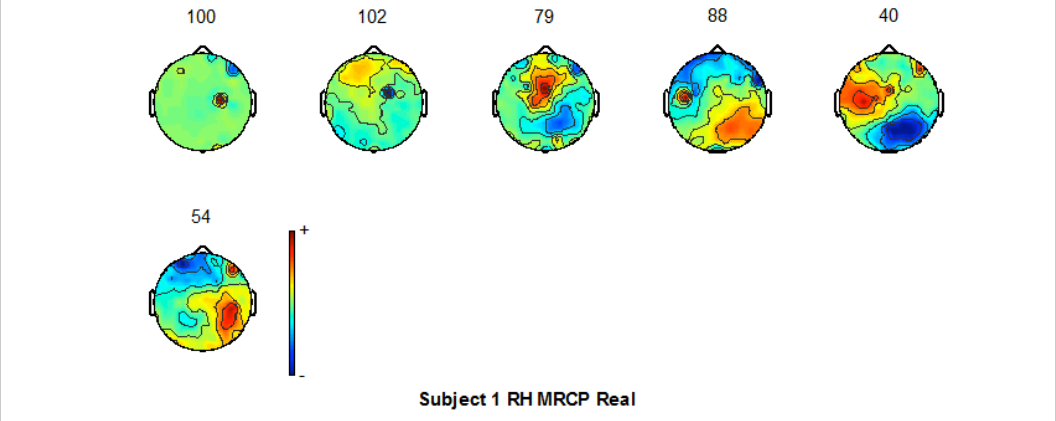

Figure A.14: Scalp plots of all visually selected ICs for subject 1's real, right hand (RH), MRCP filtered data.

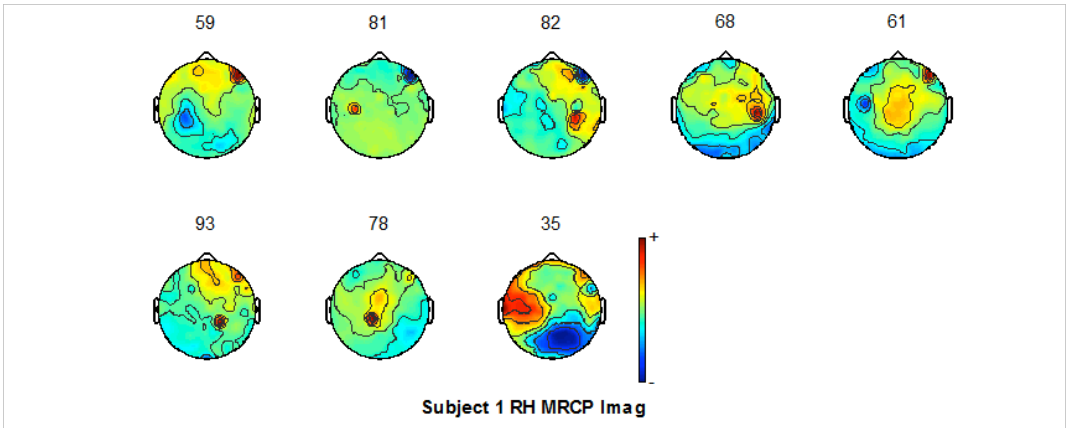

Figure A.15: Scalp plots of all visually selected ICs for subject 1's imaginary, right hand (RH), MRCP filtered data.

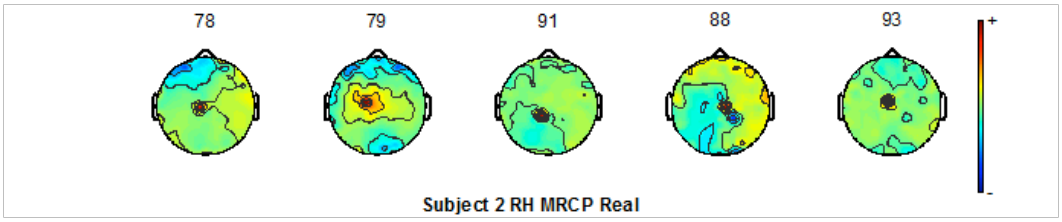

Figure A.16: Scalp plots of all visually selected ICs for subject 2's real, right hand (RH), MRCP filtered data.

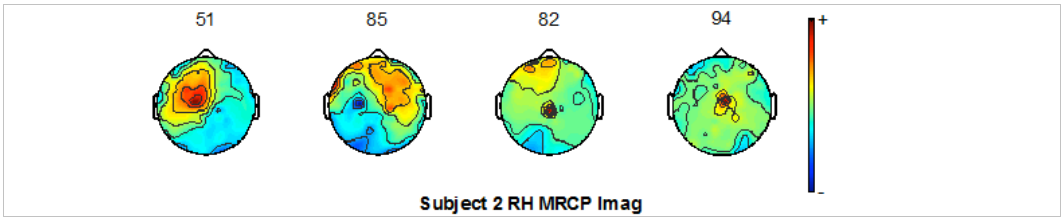

Figure A.17: Scalp plots of all visually selected ICs for subject 2's imaginary, right hand (RH), MRCP filtered data.

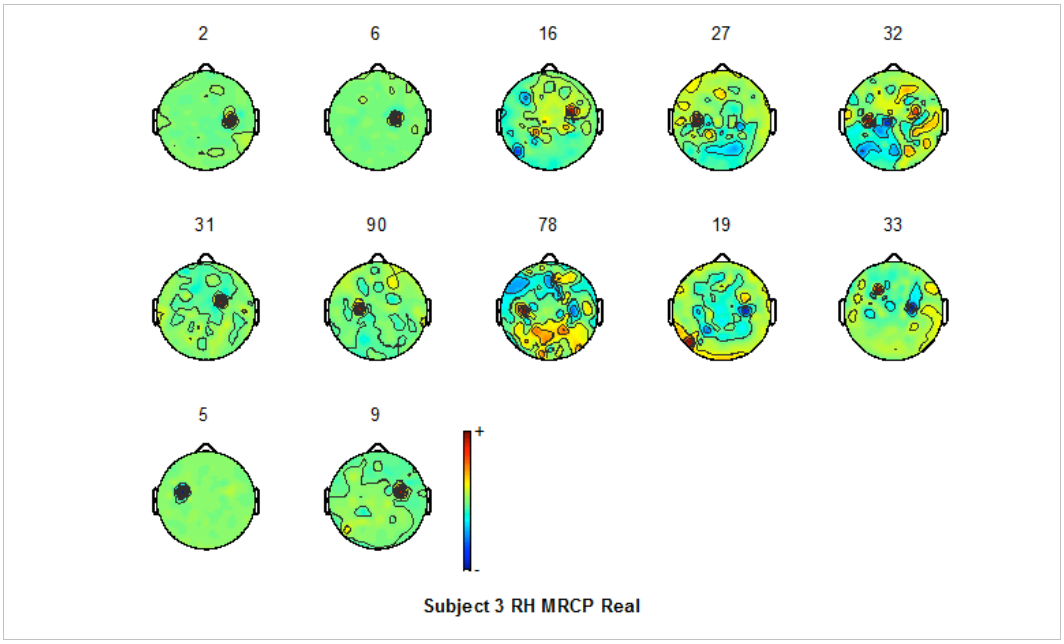

Figure A.18: Scalp plots of all visually selected ICs for subject 3's real, right hand (RH), MRCP filtered data.

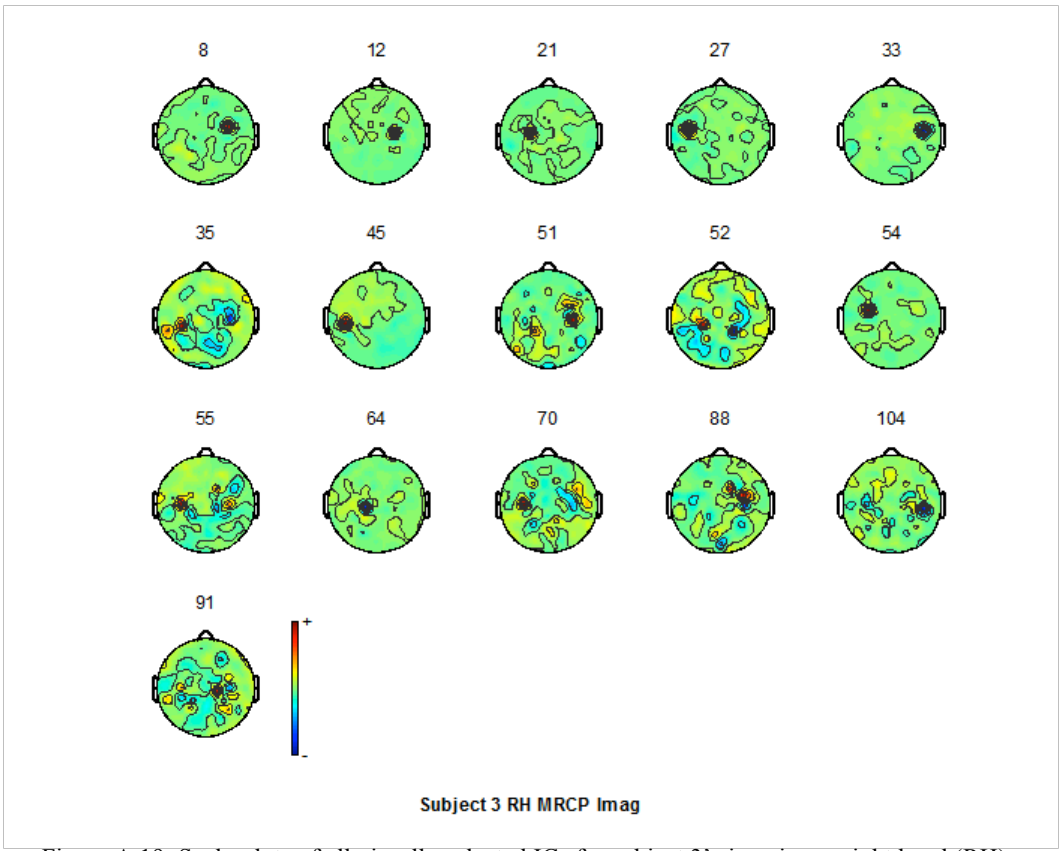

Figure A.19: Scalp plots of all visually selected ICs for subject 3's imaginary, right hand (RH), MRCP filtered data.

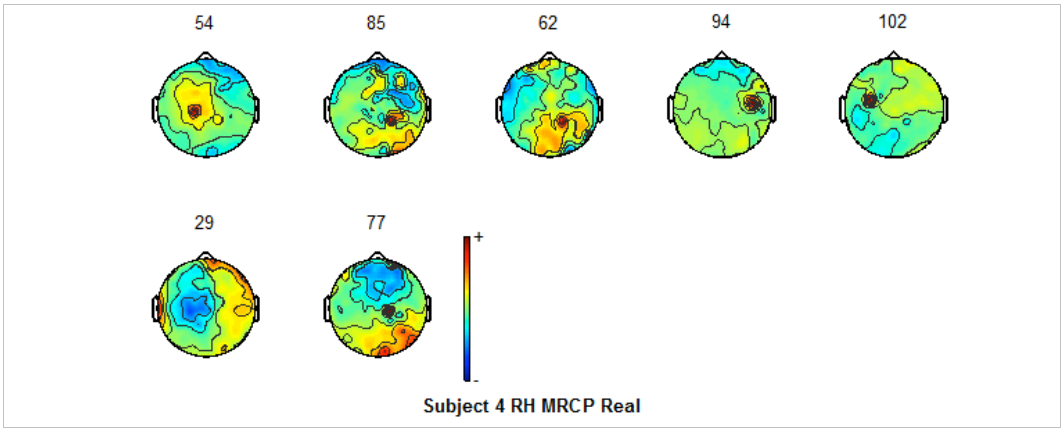

Figure A.20: Scalp plots of all visually selected ICs for subject 4's real, right hand (RH), MRCP filtered data.

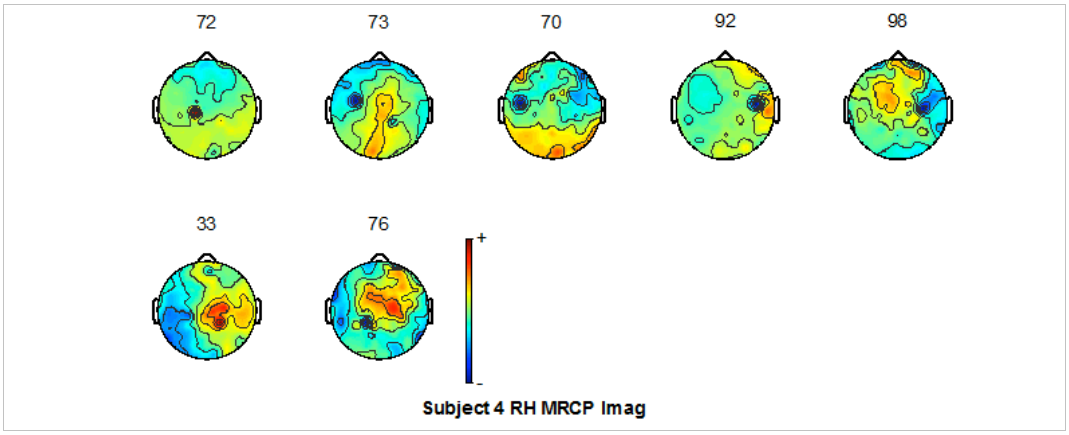

Figure A.21: Scalp plots of all visually selected ICs for subject 4's imaginary, right hand (RH), MRCP filtered data.

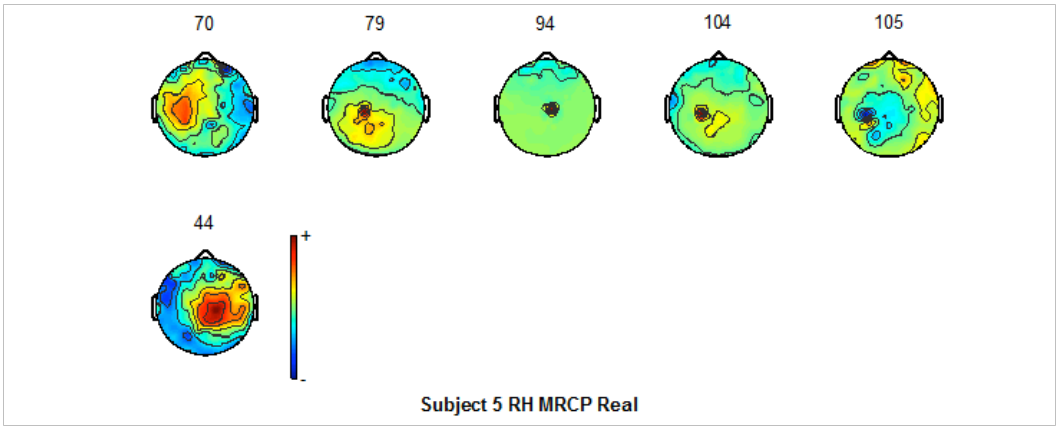

Figure A.22: Scalp plots of all visually selected ICs for subject 5's real, right hand (RH), MRCP filtered data.

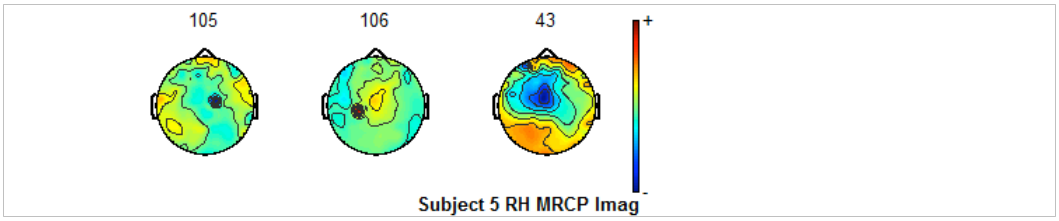

Figure A.23: Scalp plots of all visually selected ICs for subject 5's imaginary, right hand (RH), MRCP filtered data.

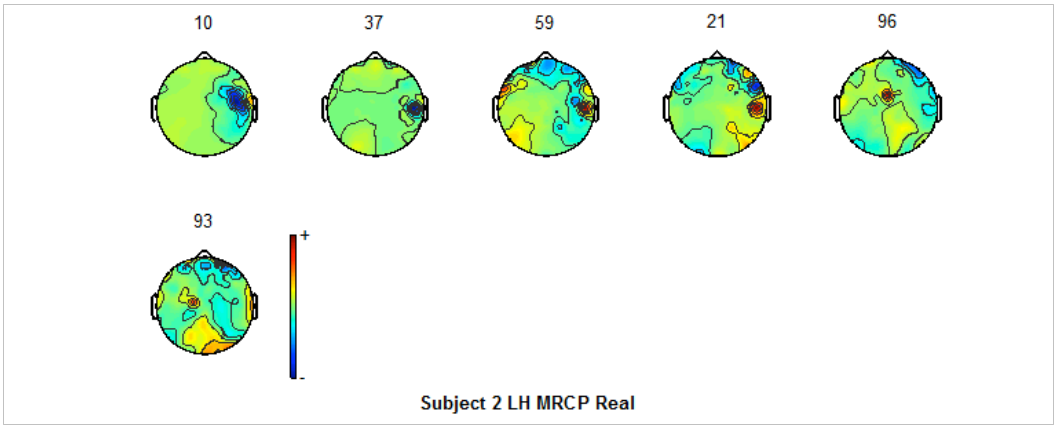

Figure A.24: Scalp plots of all visually selected ICs for subject 2's real, left hand (LH), MRCP filtered data.

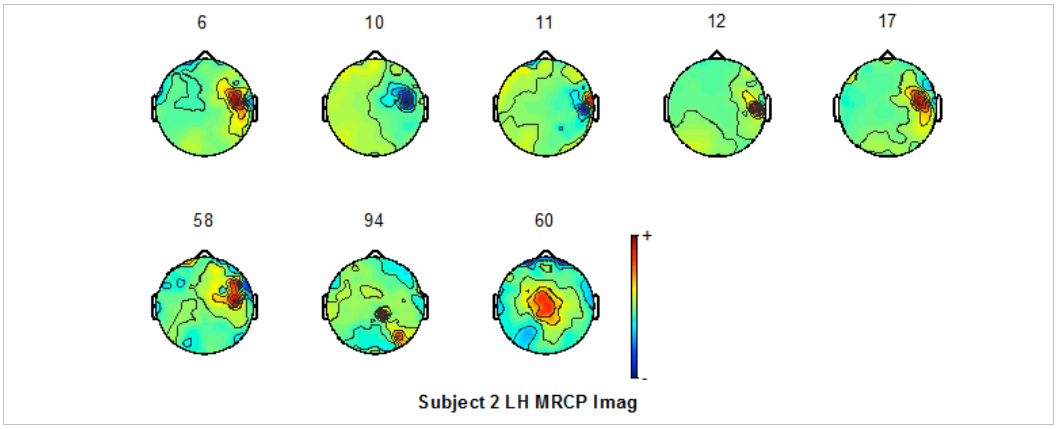

Figure A.25: Scalp plots of all visually selected ICs for subject 2's imaginary, left hand (LH), MRCP filtered data.

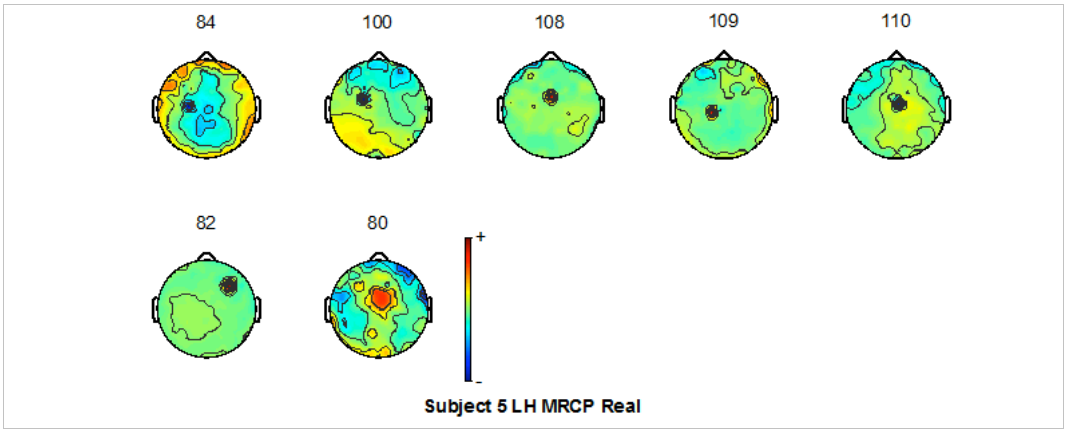

Figure A.26: Scalp plots of all visually selected ICs for subject 5's real, left hand (LH), MRCP filtered data.

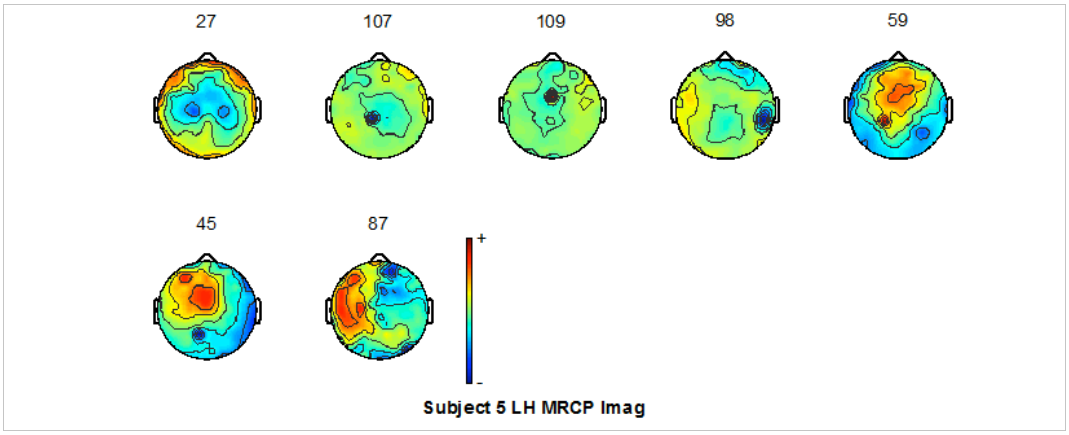

Figure A.27: Scalp plots of all visually selected ICs for subject 5's imaginary, left hand (LH), MRCP filtered data.

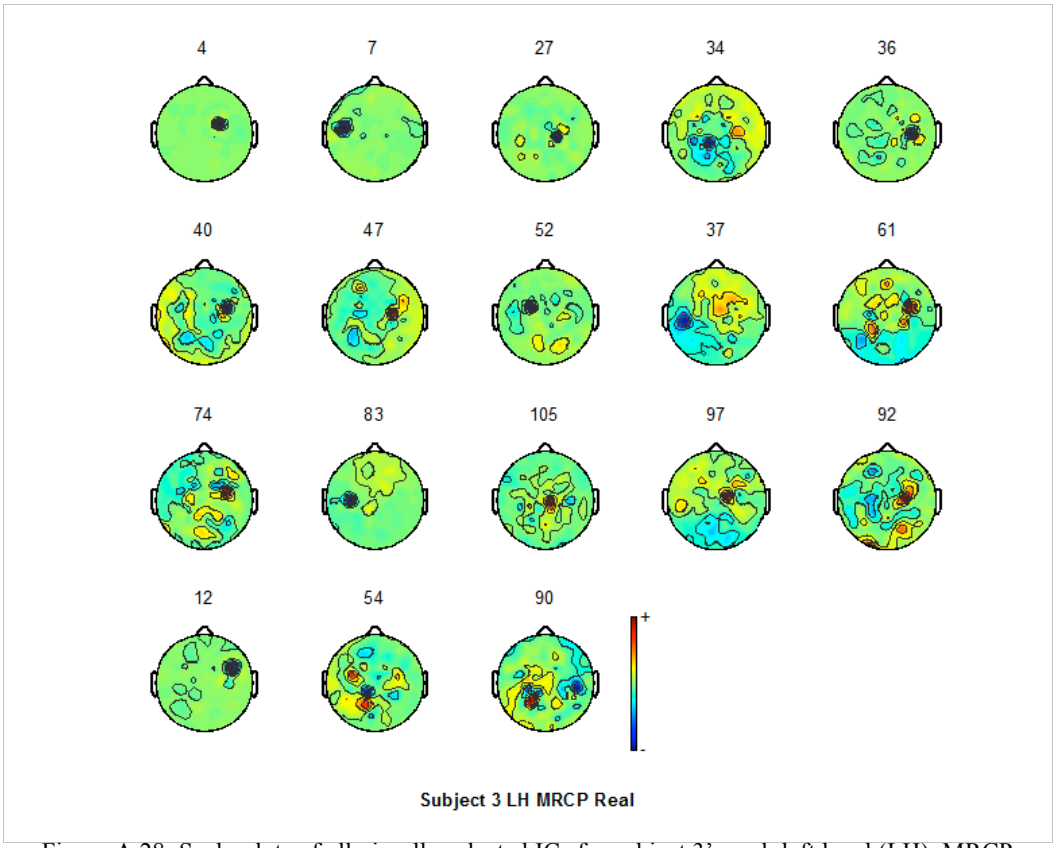

Figure A.28: Scalp plots of all visually selected ICs for subject 3's real, left hand (LH), MRCP filtered data.

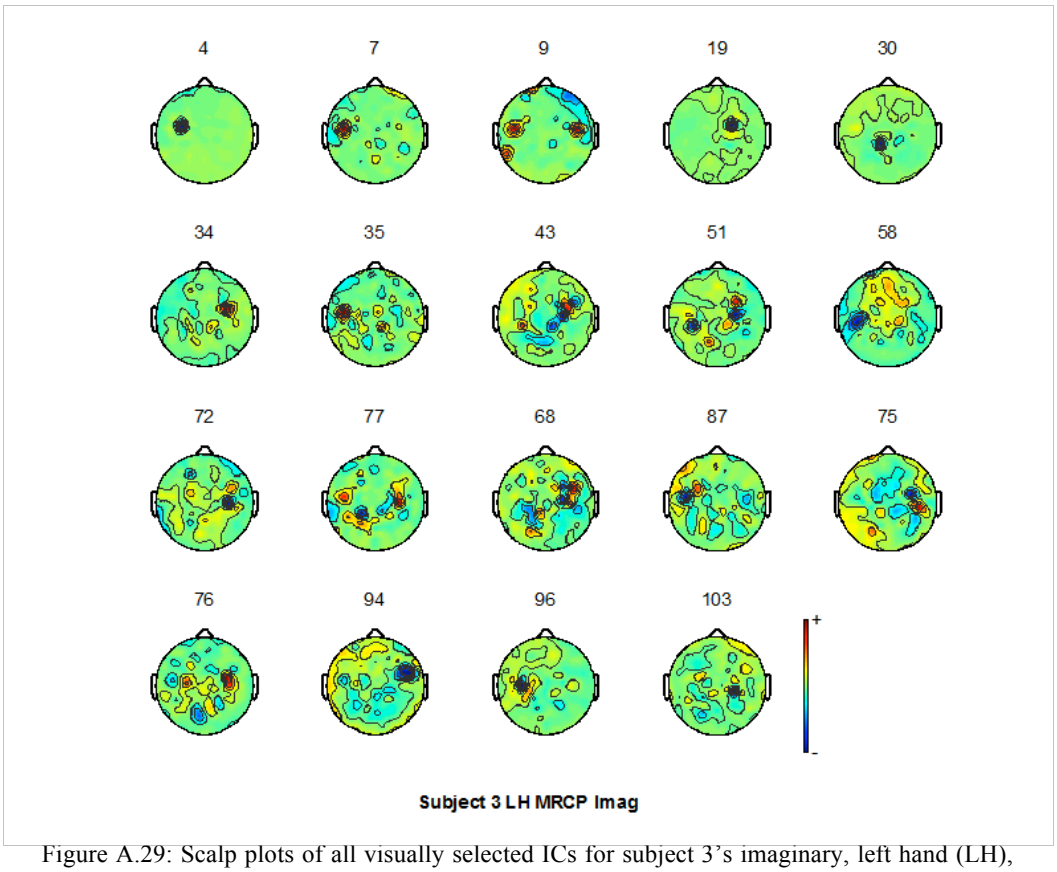

Figure A.29: Scalp plots of all visually selected ICs for subject 3's imaginary, left hand (LH), MRCP filtered data.

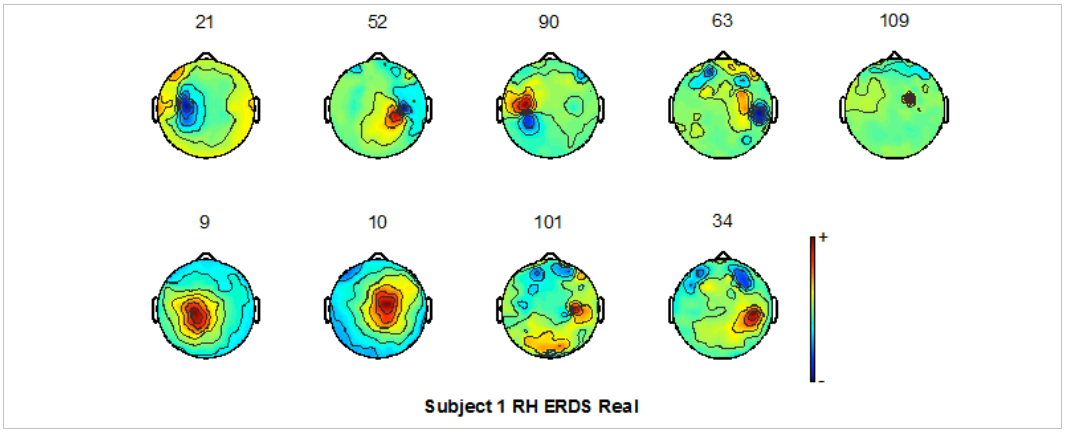

Figure A.30: Scalp plots of all visually selected ICs for subject 1's real, right hand (RH), mu and beta (ERD/ERS) filtered data.

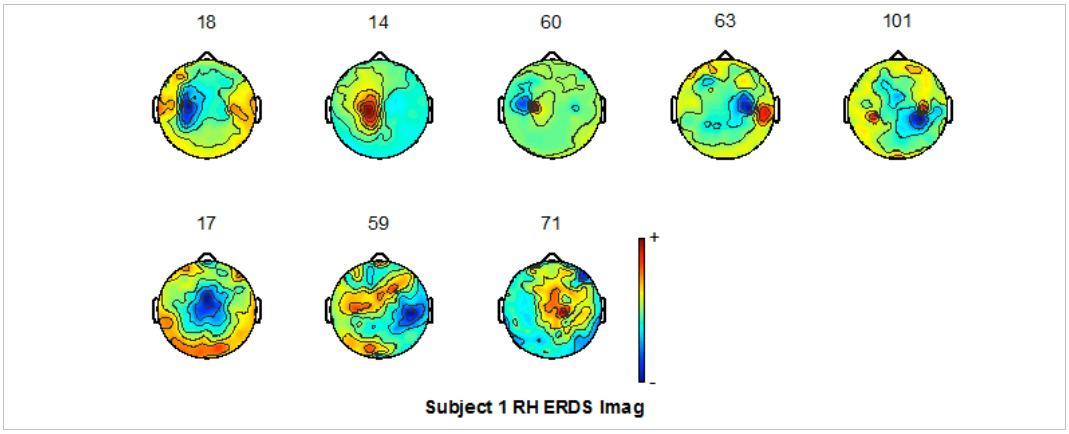

Figure A.31: Scalp plots of all visually selected ICs for subject 1's imaginary, right hand (RH), mu and beta (ERD/ERS) filtered data.

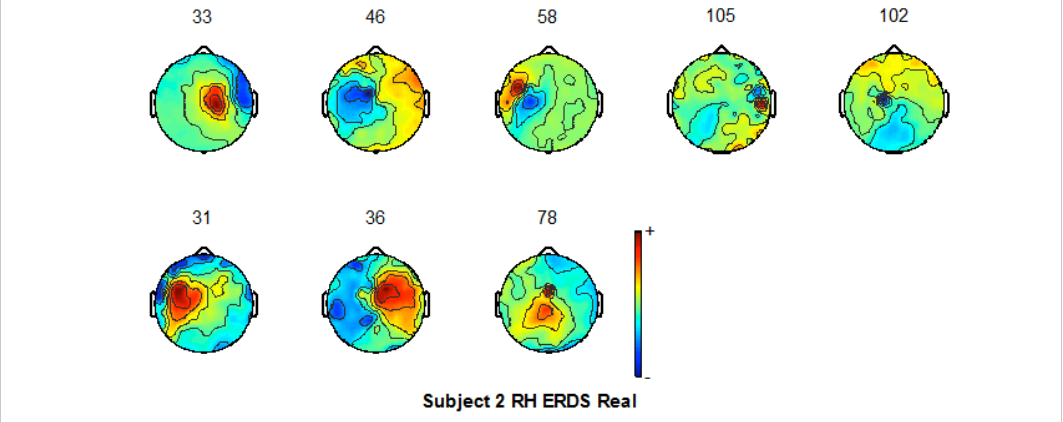

Figure A.32: Scalp plots of all visually selected ICs for subject 2's real, right hand (RH), mu and beta (ERD/ERS) filtered data.

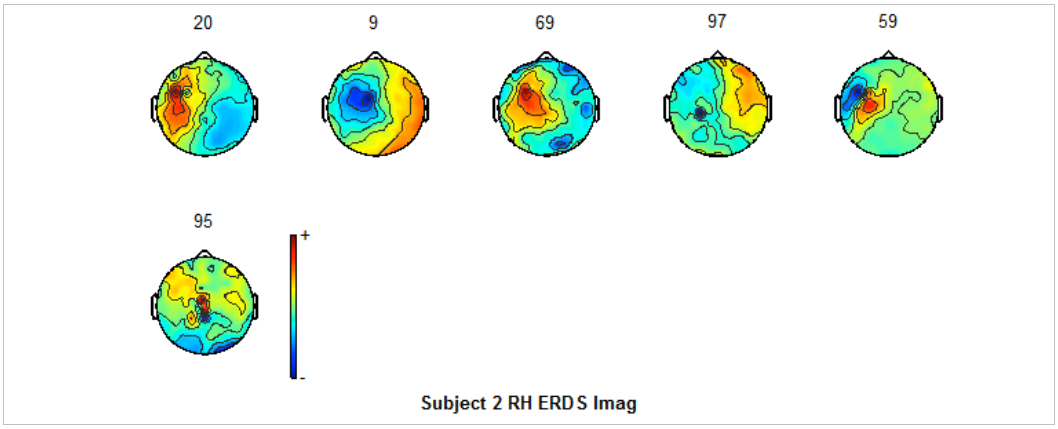

Figure A.33: Scalp plots of all visually selected ICs for subject 2's imaginary, right hand (RH), mu and beta (ERD/ERS) filtered data.

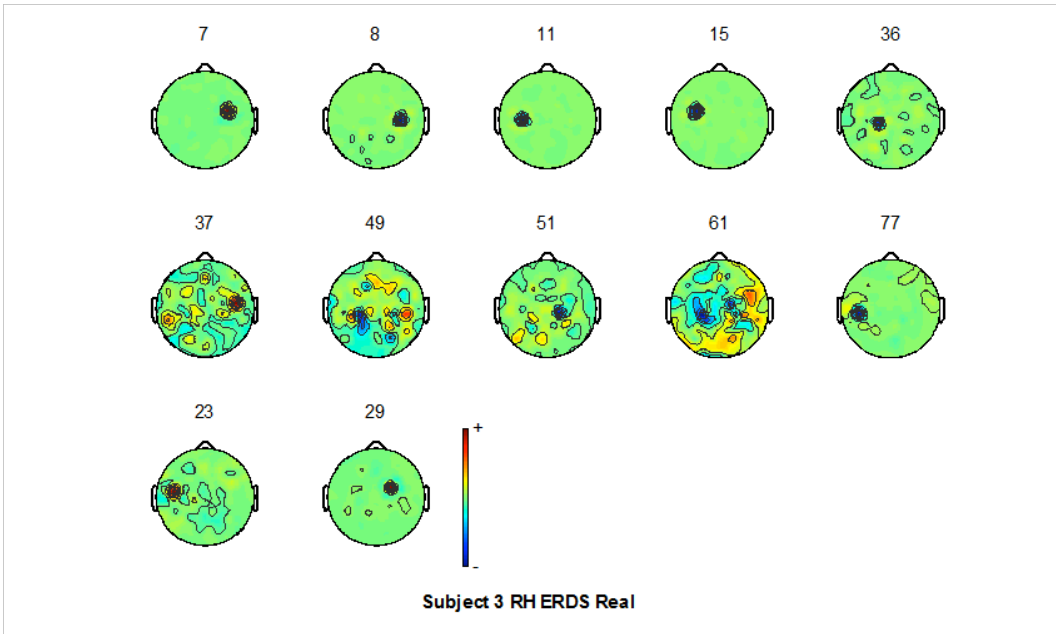

Figure A.34: Scalp plots of all visually selected ICs for subject 3's real, right hand (RH), mu and beta (ERD/ERS) filtered data.

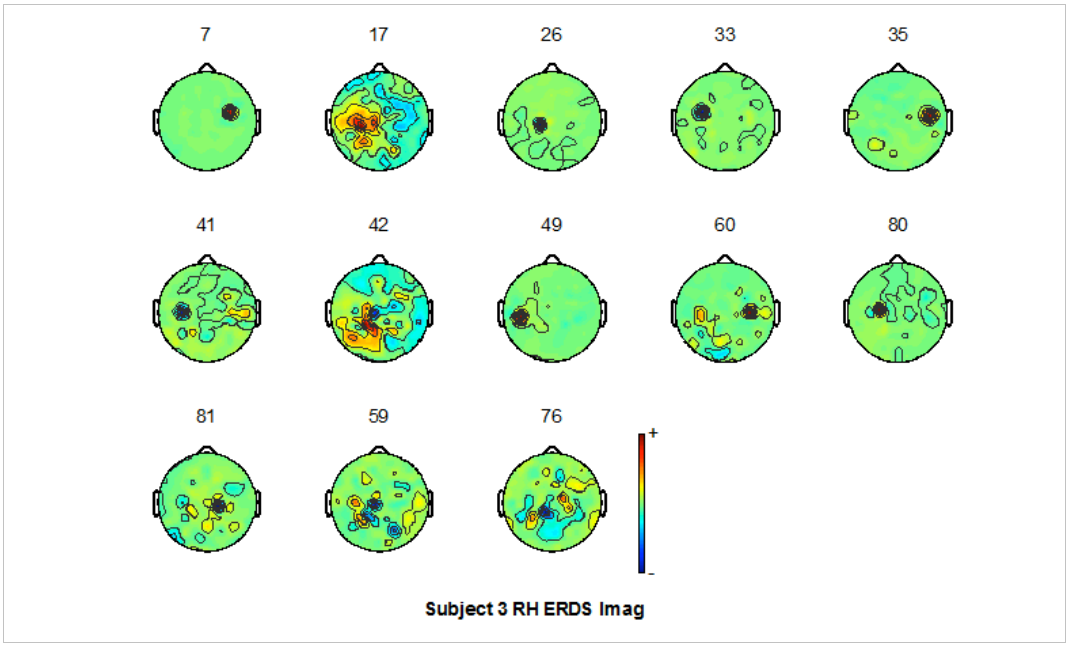

Figure A.35: Scalp plots of all visually selected ICs for subject 3's imaginary, right hand (RH), mu and beta (ERD/ERS) filtered data.

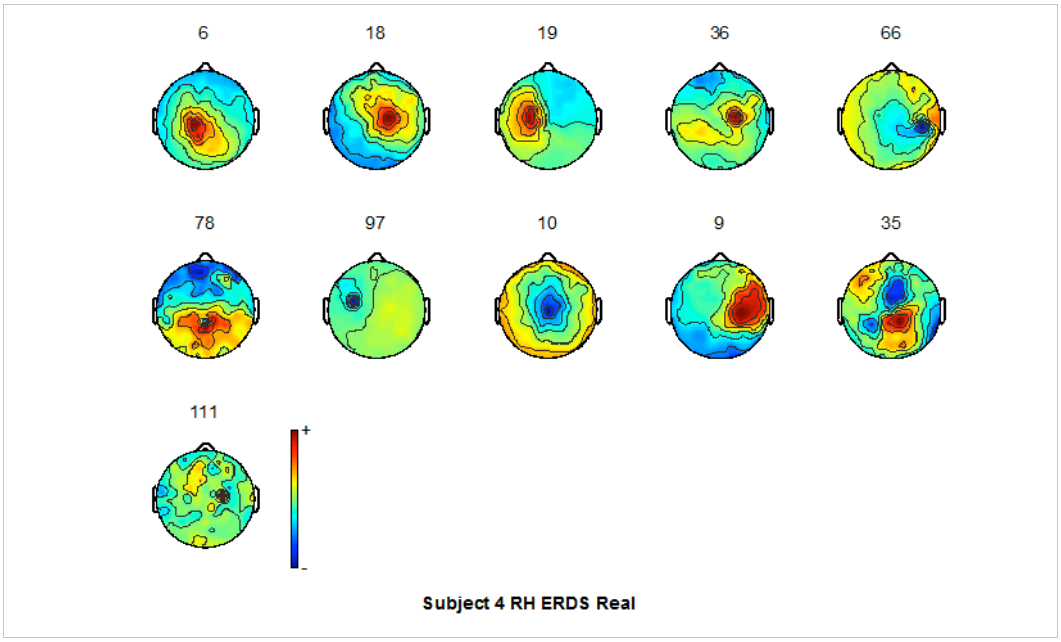

Figure A.36: Scalp plots of all visually selected ICs for subject 4's real, right hand (RH), mu and beta (ERD/ERS) filtered data.

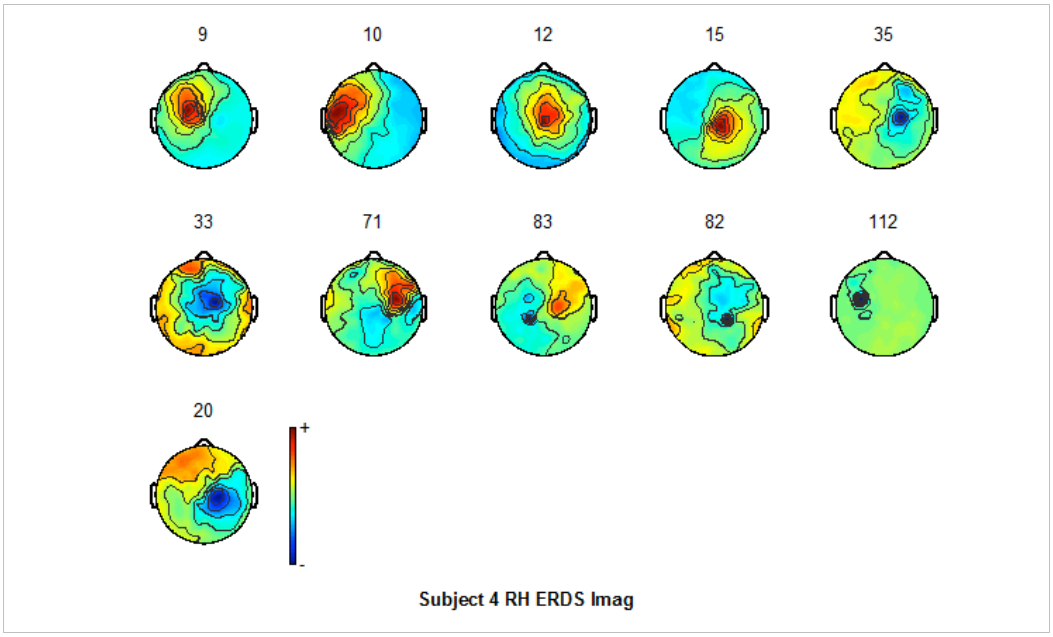

Figure A.37: Scalp plots of all visually selected ICs for subject 4's imaginary, right hand (RH), mu and beta (ERD/ERS) filtered data.

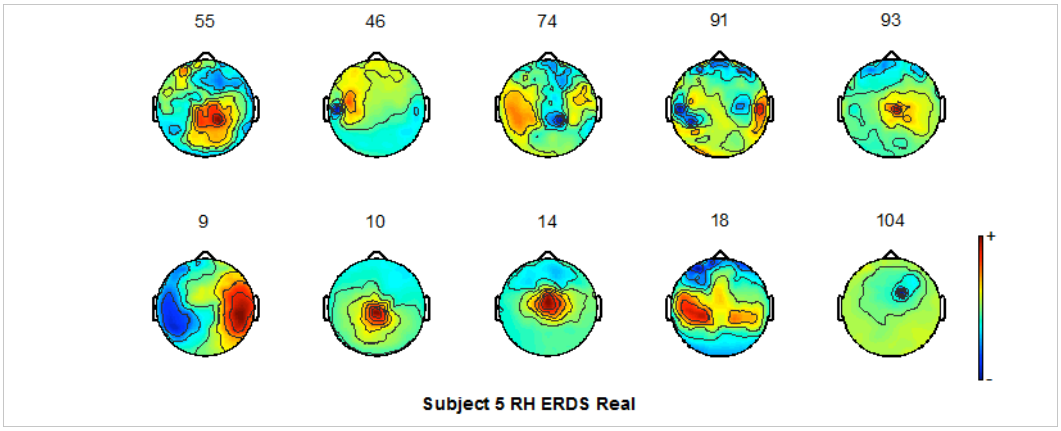

Figure A.38: Scalp plots of all visually selected ICs for subject 5's real, right hand (RH), mu and beta (ERD/ERS) filtered data.

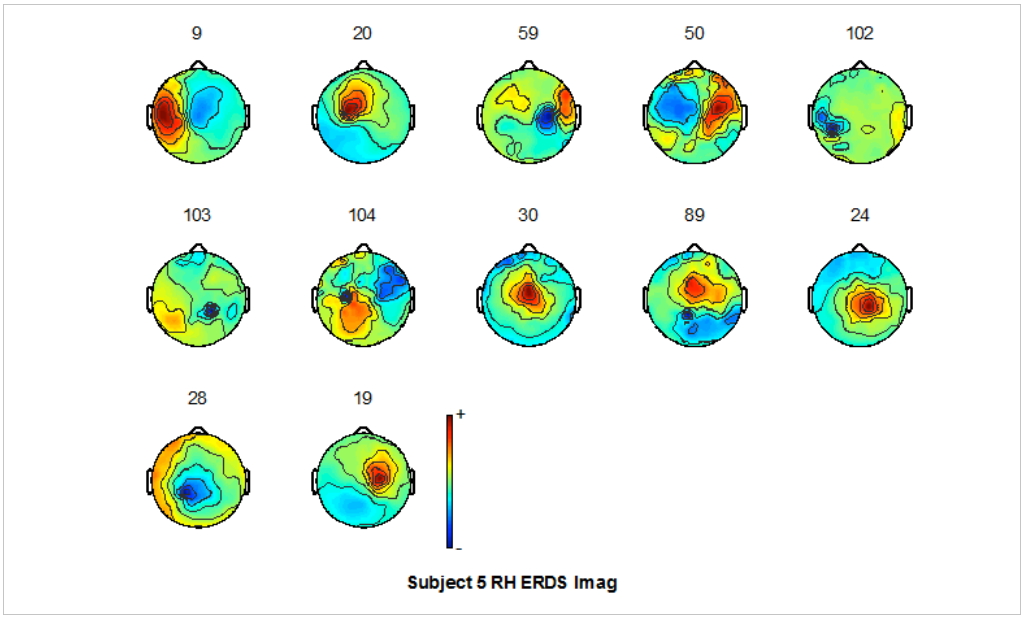

Figure A.39: Scalp plots of all visually selected ICs for subject 5's imaginary, right hand (RH), mu and beta (ERD/ERS) filtered data.

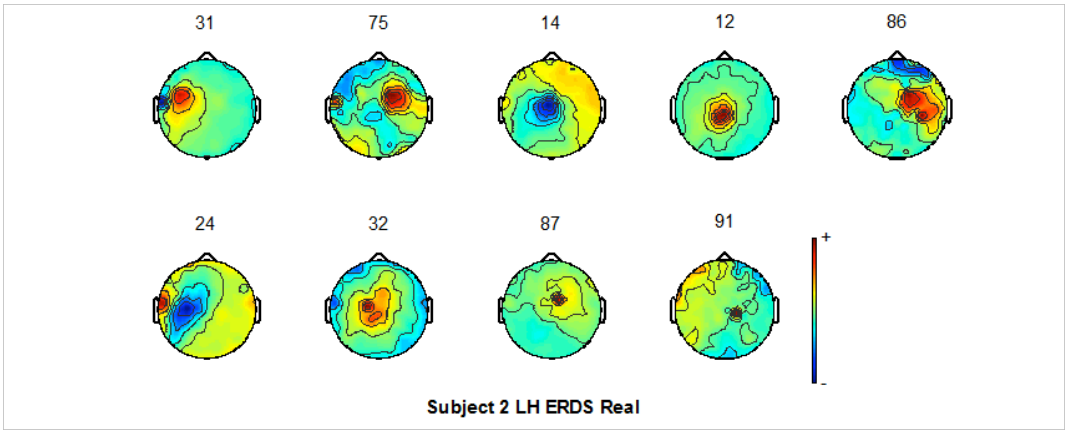

Figure A.40: Scalp plots of all visually selected ICs for subject 2's real, left hand (LH), mu and beta (ERD/ERS) filtered data.

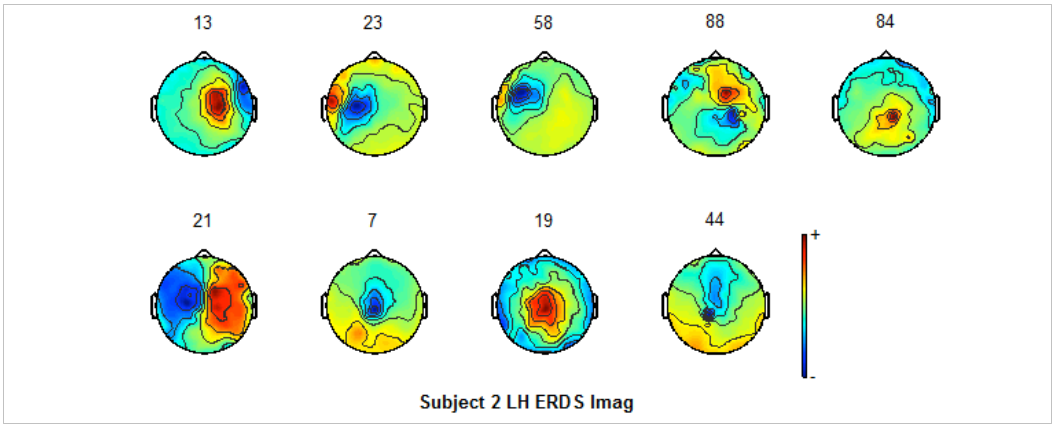

Figure A.41: Scalp plots of all visually selected ICs for subject 2's imaginary, left hand (LH), mu and beta (ERD/ERS) filtered data.

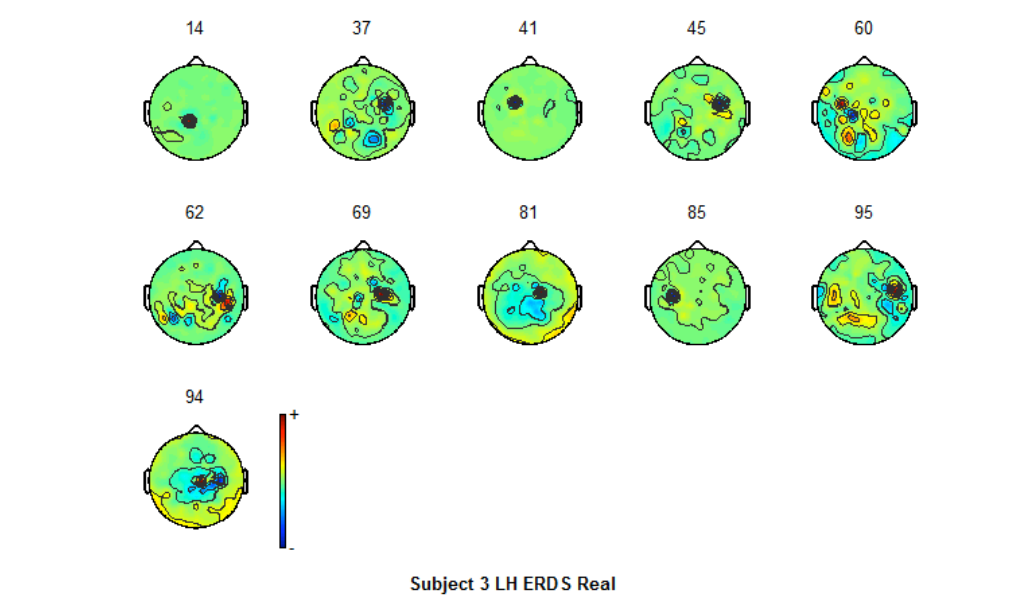

Figure A.42: Scalp plots of all visually selected ICs for subject 3's real, left hand (LH), mu and beta (ERD/ERS) filtered data.

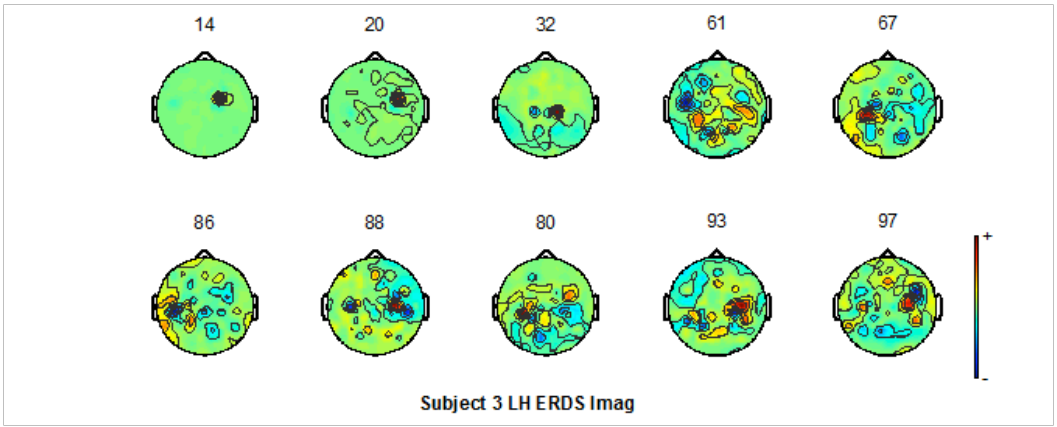

Figure A.43: Scalp plots of all visually selected ICs for subject 3's imaginary, left hand (LH), mu and beta (ERD/ERS) filtered data.

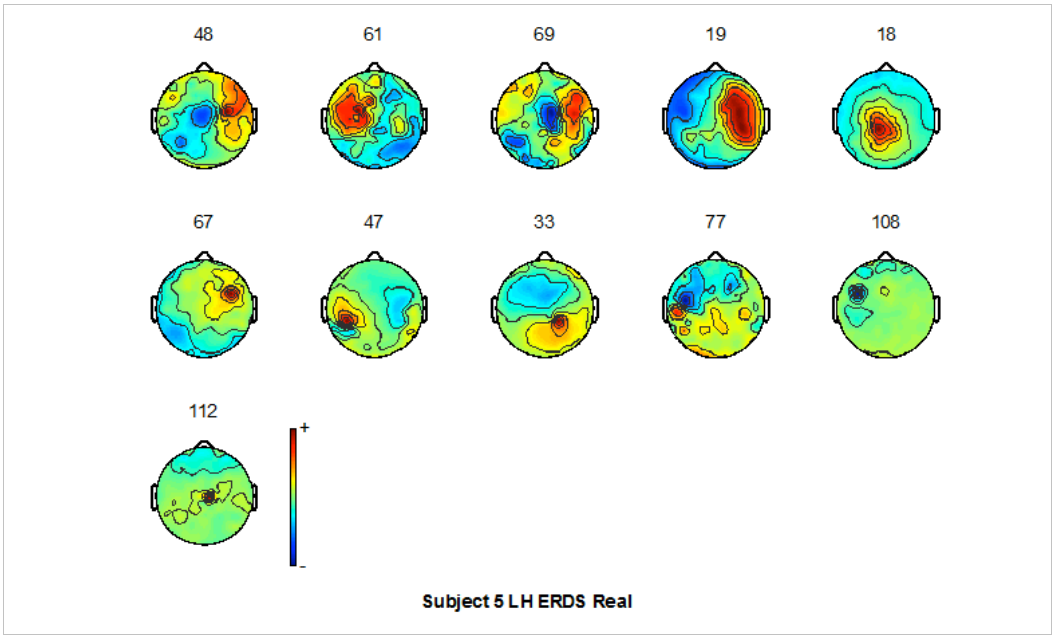

Figure A.44: Scalp plots of all visually selected ICs for subject 5's real, left hand (LH), mu and beta (ERD/ERS) filtered data.

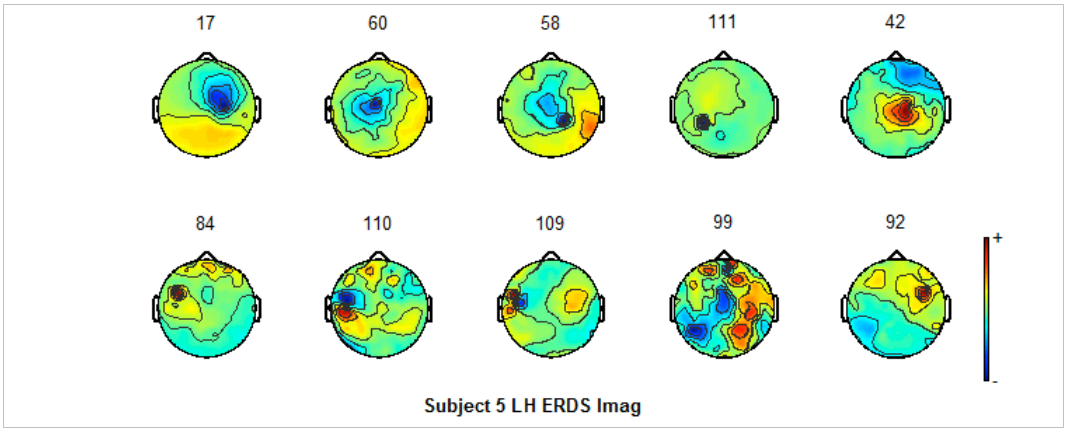

Figure A.45: Scalp plots of all visually selected ICs for subject 5's imaginary, left hand (LH), mu and beta (ERD/ERS) filtered data.

A.2 ITV ERD/ERS Plots

A.2.1 ITV ERD/ERS Plots for RLI

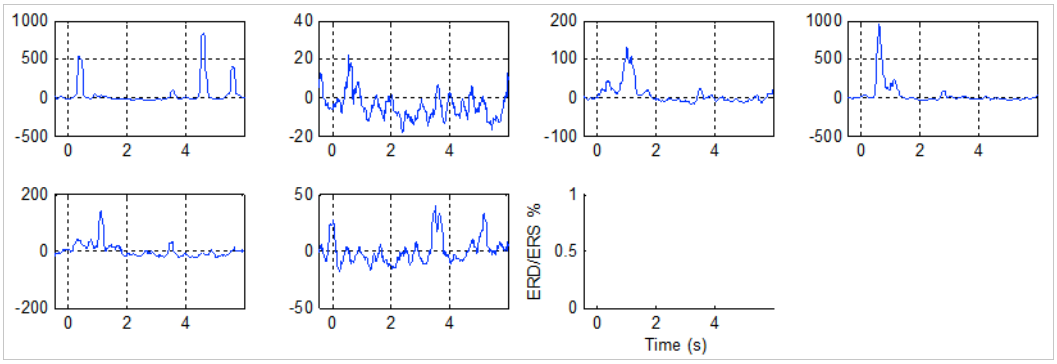

Figure A.46: ITV ERD/ERS patterns (averaged over all trials) of visually selected ICs for subject 2's real, right and left hand (RL) data.

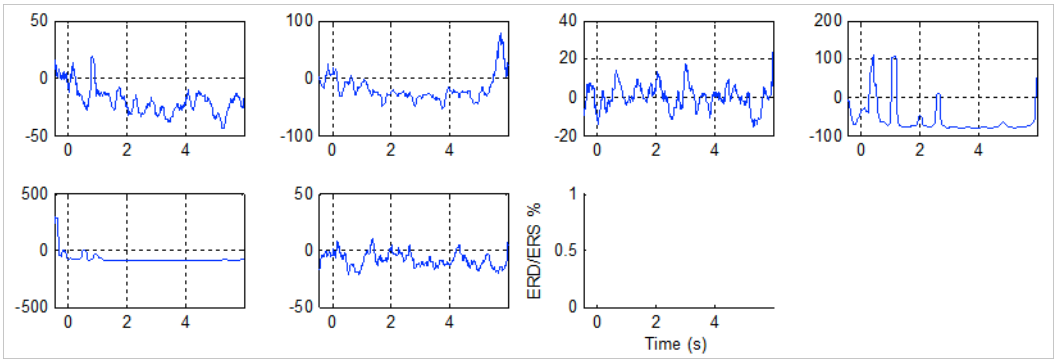

Figure A.47: ITV ERD/ERS patterns (averaged over all trials) of visually selected ICs for subject 2's imaginary, right and left hand (RL) data.

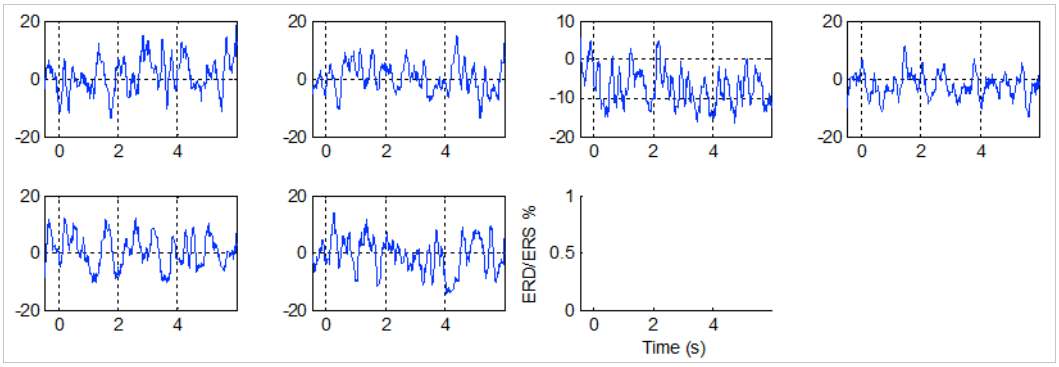

Figure A.48: ITV ERD/ERS patterns (averaged over all trials) of visually selected ICs for subject 3's real, right and left hand (RL) data.

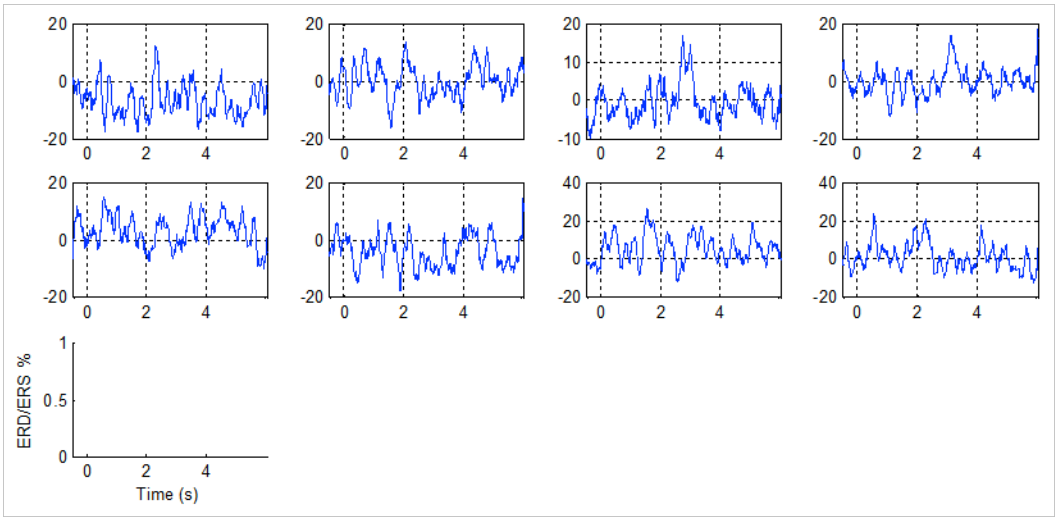

Figure A.49: ITV ERD/ERS patterns (averaged over all trials) of visually selected ICs for subject 3's imaginary, right and left hand (RL) data.

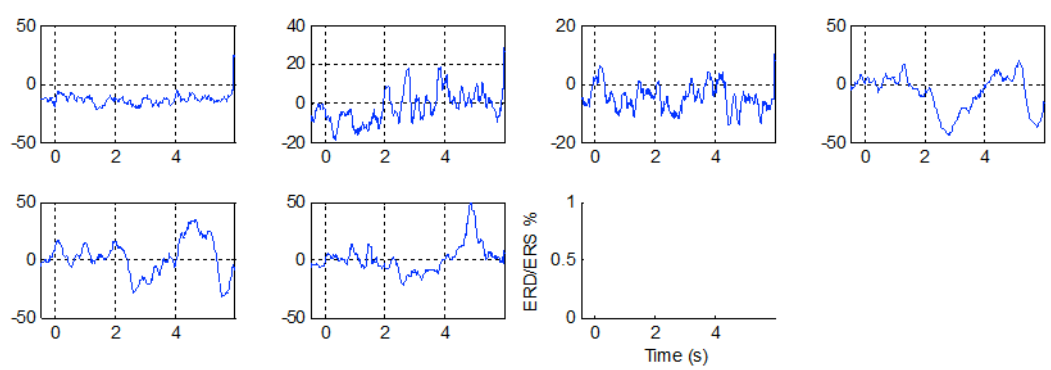

Figure A.50: ITV ERD/ERS patterns (averaged over all trials) of visually selected ICs for subject 5's real, right and left hand (RL) data.

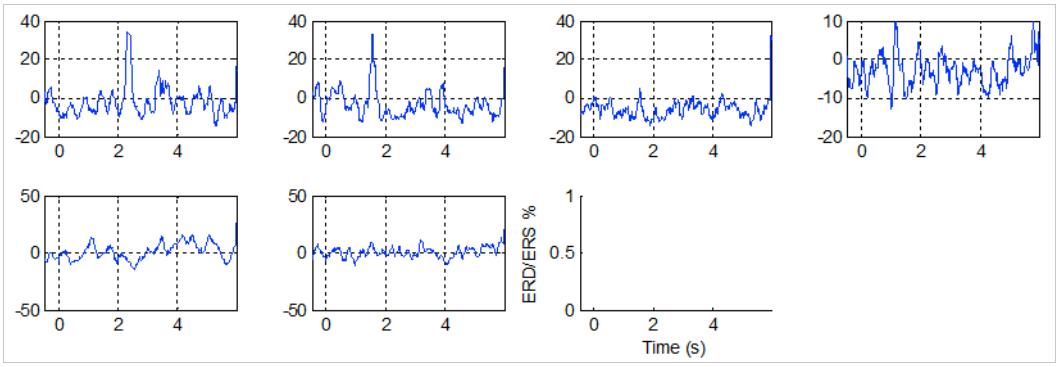

Figure A.51: ITV ERD/ERS patterns (averaged over all trials) of visually selected ICs for subject 5's imaginary, right and left hand (RL) data.

A.2.2 ITV ERD/ERS Plots for WFMI and FMDI

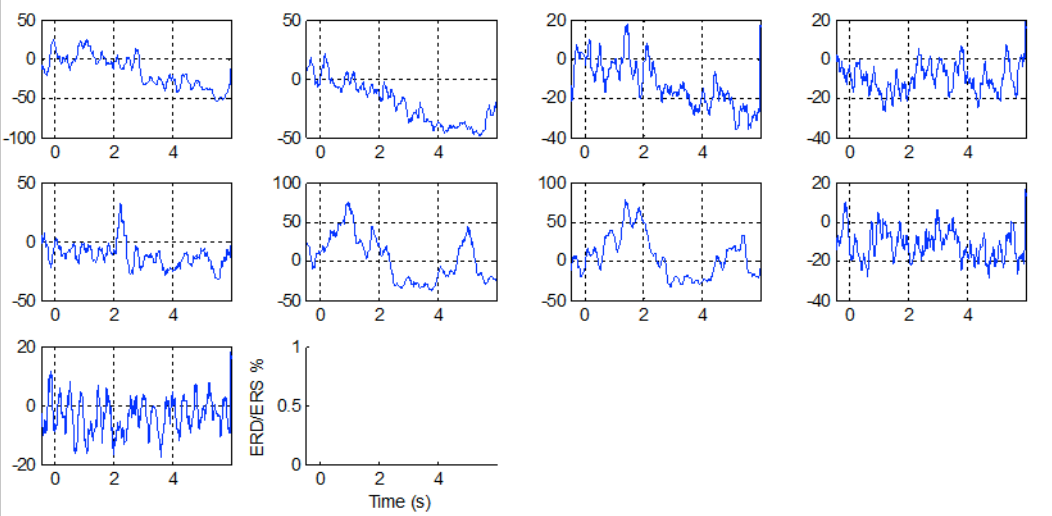

Figure A.52: ITV ERD/ERS patterns (averaged over all trials) of visually selected ICs for subject 1's real, right hand (RH) data.

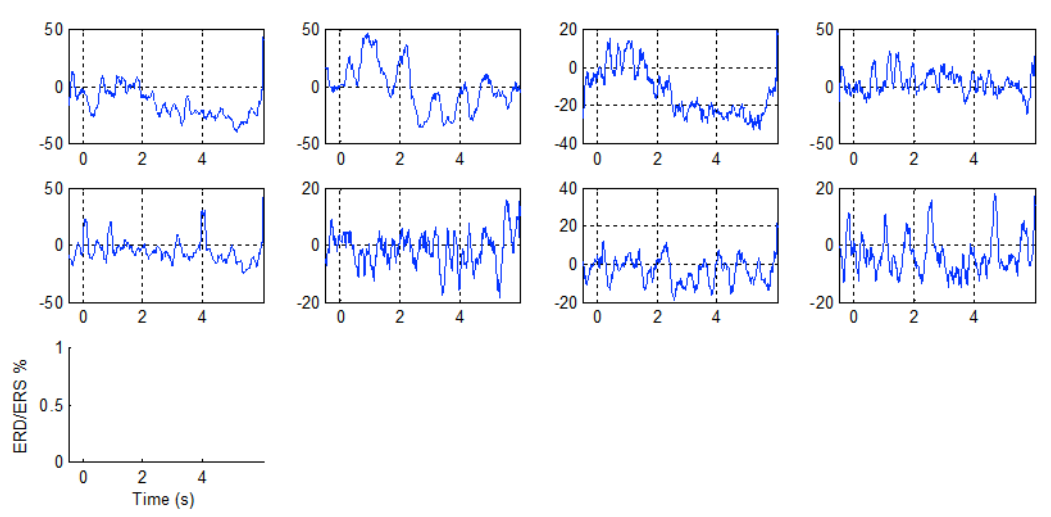

Figure A.53: ITV ERD/ERS patterns (averaged over all trials) of visually selected ICs for subject 1's imaginary, right hand (RH) data.

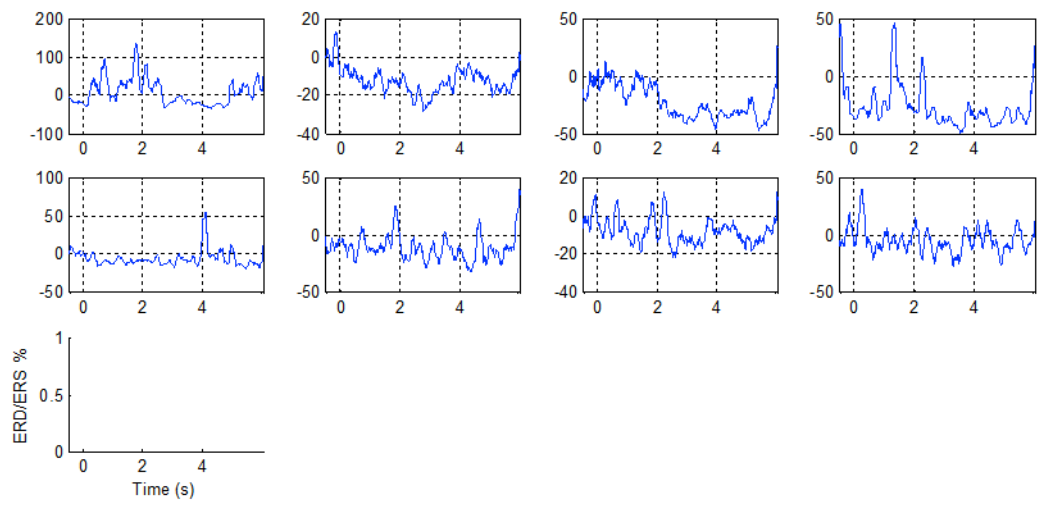

Figure A.54: ITV ERD/ERS patterns (averaged over all trials) of visually selected ICs for subject 2's real, right hand (RH) data.

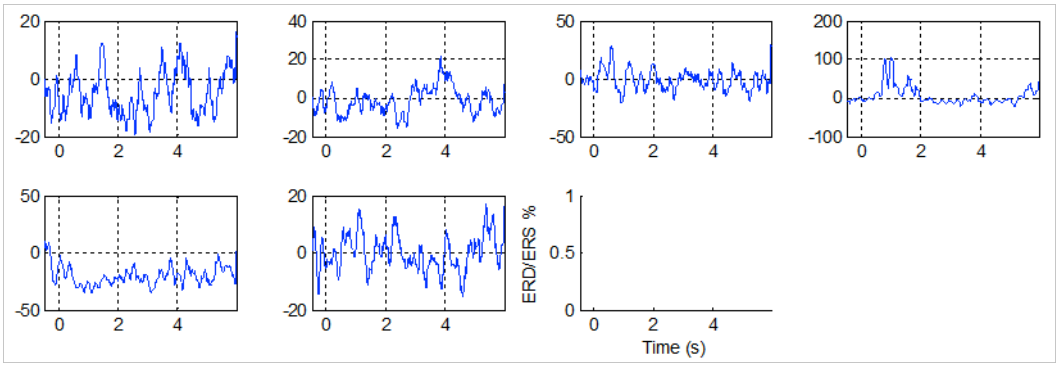

Figure A.55: ITV ERD/ERS patterns (averaged over all trials) of visually selected ICs for subject 2's imaginary, right hand (RH) data.

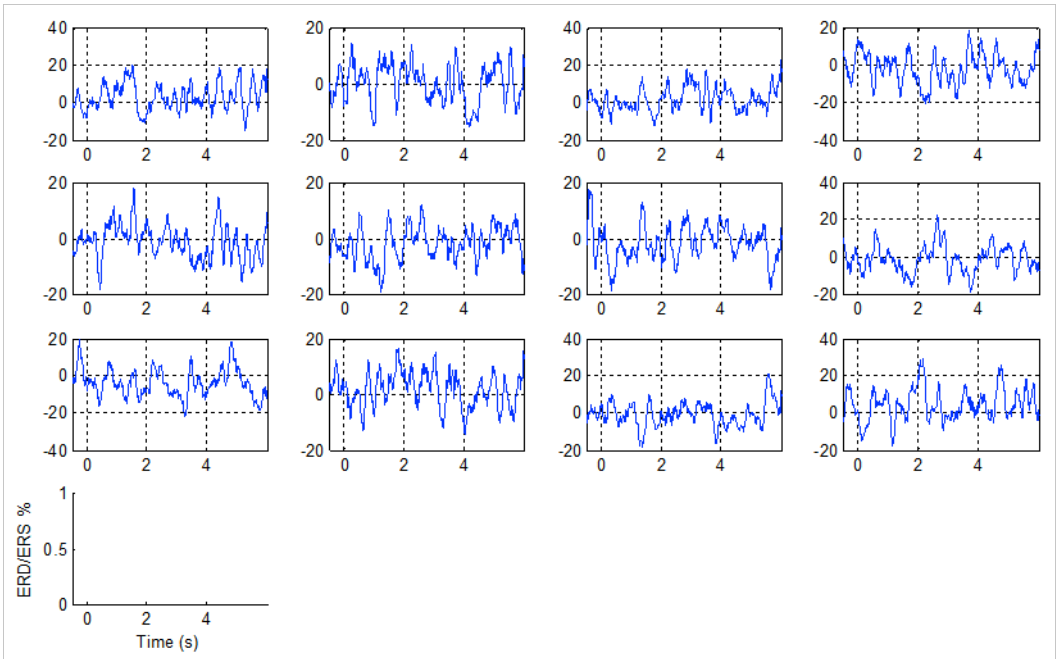

Figure A.56: ITV ERD/ERS patterns (averaged over all trials) of visually selected ICs for subject 3's real, right hand (RH) data.

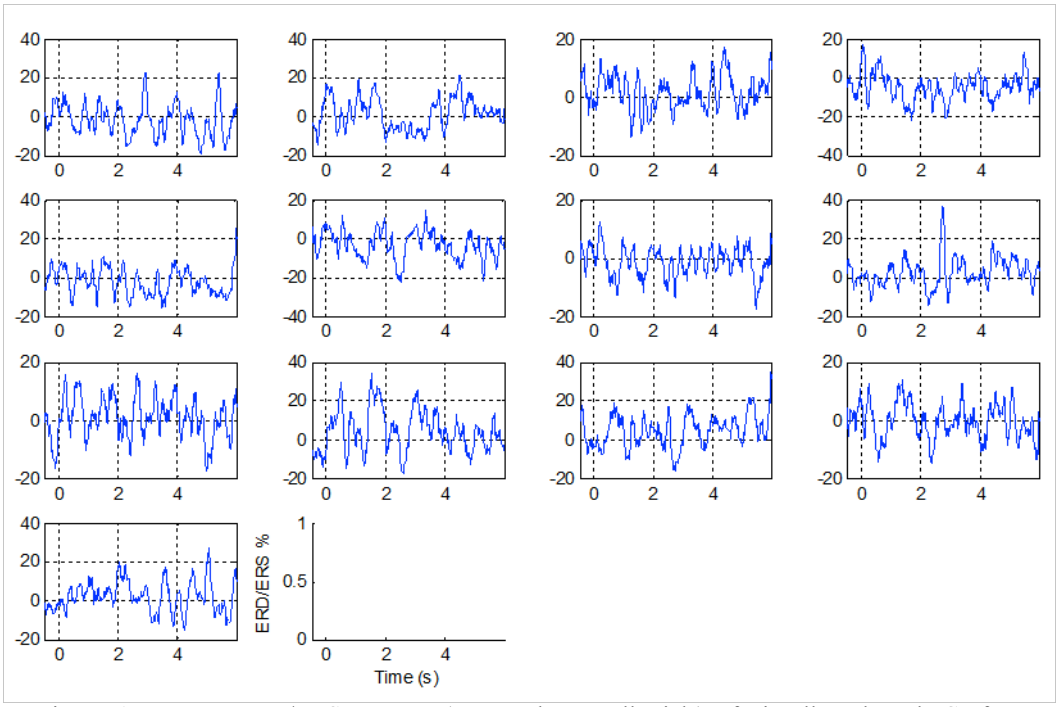

Figure A.57: ITV ERD/ERS patterns (averaged over all trials) of visually selected ICs for subject 3's imaginary, right hand (RH) data.

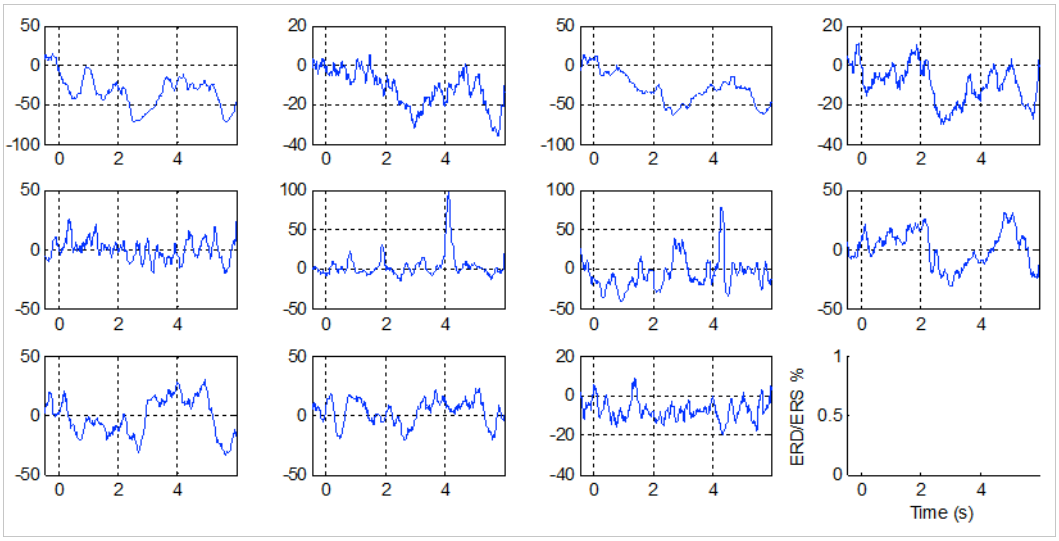

Figure A.58: ITV ERD/ERS patterns (averaged over all trials) of visually selected ICs for subject 4's real, right hand (RH) data.

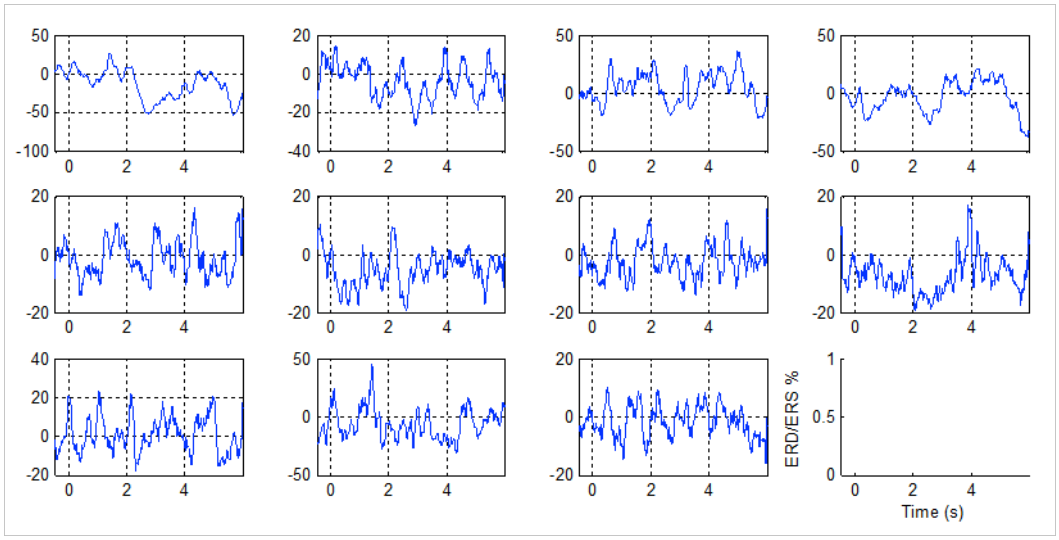

Figure A.59: ITV ERD/ERS patterns (averaged over all trials) of visually selected ICs for subject 4's imaginary, right hand (RH) data.

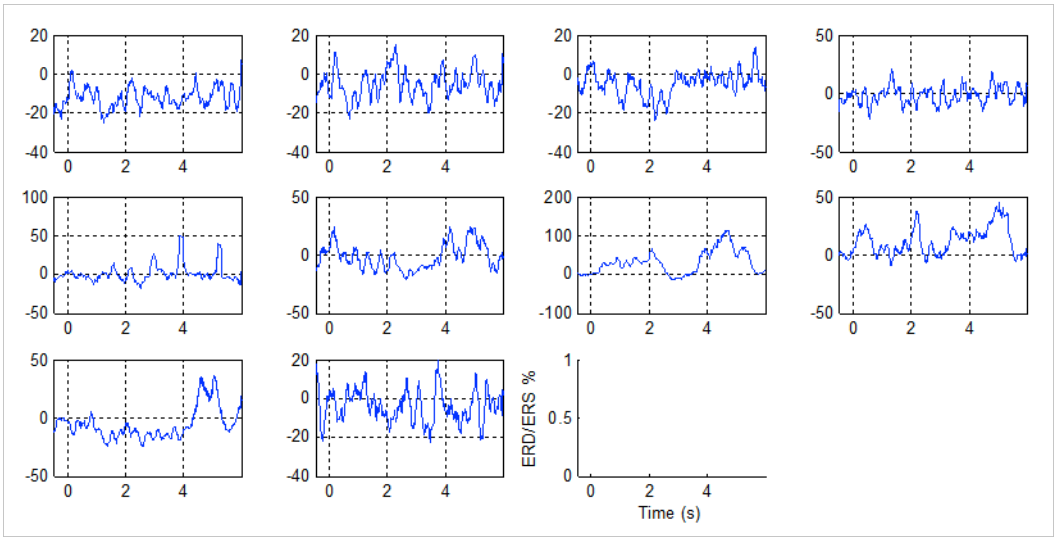

Figure A.60: ITV ERD/ERS patterns (averaged over all trials) of visually selected ICs for subject 5's real, right hand (RH) data.

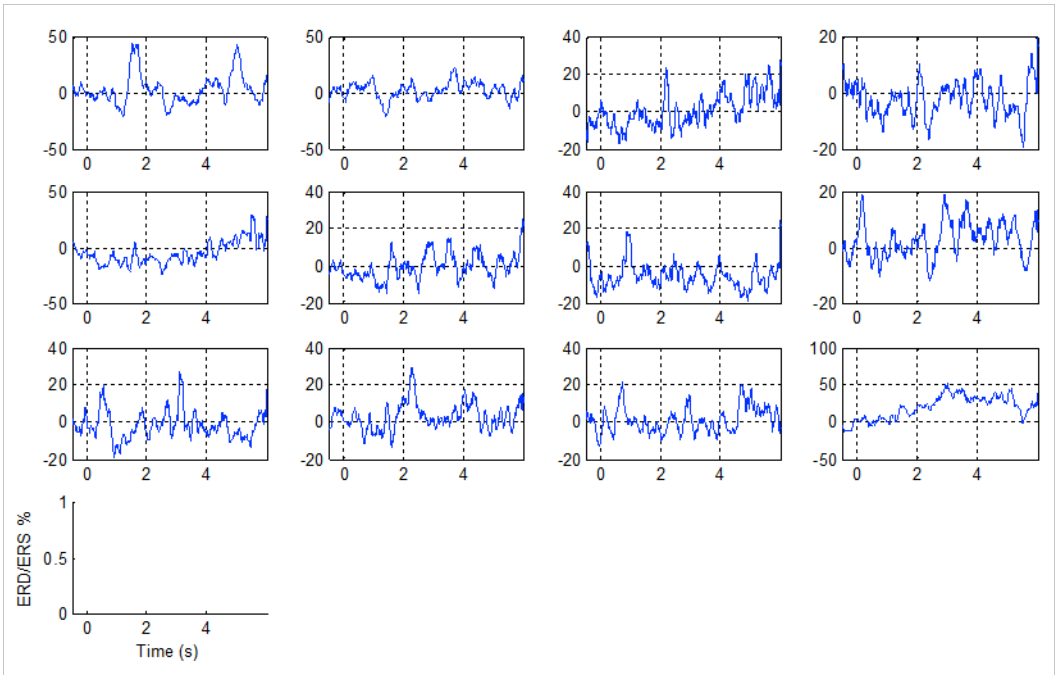

Figure A.61: ITV ERD/ERS patterns (averaged over all trials) of visually selected ICs for subject 5's imaginary, right hand (RH) data.

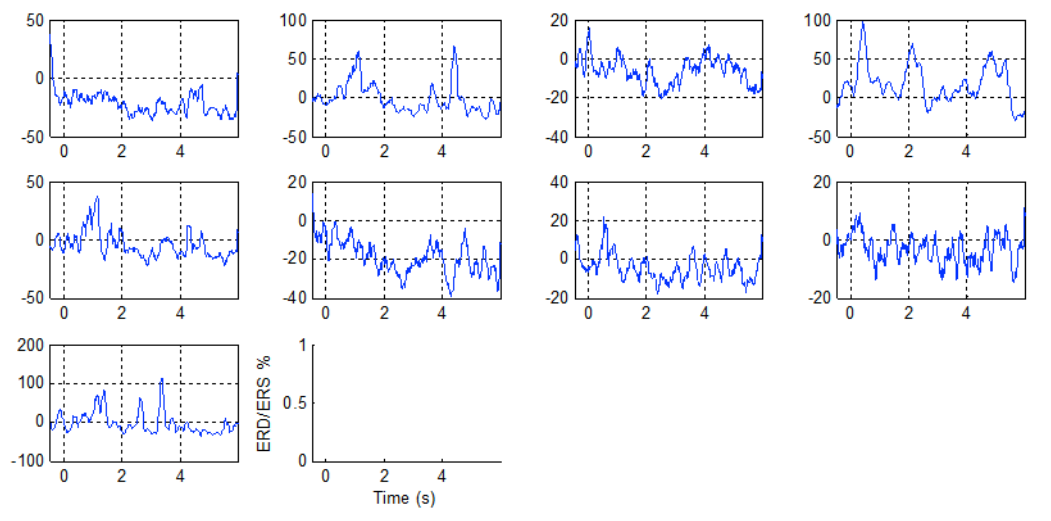

Figure A.62: ITV ERD/ERS patterns (averaged over all trials) of visually selected ICs for subject 2's real, left hand (LH) data.

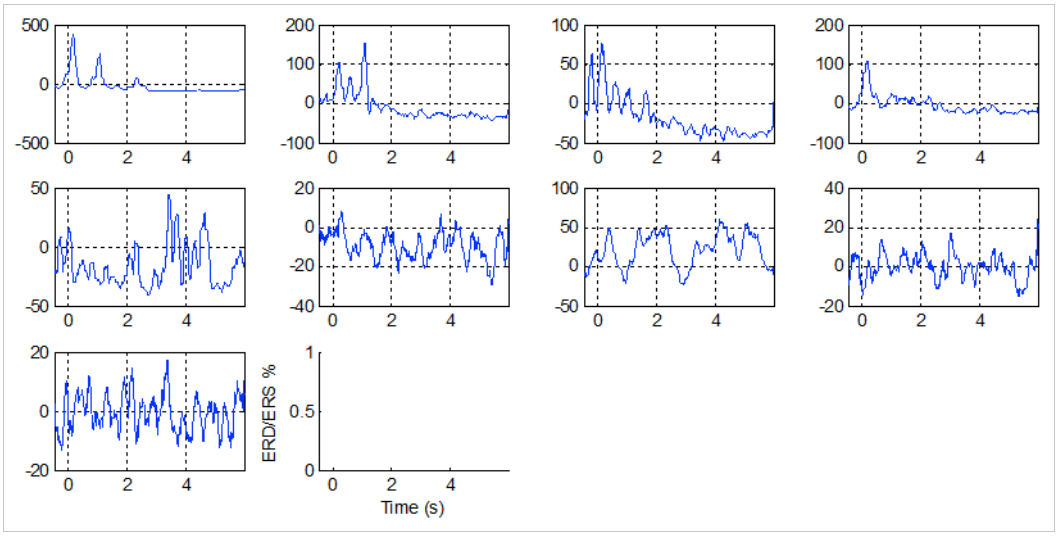

Figure A.63: ITV ERD/ERS patterns (averaged over all trials) of visually selected ICs for subject 2's imaginary, left hand (LH) data.

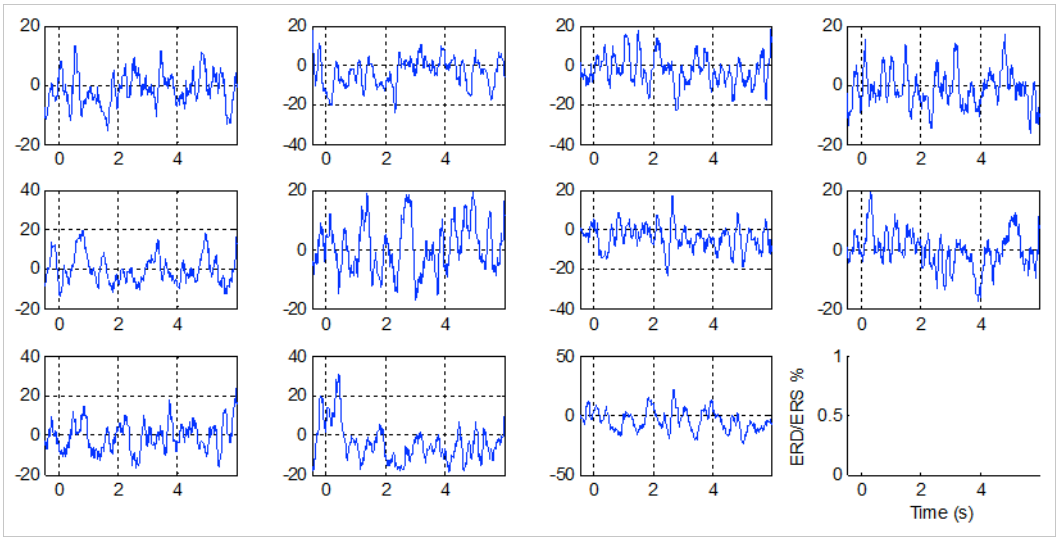

Figure A.64: ITV ERD/ERS patterns (averaged over all trials) of visually selected ICs for subject 3's real, left hand (LH) data.

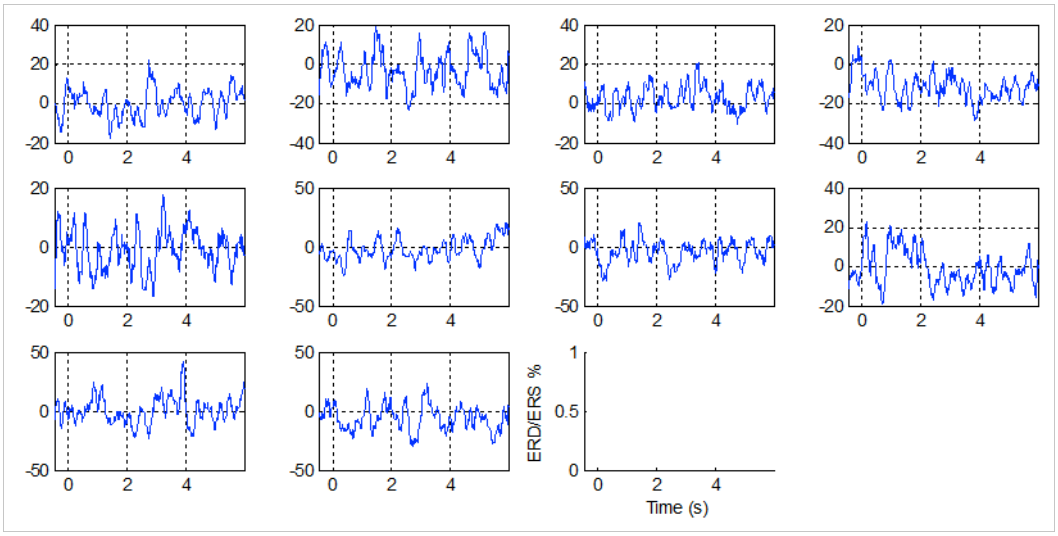

Figure A.65: ITV ERD/ERS patterns (averaged over all trials) of visually selected ICs for subject 3's imaginary, left hand (LH) data.

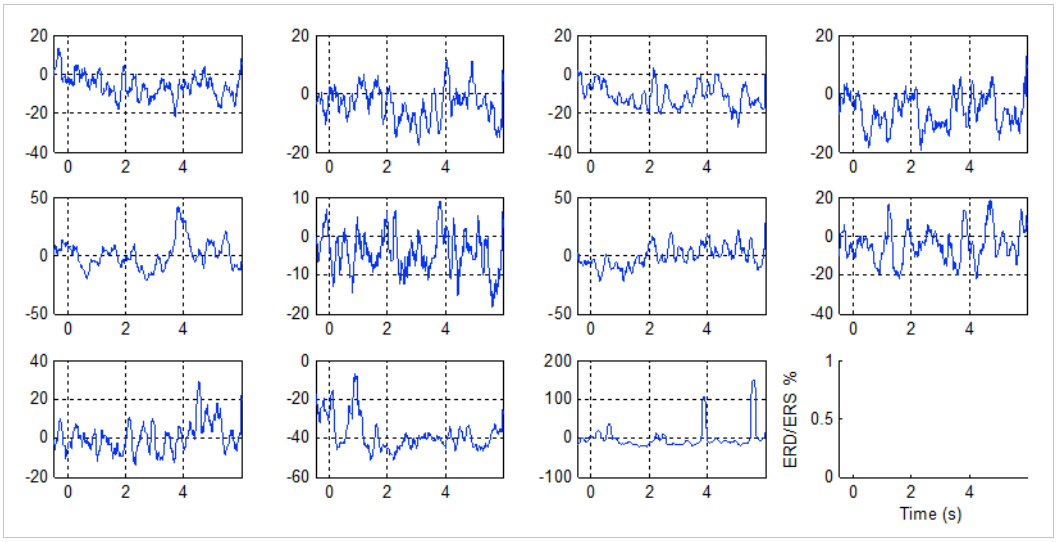

Figure A.66: ITV ERD/ERS patterns (averaged over all trials) of visually selected ICs for subject 5's real, left hand (LH) data.

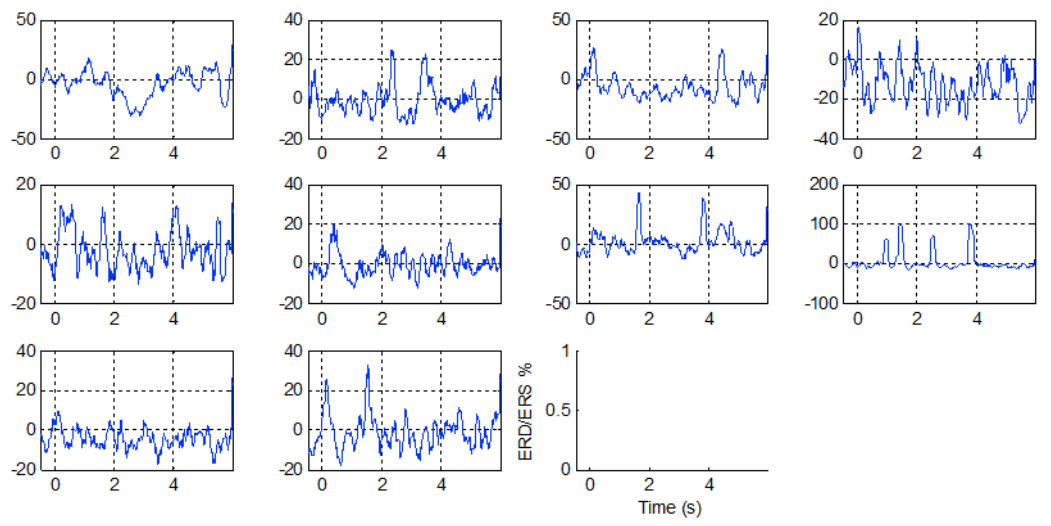

Figure A.67: ITV ERD/ERS patterns (averaged over all trials) of visually selected ICs for subject 5's imaginary, left hand (LH) data.

A.3 MRCP ERP Plots

A.3.1 MRCP ERP Plots for RLI

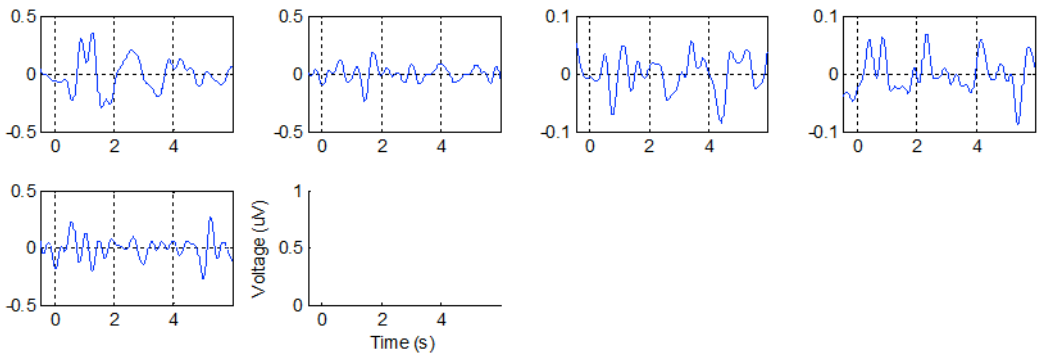

Figure A.68: MRCP ERPs (averaged over all trials) of visually selected ICs for subject 2's real, right and left hand (RL) data.

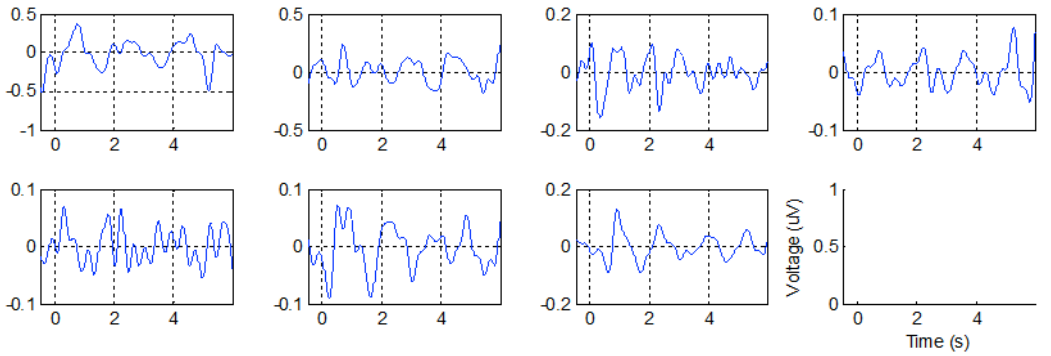

Figure A.69: MRCP ERPs (averaged over all trials) of visually selected ICs for subject 2's imaginary, right and left hand (RL) data.

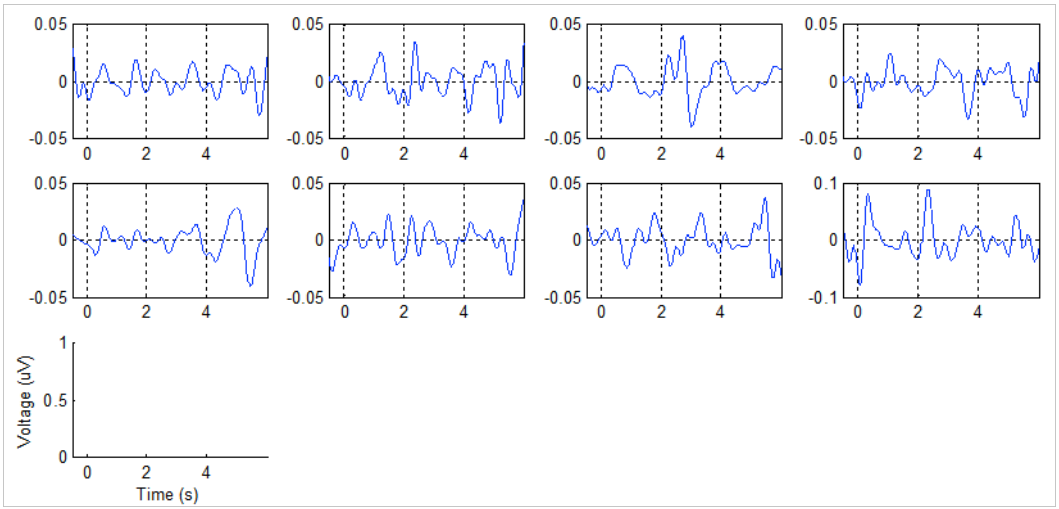

Figure A.70: MRCP ERPs (averaged over all trials) of visually selected ICs for subject 5's real, right and left hand (RL) data.

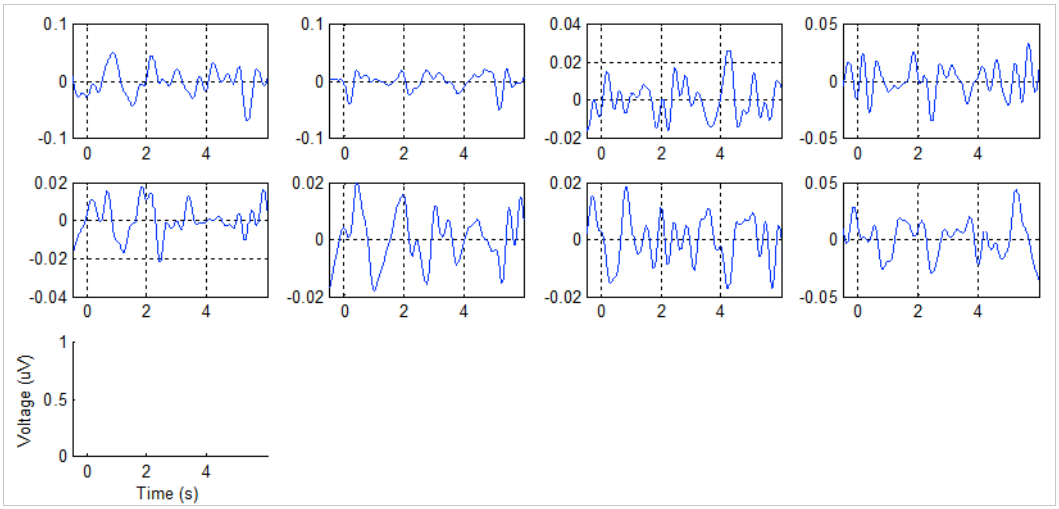

Figure A.71: MRCP ERPs (averaged over all trials) of visually selected ICs for subject 5's imaginary, right and left hand (RL) data.

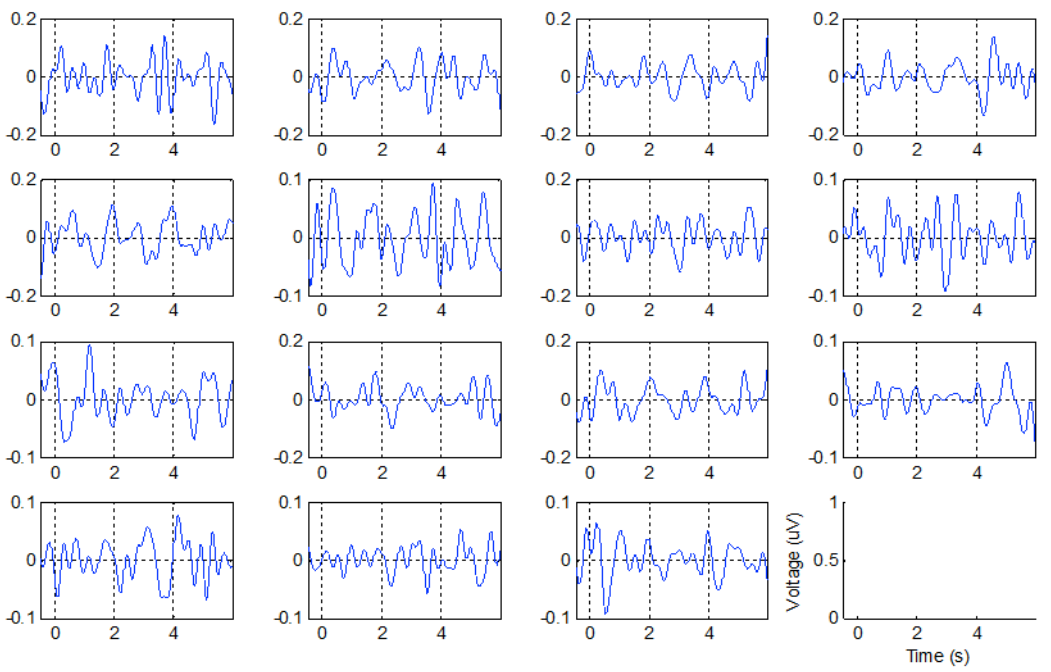

Figure A.72: MRCP ERPs (averaged over all trials) of visually selected ICs for subject 3's real, right and left hand (RL) data.

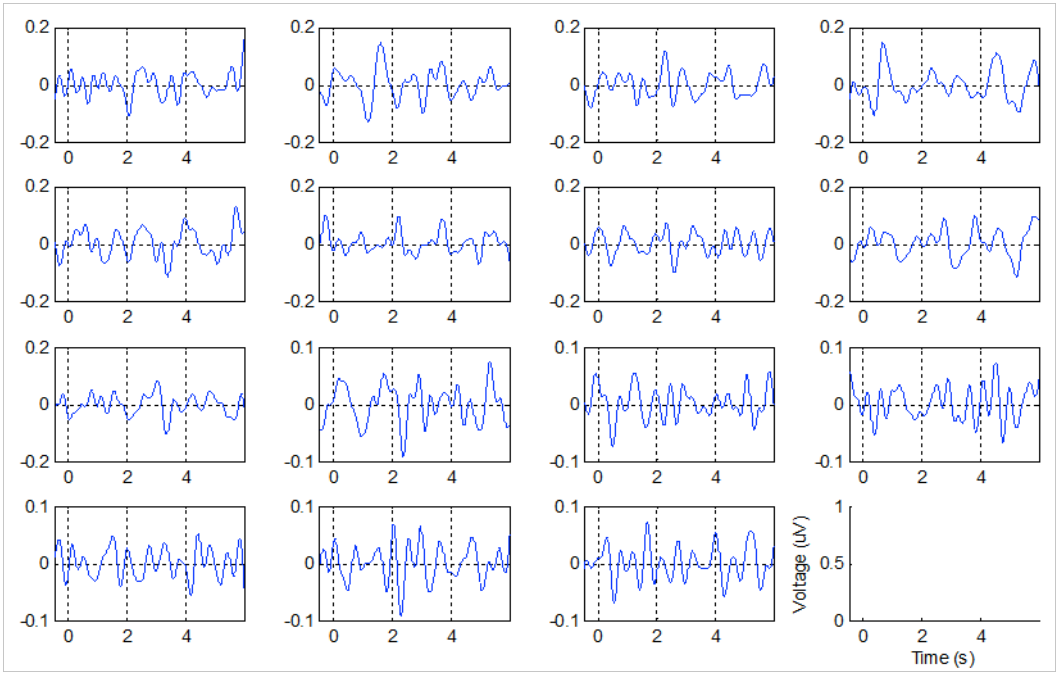

Figure A.73: MRCP ERPs (averaged over all trials) of visually selected ICs for subject 3's imaginary, right and left hand (RL) data.

A.3.2 MRCP ERP Plots for WFMI and FMDI

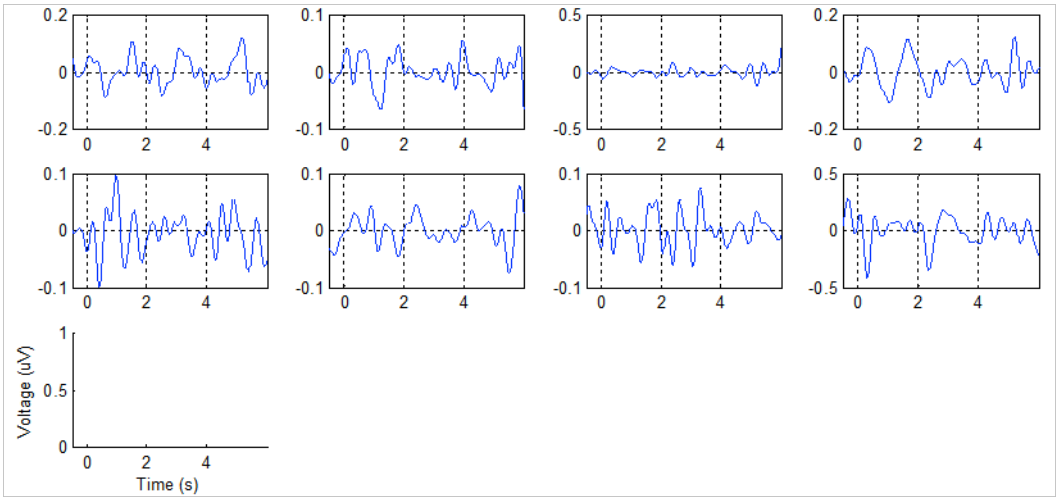

Figure A.74: MRCP ERPs (averaged over all trials) of visually selected ICs for subject 1's imaginary, right hand (RH) data.

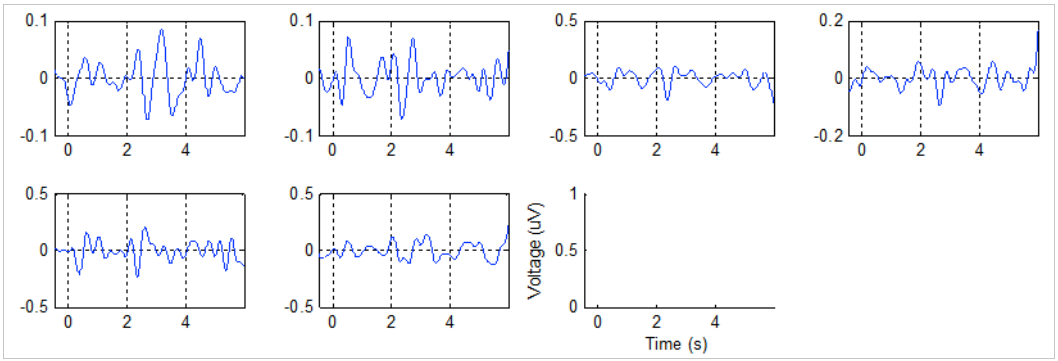

Figure A.75: MRCP ERPs (averaged over all trials) of visually selected ICs for subject 1's real, right hand (RH) data.

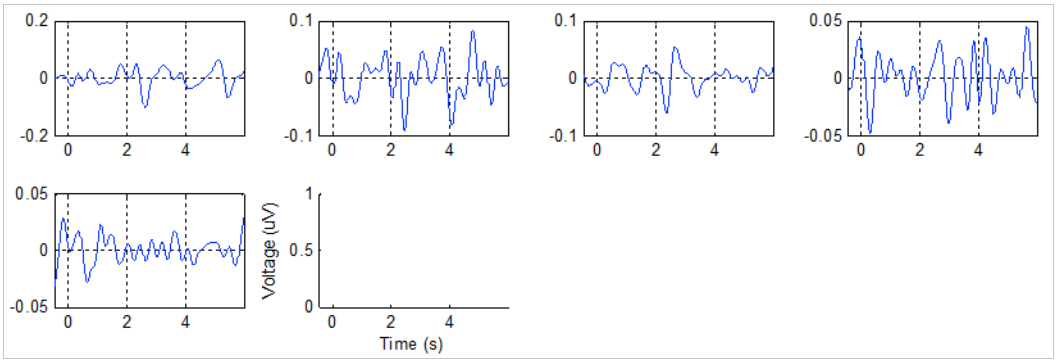

Figure A.76: MRCP ERPs (averaged over all trials) of visually selected ICs for subject 2's real, right hand (RH) data.

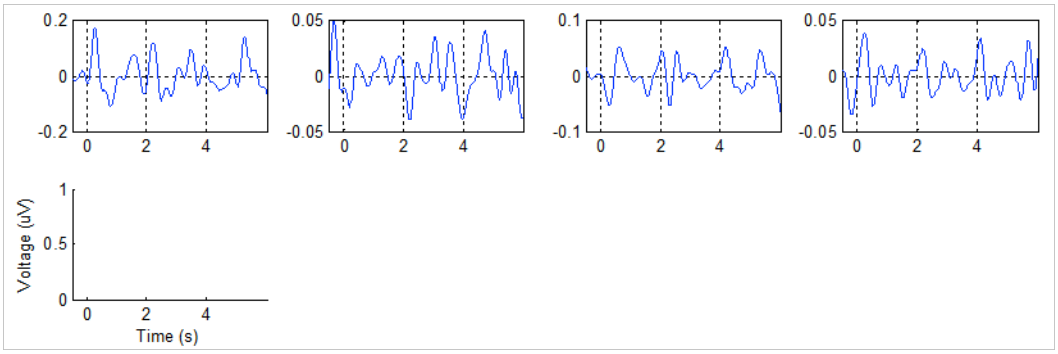

Figure A.77: MRCP ERPs (averaged over all trials) of visually selected ICs for subject 2's imaginary, right hand (RH) data.

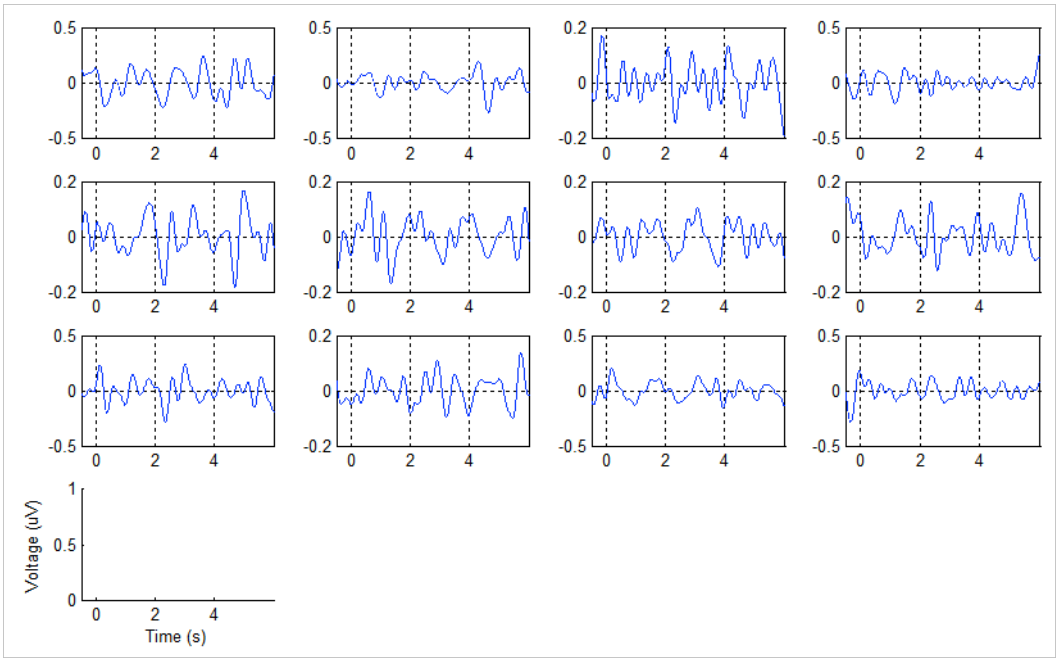

Figure A.78: MRCP ERPs (averaged over all trials) of visually selected ICs for subject 3's real, right hand (RH) data.

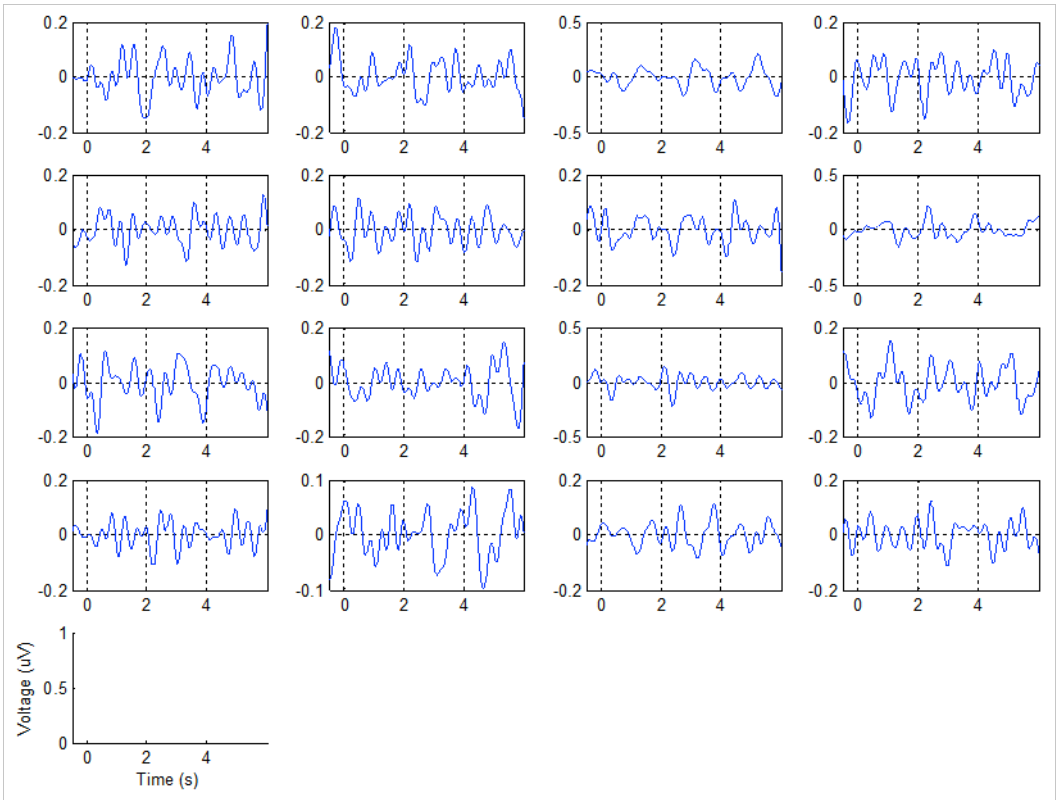

Figure A.79: MRCP ERPs (averaged over all trials) of visually selected ICs for subject 3's imaginary, right hand (RH) data.

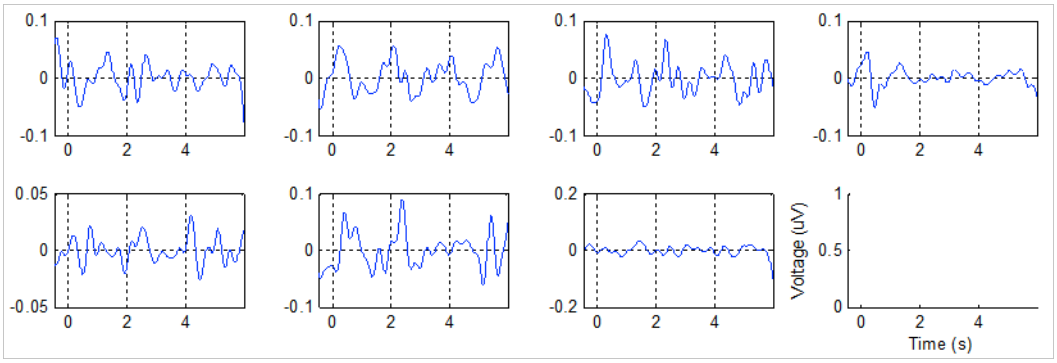

Figure A.80: MRCP ERPs (averaged over all trials) of visually selected ICs for subject 4's real, right hand (RH) data.

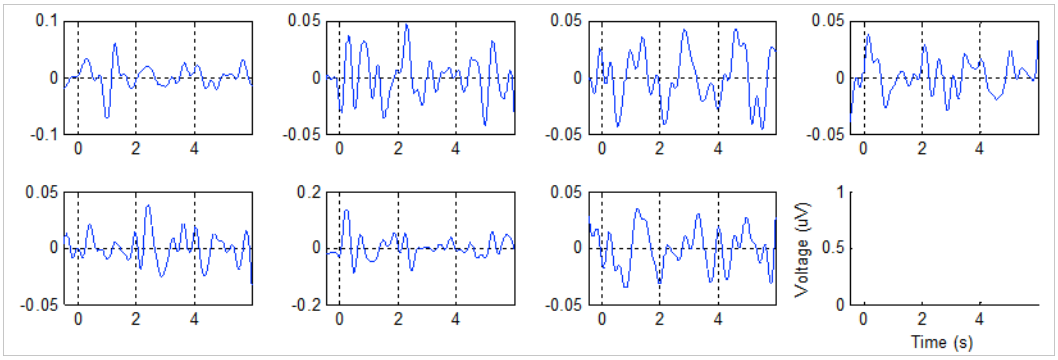

Figure A.81: MRCP ERPs (averaged over all trials) of visually selected ICs for subject 4's imaginary, right hand (RH) data.

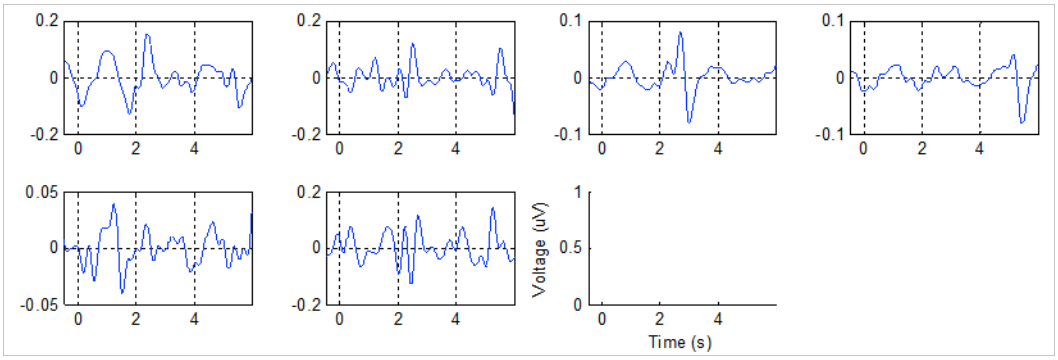

Figure A.82: MRCP ERPs (averaged over all trials) of visually selected ICs for subject 5's real, right hand (RH) data.

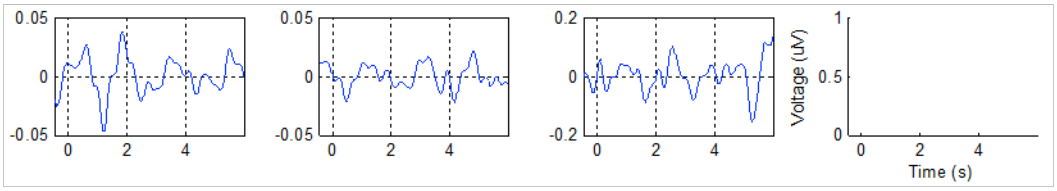

Figure A.83: MRCP ERPs (averaged over all trials) of visually selected ICs for subject 5's imaginary, right hand (RH) data.

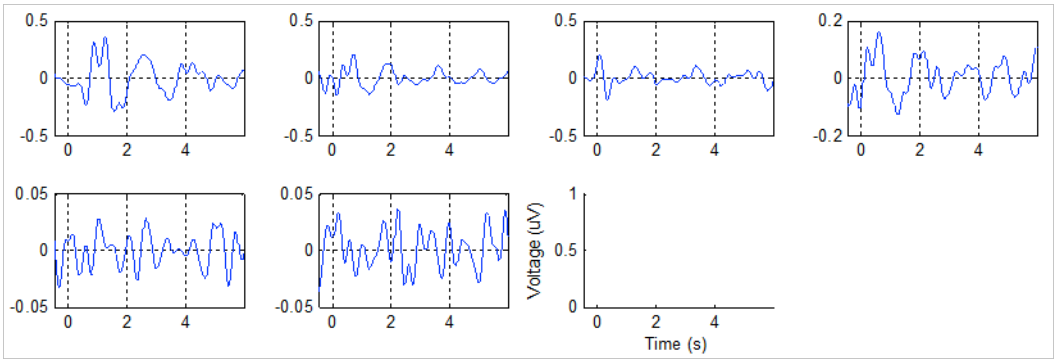

Figure A.84: MRCP ERPs (averaged over all trials) of visually selected ICs for subject 2's real, left hand (LH) data.

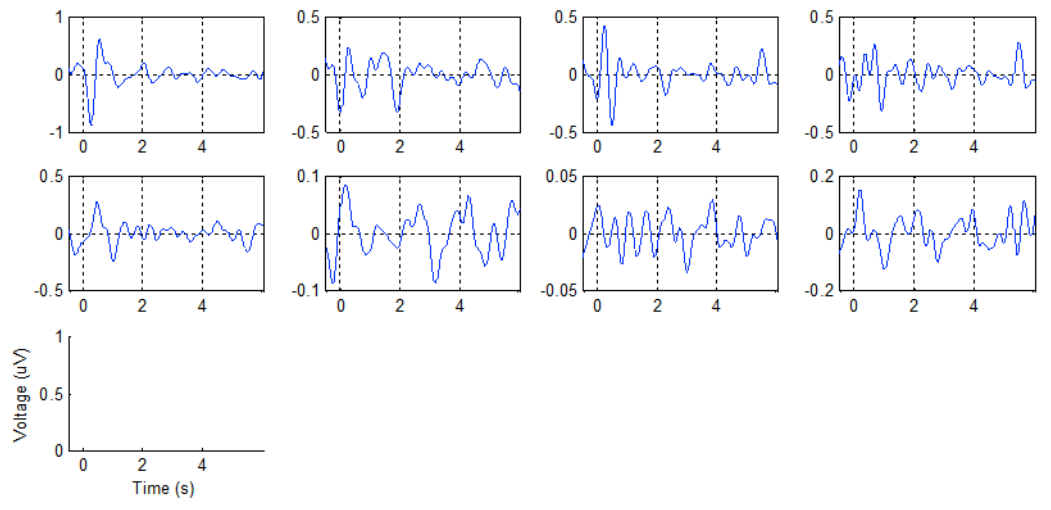

Figure A.85: MRCP ERPs (averaged over all trials) of visually selected ICs for subject 2's imaginary, left hand (LH) data.

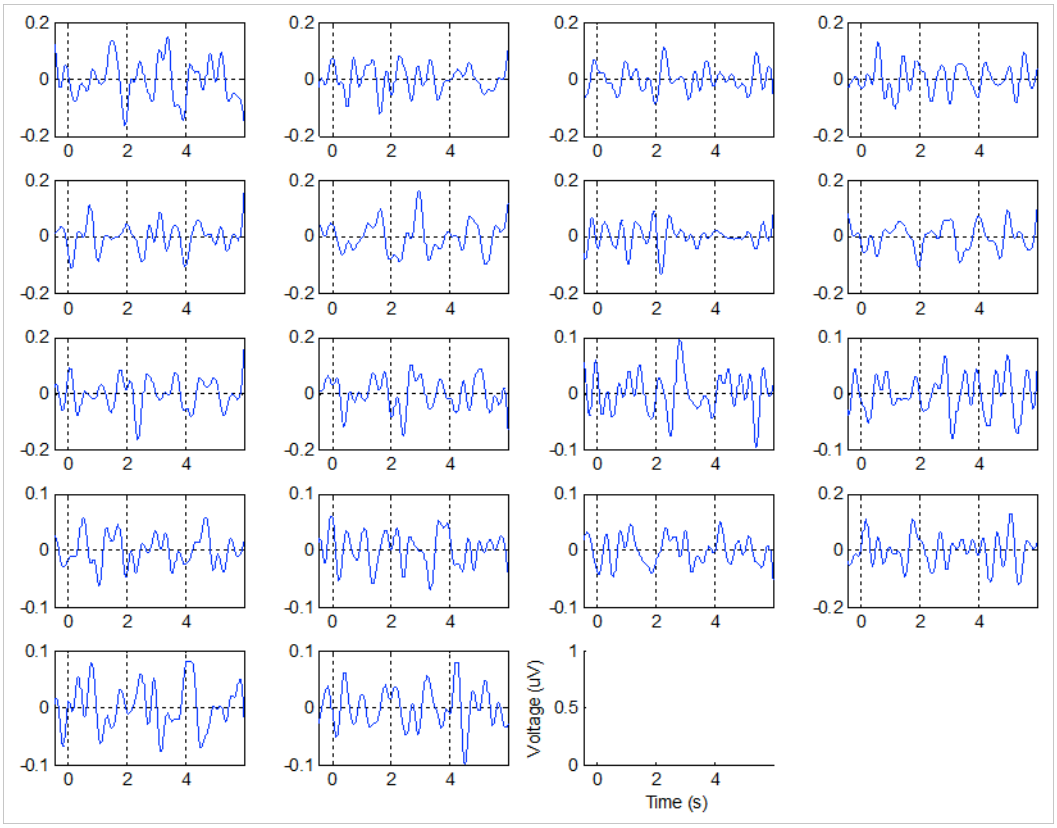

Figure A.86: MRCP ERPs (averaged over all trials) of visually selected ICs for subject 3's real, left hand (LH) data.

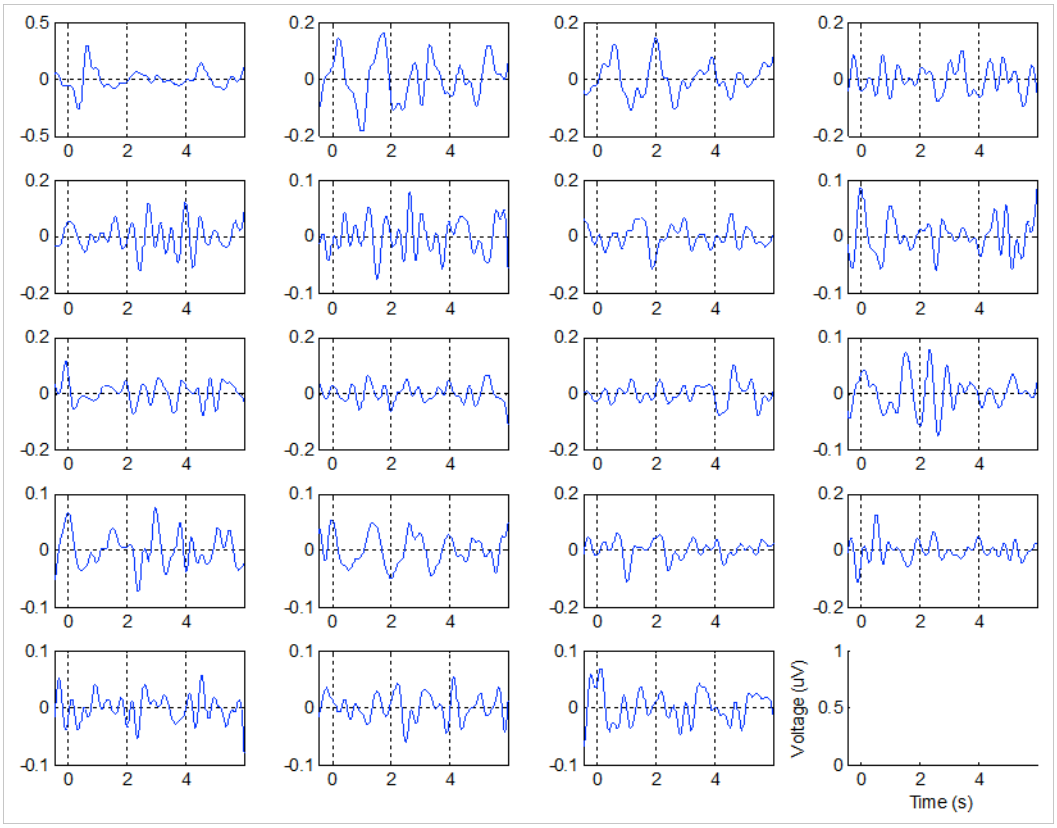

Figure A.87: MRCP ERPs (averaged over all trials) of visually selected ICs for subject 3's imaginary, left hand (LH) data.

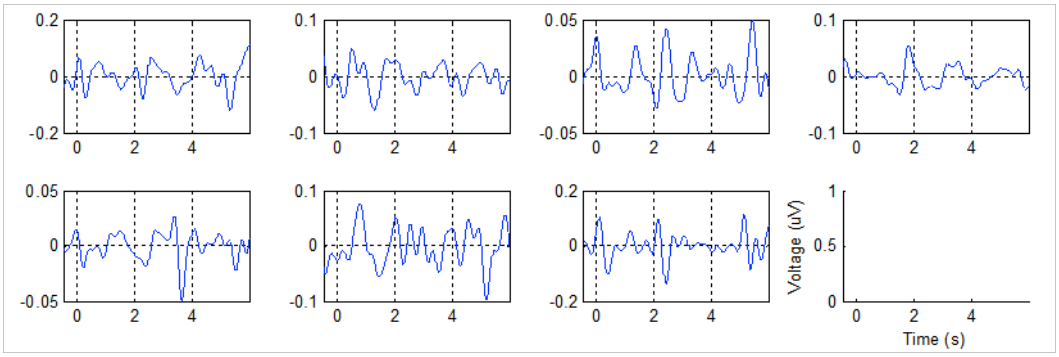

Figure A.88: MRCP ERPs (averaged over all trials) of visually selected ICs for subject 5's real, left hand (LH) data.

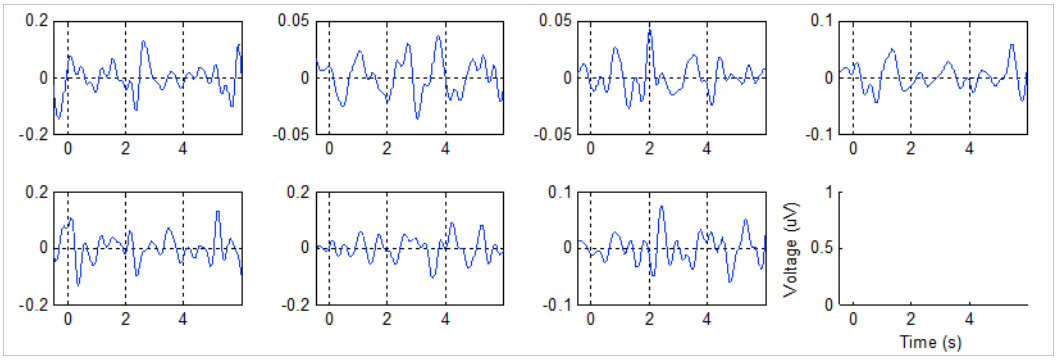

Figure A.89: MRCP ERPs (averaged over all trials) of visually selected ICs for subject 5's imaginary, left hand (LH) data.

Appendix B

Attempt at Time-Domain MRCP Feature Extraction

B.1 Introduction

The attempt at using a time-domain method of feature extraction for MRCPs is described here. The method is based on the more traditional time-domain analysis of MRCPs [24][53]. However, it proved ineffective in classifying between right and left hand movements using MD clustering in the RLI. Hence a time-frequency method was investigated for use in all three investigations (this method is described in section 5.2.6).

B.2 Feature Extraction Method

The average ERPs from the collection of ICs from all the test subjects are used to design the feature extraction method. The MRCP time-series waveform 1.5 s before movement stimulus onset up to 0.5 s after movement stimulus onset is considered (refer to timing diagram in Figure 5.3 section 5.2.1). This section of the waveform is broken up into time bands of varying lengths and the average voltages within these time bands form most of the features. This is a similar approach to that used in [63]. Time bands and time ranges for the early BP, late BP, MP, movement onset and post-movement potentials are evaluated by considering the ERPs for the different

movement types (see section 2.5.2 for additional information on the components of MRCPs). Differences between right and left, and real and imagined ERPs are also considered. Close to and during movement onset the time bands are between 50 and 100 ms wide. This is done in order to capture more detailed information during the late BP, MP and movement onset phases. During the early BP, time bands are 300 ms wide in order to capture the gradual negative slope and to reduce the effects of inter-trial variability. These time bands are shown in Figure B.1.

As shown in Figure B.**1**, the maximum voltage at the commencement of the negative slope of the BP (A1), the minimum voltage at the termination of the negative slope (A2), their associated times, and the average slope and mean voltage level between the A1 and A2 also form features. This is done since the negative slope of the BP is of key interest and it is hypothesised that the slope, amplitude and timing of the BP differs for different types of movements [24]. The peak voltage and its associated time during the overshoot at movement onset form two more features. This adds further information concerning movement onset, which strengthens the feature set.

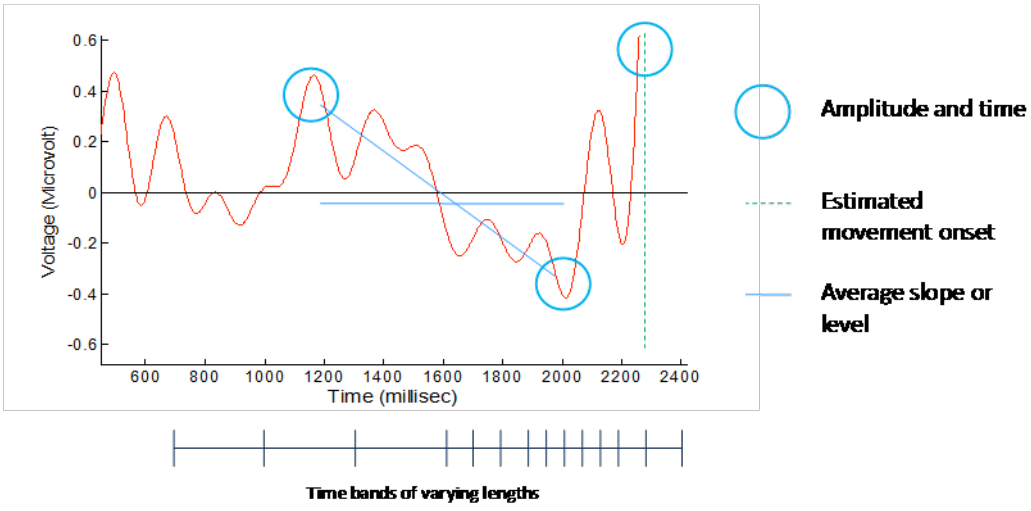

Figure B.1: Time-domain MRCP feature extraction, based on averages, slopes, peak voltage amplitudes and associated times and average voltages in time bands.

The later-mentioned set of features in combination with the former-mentioned time band features results in a total of 21 features that form the feature vector. The number of features is kept to a minimum due to the curse of dimensionality and practical

limitations of acquiring EEG data [11][41]. The final feature set is determined by iteratively adjusting and selecting features and evaluating the MD clustering accuracy.

B.3 Results and Conclusions

The results of the MD clustering of the extracted MRCP features are shown in Table B.1. The results are close to 50 % in most cases, which is not suitable.

Table B.1: Results of MD clustering for the RLI using time-based MRCP features (%)

	Subject 2	**Subject 3**	**Subject 5**
Real Movements	47.5	53.2	56.1
Imagined Movements	55.6	81.2	52.5

References

[1] Afshar P, Masuoka Y. *Neural-Based Control of a Robotic Hand: Evidence for Distinct Muscle Strategies*. Proceedings for the 2004 IEEE International Conference on Robotics and Automation (ICRA), New Orleans LA, April 2004, pp 4633 – 4638.

[2] Trombly C, Radomski M. *Occupational Therapy for physical dysfunction*. 5th edition, 2002.

[3] Smith J C. *OT for children*. *Development of hand function*. 2nd edition, 2004.

[4] Bulbulia R., Personal communication.

[5] Rybski M. *Kinesiology for Occupational Therapy*. SLACK Incorporated, New Jersey, USA, 2004.

[6] Zecca M, Micera S, Carrozza M C, Dario P. *Control of Multifunctional Prosthetic Hands by Processing the Electromyographic Signal*, Critical Reviews in Biomedical Engineering. Vol 30, 2002, pp 459 – 485.

[7] Crawford B, Miller K, Shenoy P, Rao R. *Real-Time Classification of Electromyographic Signals for Robotic Control*. AAAI'05 Proceedings of the 20th national conference on Artificial intelligence, Pittsburgh, PA, July 2005, pp 523 – 528.

[8] Otto Bock HealthCare GmbH**,** http://www.ottobock.com/cps/rde/xchg/ob_com_en/hs.xsl/384.html**,** last accessed 19 June 2008.

[9] Khezri M, Jahed M. *Real-time intelligent pattern recognition algorithm for surface EMG signals*. BioMedical Engineering OnLine 2007, Vol 6, December 2007, doi:10.1186/1475-925X-6-45.

[10] Wolpaw J R, Birbaumer N, McFarland D J, Pfurtscheller G, Vaughan T M. *Brain-computer interfaces for communication and control*. Clinical Neurophysiology, Vol 113, 2002, pp 767 – 791.

[11] Lotte F, Congedo M, Lécuyer A L, Lamarche F, Arnaldi B. *A review of classification algorithms for EEG-based brain-computer interfaces*. Journal of Neural Engineering, Vol 4, 2007, pp R1 – R13.

[12] Vuckovic, A. *Non-invasive BCI: How far can we get with motor imagination?*. Clinical Neurophysiology, Vol 120, 2009, pp 1422-1423.

[13] Guger C, Harkam W, Hertnaes C, Pfurtscheller G. *Prosthetic Control by an EEG-based Brain-Computer Interface (BCI).* In Proceedings of the 5th European Conference for the Advancement of Assistive Technology (AAATE), Germany, 1999.

[14] D.H. Plettenburg. *Basic Requirements for upper extremity prostheses: the WILMER approach*. Proceedings of the 20th Annual International IEEE EMBS Conference, Hong Kong, November 1998, pp. 2276 – 2281.

[15] Cotton D P J, Cranny A, Chappell P H, White N M, Beeby S P. *Control Strategies for a multiple degree of freedom prosthetic hand.* Measurement + Control: The Journal of the Institute of Measurement and Control, Vol 40, 2007, pp. 24 – 27.

[16] Bashashati A, Fatourechi M, Ward R K, Birch G E. *A survey of signal processing algorithms in brain-computer interfaces based on electrical brain signals*. Journal of Neural Engineering, Vol 4, 2007, pp R32 – R57.

[17] Kuiken T A, Li G, Lock B A, Lipschutz R D, Miller L A, Stubblefield K A, Englehart K B. *Targeted Muscle Reinnervation of Real-Time Myoelectric Control of Multifunctional Artificial Arms*. Journal of American Medical Association (JAMA), Vol 301, no 6, 2009, pp 619 – 628.

[18] Pistohl T, Ball T, Schulze-Bonhage A, Aertsen A, Mehring C. *Prediction of arm movement trajectories from ECoG-recordings in humans*. Journal of Neuroscience methods, Vol 167(1), 2008, pp. 105-14.

[19] Shenoy P, Miller K J, Ojemann J G, Rao R P N. *Generalized Features for Electrocorticographic BCIs*. IEEE transactions on Biomedical Engineering, Vol 55, no 1, 2008, pp 273 – 280.

[20] Shenoy P, Miller J K, Ojemann J G, Rao R P N. *Finger Movement Classification for an Electrocorticographic BCI*. Proceedings for the 3rd

International IEEE EMBS Conference on Neural Engineering, Cohala Coast, Hawaii, USA, May 2007, pp 192 – 195.

[21] Donoghue J P. *Bridging the Brain to the World: A Persepctive on Neural Interface Systems*. Neuron, Vol 60, Issue no 3, November 2008, pp 511-521.

[22] Menendez R G P, Noirhomme Q, Cincotti F, Mattia D, Aloise F, Andino S G. *Modern Electrophysiological Methods for Brain-Computer Interfaces*. Computational Intelligence and Neuroscience, Vol 2007, 2007, Article ID 56986.

[23] Matsuoka Y, Afshar P. *Neuromuscular Strategies for Dynamic Finger Movements: A Robotic Approach*. Proceedings of the 26th Annual International Conference of the IEEE EMBS, San Francisco, CA, USA, Vol 2, September 2004, pp 4649- 4652.

[24] Gu Y, Dremstrup K, Farina D. *Single-trial discrimination of type and speed of wrist movements from EEG recordings*. Clinical Neurophysiology, Vol 20, issue no 8, August 2009, pp 1596-1600.

[25] Vuckovic A, Sepulveda F. *Delta band contribution in cue based single trial classification of real and imaginary wrist movement.* Medical and Biological Engineering and Computing, Vol 46, 2008, pp 529 – 539.

[26] Navarro I, Sepulveda F, Hubais B. *A Comparison of Time, Frequency and ICA Based Features and Five Classifiers for Wrist Movement Classification in EEG Signals*. Proceedings of the 27th Annual IEEE EMBS Conference, Shanghai, 2005, pp 2118 – 2121.

[27] Brunner C, Naeem M, Leeb R, Graimann B, Pfurtscheller G. *Spatial filtering and selection of optimized components in four class motor imagery EEG data using independent component analysis*. Pattern Recognition Letters, Vol 28, June 2007, 957 – 964.

[28] Bai O, Lin P, Vorbach S, Li J, Furlani S, Hallet M. *Exploration of computational methods for classification of movement intention during human voluntary movement from single trial EEG*. Clinical Neurophysiology, Vol 118, Decemeber 2007, pp 2637–2655.

[29] Wang S, James C J. *Extracting Rhythmic Brain Activity for Brain-Computer Interfacing through Constrained Independent Component Analysis.* Computational Intelligence and Neuroscience, Vol 2007, 2007, Article ID 41468, 9 pages.

[30] Dornhege G, Blankertz B, Curio G, and Müller K-R. *Combining Features for BCI*. Advances in *Neural Information Processing Systems* (NIPS 02) Becker S. Thrun S and Obermayer K Eds, Vol 15, 2003, pp 1115–1122.

[31] Mason S G, Birch G E. *A general Framework for Brain Computer Interface Design*. IEEE Transactions on Neural Systems and Rehabilitation Engineering, Vol 11, March 2003, pp 70 – 85.

[32] Nolte J. *The Human Brain*. Mosby Year Book, third edition, 1993.

[33] Biermann-Ruben K, Salmelin R, Schnitzler A. *Right rolandic activation during speech perception in stutterers: a MEG study.* Neuroimage, Vol 25, April 2005, pp 793 – 801.

[34] Thompson M, Thompson J, Wenqing Wu. *Brodmann Areas (BA), 10-20 Sites, Primary Functions*. ADD Centers Ltd, http://www.addcentre.com/Pages/professionaltraining.html, 2007.

[35] Lu P, Ferree T. *Determination of the Geodesic Sensor Net's Average Electrode Positions and Their 10 – 10 International Equivalents*. Electrical Geodesics Inc, 2000.

[36] Frackowiak R S J. *Human Brain Function*. Academic Press, second edition, 2004 pp 7 – 22.

[37] Pfurtscheller G, Berghold A. *Patterns of cortical activation during planning of voluntary movement*. Electroencephalography and clinical Neurophysiology, Vol 72, 1989, 250 – 258.

[38] Ungureanu M, Bigan C, Strungaru R, Lazarescu V. *Independent Component Analysis Applied in Biomedical Signal Processing.* Measurement Science Review, Vol 4, 2004.

[39] Blankertz B, Tomioka R, Lemm S, Kawanabe M, Müller K R. *Optimizing Spatial Filters for Robust EEG Single-Trial Analysis.* IEEE Signal Processing Magazine, Vol 25, no 1, 2008, pp 41 – 56.

[40] Babiloni F, Babiloni C, Carducci F, Del Gaudio M, Onorati P, Urbano A. *A high resolution EEG method based on the correction of the surface Laplacian estimate for the subject's variable scalp thickness*. Electroencephalography and Clinical Neurophysiology, Vol 103, issue no 4, October 1997, Pages 486-492.

[41] Delorme A, Makeig S. *EEGLAB: an open source toolbox for analysis of single-trial EEG dynamics including independent component analysis*. Journal of Neuroscience Methods, Vol 134, 2004, pp 9-21.

[42] Babiloni F, Cincotti F, Bianchi L, Pirri G. MillánJ R, Mouriño J, Salinari S, MarcianiMG. *Recognition of imagined hand movements with low resolution surface Laplacian and linear classifiers*. Medical Engineering and Physics, Vol 23, 2001, pp 323 – 328.

[43] Townsend B, Grainmann B, Pfurtscheller G. *Continuous EEG Classification During Motor Imagery – Simulation of an Asynchronous BCI*. IEEE Transactions on Neural Systems and Rehabilitation Engineering, Vol 12, no 2, June 2004, pp 258 - 265.

[44] Pfurtscheller G, C. Brunner C, Schlögl A, Lopes da Silva F H. *Mu rhythm (de)synchronization and EEG single-trial classification of different motor imagery tasks*. NeuroImage, Vol 31, 2006, pp 153 – 159.

[45] Makeig S, Debener S, Onton J, Delorme A. *Mining event-related brain dynamics*. Trends in Cognitive Sciences, Vol 8, no 5, May 2004, 204 – 210.

[46] Hyvärinen A, Oja E. *Independent Component Analysis: Algorithms and Application.* Neural Networks, Vol 13, 2000, pp 411-430.

[47] Turner J A, Lee J S, Martinexz O, Medlin A L, Schandler S L, Cohen M J. *Somatotopy of the Motor Cortex after Long-Term Spinal Cord Injury or Amputation*, IEEE Transactions on Neural Systems and Rehabilitation Engineering, Vol 9, no 2, June 2001, pp 154 – 160.

[48] Leeb R, Friedman D, Muller-Putz G R, Scherer R, Slater M, Pfurtscheller G. *Self-Paced (Asynchronous) BCI Control of a Wheelchair in Virtual Environments: A Case Study with a Tetraplegic.* Computational Intelligence and Neuroscience, Vol 2007, 2007, Article ID 79642, 8 pages.

[49] Pfurtscheller G, Müller-Putz G R, Pfurtscheller J, Rupp R. *EEG-Based Asynchronous BCI Controls Functional Electrical Stimulation in a Tetraplegic patient*. EURASIP Journal on Applied Signal Processing, Vol 2009, 2009, pp 3152 – 3155.

[50] Kohlmorgen J, Blankertz B. *Bayesian Classification of Single-Trial Event-Related Potentials in EEG*. International Journal of Bifurcation and Chaos, Vol 14, 2004, pp 719 – 726.

[51] Hallet M, Bai O, Bonin C. *Predicting Movement: When, Which and Where*. IEEE/ICME International Conference on Complex Medical Engineering, Beijing, May 2007, pp 5 – 7.

[52] Burke D P, Kelly S P, de Chazal P, Reilly R B, Finucane C. *A Parametric Feature Extraction and Classification Strategy for Brain–Computer Interfacing*. IEEE transactions on Neural Systems and Rehabilitation Engineering, Vol 13 no 1, 2005, pp 12 – 17.

[53] Shibasaki H, Hallett M. *What is the Bereitschaftspotential?*. Clinical Neurophysiology, Vol 117, November 2006, pp 2341–2356.

[54] Babiloni C, Carducci F, Cincotti F, Rossini P M, Neuper C, Pfurtscheller G, Babiloni F. *Human Movement-Related Potentials vs Desynchronization of EEG Alpha Rhythm: A High-Resolution EEG Study*. Neuroimage, Vol 10, December 1999, pp 658–665.

[55] Khan Y U, Sepulveda F. *Brain–computer interface for single-trial EEG classification for wrist movement imagery using spatial filtering in the gamma band*. IET Signal Processing, Vol 4, 2010, pp 510 – 517.

[56] Pfurtscheller G, Lopes da Silva F H. *Event-related EEG/MEG synchronization and desynchronisation: basic principles*. Clinical Neurophysiology, Vol 110, 1999, pp 1845 – 1857.

[57] Neuper C, Pfurtscheller G. *Event-related dynamics of cortical rhythms: frequency-specific features and functional correlates*. International Journal of Psychophysiology, Vol 43, 2001, pp 41 – 58.

[58] Kalcher J, Pfurtscheller G. *Discrimination between phase-locked and non-phase-locked event-related EEG activity*. Electroencephalography and clinical Neurophysiology, Vol 94, 1995, pp 381-384.

[59] Åberg M CB, Wessberg J. *Evolutionary optimization of classifiers and features for single-trial EEG Discrimination*. BioMedical Engineering OnLine, Vol 6, August 2007.

[60] Dornhege G, Blankertz B, Curio G. *Speeding up classification of multi-channel Brain-computer interfaces: Common spacial patterns for slow cortical potentials*. In Proceedings of the 1st International IEEE EMBS Conference on Neural Engineering, Capri, 2003, pp 591 – 594.

[61] Logar V, Skrjanc I, Belic A, Brezan S, Koritnik B, Zidar J. *Identification of the phase code in an EEG during gripping-force tasks: A possible alternative approach to the development of the brain-computer interfaces.* Artificial Intelligence in Medicine, Vol 44, issue no 1, September 2008, pp 41 – 49.

[62] Ben Dayan Rubin D D, Baselli G, Inbar G F, Cerutti S. *An adaptive neuro-fuzzy method (ANFIS) for estimating single-trial movement-related potentials*. Biological Cybernetics, Vol 91, August 2004, pp 63 – 75.

[63] Slobonouv S, Chiang H, Johnston J, Ray W. *Modulated cortical control of individual fingers in experienced musicians: an EEG study*. Clinical Neurophysiology, Vol 113, 2002, pp 2013 – 2024.

[64] do Nascimento O F, Farina D. *Movement-related cortical potentials allow discrimination of rate of torque development in imaginary isometric plantar flexion*. IEEE Transactions on Biomedical Engineering, Vol 55, November 2008, pp 2675 – 2678.

[65] Pfurtscheller G, Ch. Neuper Ch, Flotzinger D, Pregenzer M. *EEG-based discrimination between imagination of right and left hand movement*. Electroencephalography and clinical Neurophysiology, Vol 103, 1997, pp. 642 – 651.

[66] Babiloni F, Bianchi L, Semeraro F, del R Millan J, Mourino J, Cattini A, Salinari S, Marciani M G, Cincotti F. *Mahalanobis Distance-Based Classifiers Are Able to Recognize EEG Patterns by Using Few EEG Electrodes*. Proceedings of the 23rd Annual International Conference of the IEEE EMBS, Istanbul, October 2001.

[67] Morash V, Bai O, Furlani S, Lin P, Hallett M. *Classifying EEG signals preceding right hand, left hand, tongue,and right foot movements and motor imagery.* Clinical Neurophysiology, Vol 119, November 2008, pp 2570 – 2578.

[68] Pfurtscheller G, Neuper C. *Event-related synchronization of mu rhythm in the EEG over the cortical hand area in man*. Neuroscience Letters, Vol 174, 1994, pp 93 – 96.

[69] Pfurtscheller G, Neuper C, Andrew C, Edlinger G. *Foot and hand movement mu rhythms*, International Journal of Psychophysiology. Vol 26, 1997, pp 121 – 135.

[70] Farina D, do Nascimento O F, Lucas M F, Doncarli C. *Optimization of wavelets for classification of movement-related cortical potentials generated by variation of force-related parameters*. Journal of Neuroscience Methods, Vol 162, 2007, pp 357 – 363.

[71] Obermaier B, Neuper C, Guger C, Pfurtscheller G. *Information transfer rate in a five-class brain-computer interface*. IEEE Transactions on Neural Systems and Rehabilitation Engineering, Vol 9, September 2001, pp 283–288.

[72] PhysioForum. *Muscles associated with basic limb pattern movement of the upper extremity in the PNF technique*. http://www.physiobob.com/forum/neuro-physiotherapy/4194-muscle-associated-basic-limb-pattern-movement-upper-extremity-pnf-te.html, Last accessed 09 February 2011.

[73] Scherer R, Zanos S P, Miller K J, Rao R P N, Ojemann J G. *Classification of contralateral and ipsilateral finger movements for electrocorticographic brain-computer interfaces*. Neurosurg Focus, Vol 27, July 2009, E12.

[74] Miller J K, Zanos S, Fetz E E, den Nijis M, Ojemann J G. *Decoupling the Cortical Power Spectrum Reveals Real-Time Representation of Individual Finger Movements in Humans*. The Journal of Neuroscience, Vol 29, March 2009, pp 3132 – 3137.

[75] Vuckovic A, Sepulveda F. *A four-class BCI based on motor imagination of the right and the left hand wrist*. First International Symposium on Applied Sciences on Biomedical and Communication Technologies (ISABEL), Aalborg, October 2008.

[76] Kubler A, Nijboer F, Mellinger J, Vaughan T M, Pawlezik H, Schalk G, Mcfarland D J, Birbaumer N, Wolpaw J R. *Patients with ALS can use sensorimotor rhythms t operate a brain-computer interface*. Neurology, Vol 64, 2005, pp. 1775-1777.

[77] Blankertz B, Curio G, Müller K R. *Classifying Single Trial EEG: Towards Brain Computer Interfacing*. Advances in Neural Information Processing Systems, Vol 14, 2002, pp 157 – 164.

[78] Neuper C, Scherer R, Reiner M, Pfurtscheller G. *Imagery of motor actions: Differential effects of kinesthetic and visual–motor mode of imagery in single-trial EEG*. Cognitive Brain Research, Vol 25, October 2005. pp 668 – 677.

[79] Nabney I. *Netlab: Algorithms for Pattern Recognition*. Springer, London, 2004.

[80] Zhao Q, Zhang L. *Temporal and Spatial Features of Single-Trial EEG in a Brain-Computer Interface*. Computational Intelligence and Neuroscience, Vol 2007, 2007, Article ID 37695, 14 pages, doi:10.1155/2007/37695.

[81] Psychology Software Tools Inc. E-Prime 2, http://www.pstnet.com/eprime.cfm, Last accessed 11 Janaury 2011.

[82] EGI, http://www.egi.com/research-division-research-products/eeg-systems/191-ges300mr, Last accessed 13 April 2009.

[83] Bind UDA. *Behavioral Imaging and Neural Dynamics Center*. http://bindcenter.eu/?page_id=12#eeg, Last accessed 29th November 2010.

[84] Electrical Geodesics Inc. *Geodesic Sensor Net Technical Manual*, Electrical Geodesics Inc. http://www.egi.com, January 2007, S-MAN-200-GSNR-001.

[85] Gu Y, Farina D, Murguialday A R, Dremstrup K, Montoya P, Birbaumer N. *Offline identification of imagined speed of wrist movements in paralyzed ALS patients from single-trial EEG.* Frontiers in Neuroscience, Vol 3, August 2009, Article 62, 7 pages.

[86] Kauhanen L. Nykopp T, Lehtonen J, Jylänki P, Heikkonen J, Rantanen P, Alaranta H, Sams M. *EEG and MEG in Brain Computer Interfaces for Tetraplegic Patients*. IEEE Transactions on Neural Systems and Rehabilitation Engineering, Vol 14, no 2, June 2006, pp 190 – 193.

[87] G´omez-Herrero G. *Automatic Artifact Removal (AAR) toolbox v1.3 (Release 09.12.2007) for MATLAB,* Tampere University of Technology, December 2007.

[88] Knight J N. *Signal Fraction Analysis and Artifact Removal in EEG*, Department of Computer Science, Colorado State University, Fort Collins, Colo, US, 2003.

[89] Haitsma J A, Kalker T. *A Highly Robust Audio Fingerprinting System*, Proceedings for International Conference on Music Information Retrieval, Vol 2002, 2002, pp 107 – 115.

[90] Bhattacharyya A. *On a measure of divergence between two statistical populations defined by their population distributions*. Bulletin of Calcutta Mathematical Society, Vol 35, 1943, pp 99 – 110.

[91] Nielsen F, Boltz F, Schwander O. *Bhattacharyya Clustering with Applications to Mixture Simplifications*. 20th Annual International Conference on Pattern Recognition (ICPR), Istanbul, August 2010, pp 1437 – 1440.

[92] Tiwari K, Mehta K, Jain N, Tiwari R, Kanda G. *Selecting the Appropriate Outlier Treatment for Common Industry Applications*. NESUG Conference Proceedings on Statistics and Data Analysis, Baltimore, Maryland, USA, November 2007.

[93] Jarrell M G. *A comparison of Two Procedures, the Mahalanobis Distance and the Andrews-Pregibon Statistic for Identifying Multivariate Outliers*. Research in the Schools, Vol 1, 1994, 49 – 58.

[94] Hawkins D M. *Identification of Outliers*. Chapman and Hall, New York, 1980.

[95] De Maesschalck R, Jouan-Rimbaud D, Massart D L. *The Mahalanobis distance*. Chemometrics and Intelligent Laboratory Systems, Vol 50, 2000, pp 1–18.

[96] Gurner K. *An Introduction to Neural Networks*. CRC Press, 2003.

[97] Bosque M. *Understanding 99% of Artificial Neural Networks*. Writers Club Press, New York, 2002.

[98] Peat J, Parton B. *Medical Statistics: A Guide to Data Analysis and Critical Appraisal*. Blackwell publishing, 2005, pp 282 – 283.

[99] Schogl A, Lee F, Bischof H, Pfurtscheller G. *Characterization of four-class motor imagery EEG data for the BCI-competition.* Journal of Neural Engineering, Vol 2, 2005, pp L14 – L22.

[100] Bai O, Lin P, Vorbach S, Floeter M K, Hattori N, Hallet M. *A high performance sensorimotor beta rhythm-based, brain-computer interface associated with human natural motor behavior*. Journal of Neural Engineering, Vol 5, 2008, pp 24 – 35.

[101] Erfanian A, Erfani A. *ICA-Based Classification Scheme for EEG-based Brain-Computer Interface: The Role of Mental Practice and Concentration Skills*. Proceedings of the 26th Annual IEEE EMBS Conference, San Fransisco, CA, USA, September 2004, pp 235 – 238.

[102] Date A. *An Information Theoretic Analysis of 256- Channel EEG Recordings: Mutual Information and Measurement Selection Problem.* 3rd International Conference on Independent Component Analysis and Blind Signal Separation (ICA2001), San Diego, California, Decemeber 2001, pp. 185-188.